A COMPARATIVE STUDY OF PASSIVE CONTROL OF STRUCTURES

by

Aykut Erkal

B.S. in C.E., Yıldız Teknik University, 1998

Submitted to the institute for Graduate Studies in
Science and Engineering in partical fulfillment of
The requirements for the degree of
Master of Science
in
Civil Engineering

Boğaziçi University

2001

ACKNOWLEDGMENTS

I would like to express my sincere gratitude to my thesis supervisor, Prof. Dr. Semih S. Tezcan, for his continuous support, guidance, inspiration and encouragement. My special thanks are also due to members of my thesis jury; Prof. Dr. Hasan Boduroğlu and Dr. Sami And Kılıç.

I would also like to express grattitude to; Mr. Yavuz Kaya, Miss Serra Cimilli, Miss Esma Gülşen, Mr. Turgut Ersavaş, Mr. Gökhan Çapraz and Mr. Ufuk Hancılar, for their assistance and support during the preparation of this thesis.

Finally, heartfelt thanks are also due to my family for their affection and understanding.

ABSTRACT

A COMPARATIVE STUDY OF PASSIVE CONTROL OF STRUCTURES

Passive energy dissipation systems are described for the control of structures against earthquake vibrations. Classification of passive energy dissipation systems is made and discussion of the behaviour of individual passive devices and systems are provided. Hysteretic systems, viscoelastic systems, re-centering systems, dynamic vibration absorbers and base isolation system components are discussed.

In order to investigate the effects of these systems on the response of structures, a typical model building is selected. Passive energy dissipation systems are applied to the model building and the results are then compared.

First, in order to meet scientific objectives, a control theoretical four-story frame building was modelled without any passive energy dissipation systems. In a second model, isolators were used at the base level of the building. In a third, viscoelastic dampers are fixed at each storey. In the fourth model isolaters are at the base level together with viscoelastic dampers at each storey. In each scenario calculations have been carried out according to the equivalent seismic load method and linear time history analyses. Linear time history analyses have been carried out by simulating two earthquakes using 0.13sec. and 1.43sec. predominant periods and a 3.96m/sn^2 maximum acceleration. The different effects of the two periods are also presented.

Results of base shears of the models, storey displacements, the bending moments at the top of the columns, and interstorey drift ratios are presented. Conclusions are drawn.

ÖZET

PASİF KONTROLLU YAPILARIN KARŞILAŞTIRILMALI ÇALIŞMASI

Deprem sarsıntılarını kontrol altına almak amcıyla pasif enerji emici cihazlar tanımlandı. Pasif enerji emici cihazlar sınıflandırıldı ve bu cihazların davranışı hakkında bilgi verildi. Histeresis sistemler, viskoelastik sistemler, otomatik merkezileşen sistemler, dinamik tireşim söndürücüleri ve bina izolasyon aletleri anlatıldı.

Bu cihazların binalar üzerindeki etkilerini anlamak amacıyla bir model bina seçildi. Seçilen bu bina üzerinde pasif enerji emici cihazlar kullanıldı ve sonuçlar karşılaştırılmalı olarak incelendi.

Bu çalışmanın amacı doğrultusunda dört katlı bir çerçeve ilk olarak, pasif enerji emici cihaz kullanılmadan modellendi. İkinci olarak, bina zemin seviyesinde izolatörler konularak modellendi. Üçüncü olarak katlara viskoelastik söndürücüler yerleştirildi. Son olarak ise, bina aynı anda hem izolatörler hem viskoelastik söndürücüler kullanılarak modellendi. Bu dört model için, zemin hakim periyotları 0.13sn. ve 1.43sn. olan ve maksimum ivmeleri 3.96m/sn^2 olan, zaman tanım alanında doğrusal deprem davranış analizlerine ve eşdeğer deprem yüklerine göre hesap yapıldı. Depremlerin periyotlarındaki değişimin, binaların deprem davranışları üzerindeki etkileri de ayrıca incelendi.

Modellerin taban kesme kuvvetleri, kat deplasmanları, kolonların üst uçlarındaki eğilme momentleri ve katların yerdeğiştirme oranları gösterildi. Sonuçlar özetlendi.

TABLE OF CONTENTS

LIST OF FIGURES

LIST OF TABLES

LIST OF SYMBOLS

A	Area of the disc
A(T)	The spectral acceleration coefficient
A_o	Effective ground acceleration coefficient
A_{lead}	Plug area
A_{loop}	Loop area
B	Reduction factor of the response spectrum
C_0	Zero-frequency damping coefficient
C	Damping coefficient
c_e	Linear effective damping
cexp	Damping exponent
C_{VD}, C_{AD}	Design level seismic coefficients
C_{VM}, C_{AM}	Maximum capable earthquake level seismic coefficients
D	Diameter of the disc
dj2	Distance of the shear spring to joint j
d_k	Deformation across the spring
$\dot{d}_c$	Deformation rate across the damper
d_D	Design displacement
d_M	Maximum displacement
d_l	Plug diameter
E	Absolute energy input from the earthquake motion
E_k	Absolute kinetic energy
E_s	Recoverable elastic strain energy
E_h	Irrecoverable energy dissipated by the structural system through inelastic or other forms of action
E_d	Energy dissipated by supplemental damping devices
E_c	Composite compression Modulus
$E_{eff,v}$	Effective vertical modulus
F_t	Frictional force μ
F_n	Normal force

f_{u1}, f_{u2}, f_{u3}	Internal-spring forces
f_{r1}, f_{r2}, f_{r3}	Internal-spring moments
G′(ω)	Shear storage moduli
G″(ω)	Shear loss moduli
G(t)	Stress relaxation modulus
G_e	Rubbery modulus
G_g	Glassy modulus
G	Shear Modulus and gravity
I	Building importance factor
K	Stiffness
k_{u1}, k_{u2} , k_{u3}	Linear translational stiffness coefficients
k_{r1} , k_{r2} , k_{r3}	Linear rotational stiffness coefficients
k_2	Elasto-plastic stiffness of rubber
k_e	Effective stiffness
k_v	Vertical stiffness
k2, k3	Elastic spring constants
$k_{D,min}$	Minimum stiffness that correspond to the Design Based Earthquake response
$k_{M,min}$	Minimum stiffness that correspond to the Maximum Capable Earthquake response
M	Mass
M_M	Maximum capable earthquake response coefficient
N_v	Near source factor
N_a	Seismic source factor
P_{cr}	Buckling load
Q_y	Yield force
R_i	Reduction factor
R_i	Reduction factor of the isolated building
ratio2, ratio3	Ratios of post-yield stiffnesses to elastic stiffnesses
SR	Slip Rate
S	Shape factor of rubber layers and site soil profile type
S(T)	Spectral design acceleration spectra
T_D	Target design level period

T_M	Target maximum capable period
T_v	Vertical period
T_h	Horizontall period
T_A, T_B	Spectrum characteristic periods
t_0	Relaxation time
t_o	Thickness of rubber layers
t	Thickness of the isolator pad
u_1	Displacement at time t_1
u_2	Displacement at time t_2
V_{fixed}	Base shear of fixed base building
V_S	Minimum design lateral force
V_D	Design base shear
V_t	Total equivalent seismic load
W	Weight of the building
yield2, yield3	Yield forces
Z	Seismic zone factor
z_2, z_3	Internal hysteretic variables
x_o	Displacement amplitude
α	Real constant
β_{eff}	Critical damping ratio
Δt	Vertical displacement
γ	Shear strain
τ	Shear stress
τ_y	Yield stress
λ	Relaxation time
υ	Damping ratio
μ	Coefficient of friction
$\eta(\omega)$	Loss factor Shear strain
γ_v	Shear strain due to vertical load
γ_s	Shear strain due to lateral load
γ_{max}	Max shear strain
ω	Circular frequency

1. INTRODUCTION

1.1. Seismic Design

A large proportion of the world's population lives in regions of seismic hazard, at risk from earthquakes of varying severity and varying frequency of occurrence. Earthquakes cause significant loss of life and damage to property every year. Many aseismic construction designs have been developed over the years in attempts to mitigate the effects of earthquakes on buildings, bridges, and potentially vulnerable contents.

In conventional seismic design, acceptable performance of a structure during earthquake shaking is based on the lateral force resisting system, being able to absorb and dissipate energy in a stable manner for a large number of cycles. Energy dissipation occurs in specially detailed regions. These are ductile plastic hinge regions of beams and column bases, which also form part of the gravity load carrying system. Plastic hinges are regions of concentrated damage to the gravity frame, which is often irreparable. Nevertheless, this design approach is acceptable because of economic considerations provided, of course, that structural collapse is prevented and life safety is ensured.

Situations exist in which the conventional design approach is not applicable. When a structure must remain functional after an earthquake, as is the case of important structures (hospitals, police station, etc), the conventional design approach is inappropriate. For such cases, the structure may be designed with sufficient strength so that inelastic action is either prevented or is minimal, an approach that is very costly. Moreover, in such structures, special precautions need to be taken in safeguarding against damage or failure of important secondary systems, which are needed for continuing serviceability.

Moreover a large number of older structures have insufficient lateral strength and lack the detailing required for ductile behavior. Seismic retrofitting of these structures is necessary and may be achieved by conventional seismic design, although often at significant cost and with undesirable disruption of architectural features. The latter is a

significant consideration in the seismic retrofit of historic structures with important architectural features.

Alternate design procedures have been developed which incorporate earthquake protective systems in the structures. These systems may take the form of seismic isolation systems or supplemental energy dissipation devices. An examination of the behavior and effects of these systems may begin with the consideration of the distribution of the energy within a structure. This input energy is transformed into both kinetic and potential (strain) energy, which must be either absorbed or dissipated through heat. If there were no damping, vibrations exist for all time. However there is always some level of inherent damping, which withdraws the energy from the system and therefore reduces the amplitude of vibration until the motion ceases. The structural performance can be improved if a portion of the input energy can be absorbed, not by the structure itself, but by some type of supplemental device. This is made by considering the conservation of energy relationship:

$$E = E_k + E_s + E_h + E_d$$

where E is the absolute energy input from the earthquake motion, E_k is the absolute kinetic energy, E_s is the recoverable elastic strain energy, E_h is the irrecoverable energy dissipated by the structural system through inelastic or other forms of action, and E_d is the energy dissipated by supplemental damping devices. The absolute energy input E, represents the work done by the total base shear force at the foundation on the ground (foundation) displacement. It, thus, contains the effects of the inertia forces of the structure.

In the conventional design approach, acceptable structural performance is accomplished by the occurrence of inelastic deformations. This has the direct effect of increasing energy E_h. It also has an indirect effect. The occurrence of inelastic deformations results in softening of the structural system which itself modifies the absolute input energy. In effect, the increased flexibility acts as a filter which reflects a portion of the earthquakes' energy. The significant result is that it leads to reduced accelerations and reduced strains in regions away from the plastic hinges.

The technique of seismic isolation accomplishes the same task by the introduction of base isolation components at the foundation of a structure. This is a system which is characterized by flexibility and energy absorption capability. The flexibility alone, typically expressed by a period of the order of 2 seconds, is sufficient to reflect a major portion of the earthquake energy so that inelastic action does not occur. Energy dissipation in the isolation system is then useful in limiting the displacement response and in avoiding resonances.

Modern seismic isolation systems incorporate energy dissipating mechanisms. Examples are high damping elastomeric bearings, lead plugs in elastomeric bearings, mild steel dampers, fluid viscous dampers, and friction in sliding bearings.

Another approach to improving earthquake response performance and damage control is that of supplemental energy dissipation systems. In these systems, mechanical devices are incorporated into the frame of the structure and dissipate energy throughout the height of the structure. The means by which energy is dissipated is either yielding of mild steel, sliding friction, motion of a piston or a plate within a viscous fluid, orificing of fluid, or viscoelastic action in polymeric materials.

In addition to increasing the energy dissipation capacity per unit drift of a structure, some energy dissipation systems also increase the strength and stiffness. Such systems include the following types of energy dissipating devices: metallic-yielding, friction, and viscoelastic. Energy dissipation systems utilizing fluid viscous dampers will not generally increase the strength or stiffness of a structure unless the excitation frequency is high. The addition of energy dissipation systems increases the strength and/or stiffness of the structures. In general, the addition of energy dissipation system will result in a reduction in drift and, therefore, reduction of damage (due to energy dissipation) and an increase in the total lateral force exerted on the structure (due to increased strength and/or stiffness). Reduction of both drift and total lateral force may be achieved only when deformations are reduced to levels below the elastic limit.

1.2. Motion Control Systems

Seismic isolation and energy dissipation systems are classified as earthquake protection systems since their function is to mitigate earthquake hazard. Mitigation is defined as the action taken to reduce the consequences of earthquakes, such as seismic strengthening or upgrading, installation of a seismic isolation or energy dissipation system, etc. However, energy dissipation systems are also useful in reducing dynamic response under wind and other types of service loads. Thus in general, seismic isolation and energy dissipation systems may be termed motion control systems.

Dynamic vibration absorbers are oscillators which, when attached to a structure and tuned to a frequency close to that of a vibrating mode, cause an increase in damping of this mode as a result of transfer of kinetic energy among vibrating modes. Dynamic vibration absorbers may take the form of tuned mass dampers, tuned liquid dampers, tuned liquid column dampers as well as the form of arrays of such devices, each one tuned at a different frequency.

Dynamic vibration absorbers have been used for the reduction of response of structures subjected to wind excitation, occupant activity and machine vibration. Typically, the application is restricted to structures which remain in the elastic range. Many of the applications are in tall modern buildings with very small inherent damping. In these cases, dynamic vibration absorbers can enhance damping by a small amount (typically, less than about 5% of critical), which is sufficient to suppress wind induced motion for the comfort of occupants. The effectiveness of dynamic vibration absorbers is significantly reduced when the structural system undergoes inelastic action. The reasons for this reduction in effectiveness are (a) de-tuning of the absorbers when inelastic action occurs, and (b) the enhancement of damping is insignificant in comparison to that generated by inelastic action.

A passive control system, whether an energy dissipation system or a dynamic absorber (or even a seismic isolation system), develops motion control forces at the points of attachment of the system. The power needed to generate these forces is provided by the motion of the points of attachment during dynamic excitation. The relative motion of these

points of attachment determines the amplitude and direction of the control forces. For example, the seismic isolation system of the San Bernardino County Medical Center includes 184 passive fluid viscous dampers, each capable of delivering 1400 kN force at velocity of 1.5m/s and stroke of ± 0.6m. The power needed to operate each of these devices 2100 kW or about 2800 hp. This power is provided by the relative motion of the isolation basemat and foundation to which these devices are attached.

1.3. Classification of Passive Energy Dissipation Systems

Passive energy dissipation systems are classified herein as hysteretic, viscoelastic and others. Examples of hysteretic systems include devices based on yielding of metals or through sliding friction. Figure 1.1 shows typical force-displacement loops hysteretic energy dissipation systems. The simplest models of hysteretic behavior involve algebraic relations between force and displacement. Hence, hysteretic systems are often called displacement dependent. In this respect, shape memory alloy devices are also classified as hysteretic (or displacement-dependent) systems despite the fact that their force-displacement loops resemble those of Figure 1.3 for other systems rather than those of Figure 1.1 for hysteretic systems.

Viscoelastic energy dissipation systems include devices consisting of viscoelastic solid materials, devices operating on the principle of fluid orificing (e.g. viscous fluid dampers) and devices operating by deformation of viscoelastic fluids. Figure 1.2 shows force-displacement loops of these devices. Typically, these devices exhibit stiffness and damping coefficients which are frequency dependent. Moreover, the damping force in these devices is proportional to velocity, that is, the behavior is viscous. Accordingly, they are classified as viscoelastic systems. A purely viscous device is a special case of a viscoelastic device with zero stiffness and frequency independent properties.

Energy dissipation systems which cannot be classified by one of the basic types depicted in Figure 1.1 and 1.2 are classified as other systems. Examples are friction-spring devices with re-centering capability and fluid restoring force and damping devices. Figure 1.3 illustrates the behavior of these devices. While the illustrated loops of appear very different from those of Figures 1.1 and 1.2, in reality these devices originate from either

hysteretic devices (a friction device with an innovative re-centering mechanism) or fluid viscous devices (a pressurized to develop preload and re-centering capability, together with fluid orificing for energy dissipation).

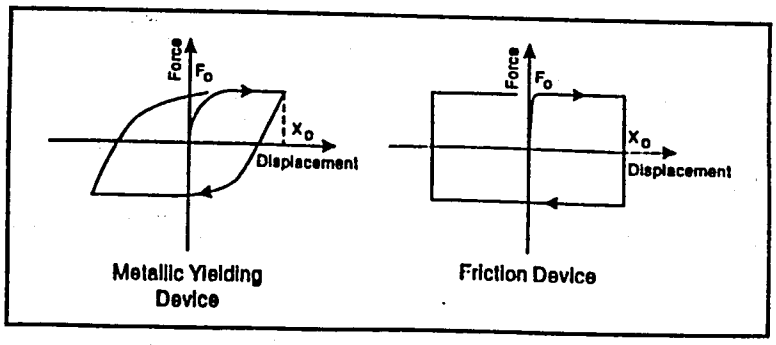

Figure 1.1. Idealized force-displacement loops of hysteretic energy dissipation devices

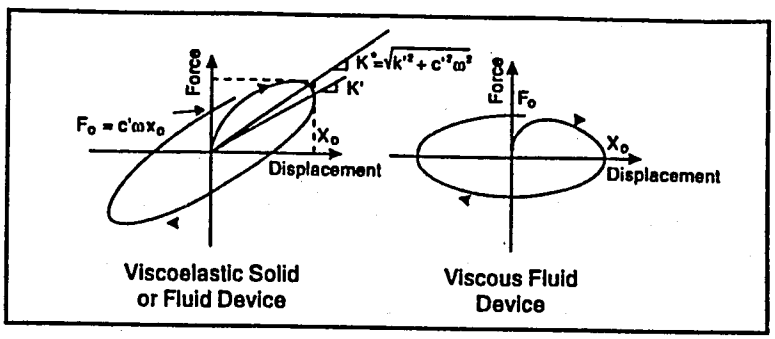

Figure 1.2. Idealized force-displacement loops of viscoelastic energy dissipation devices

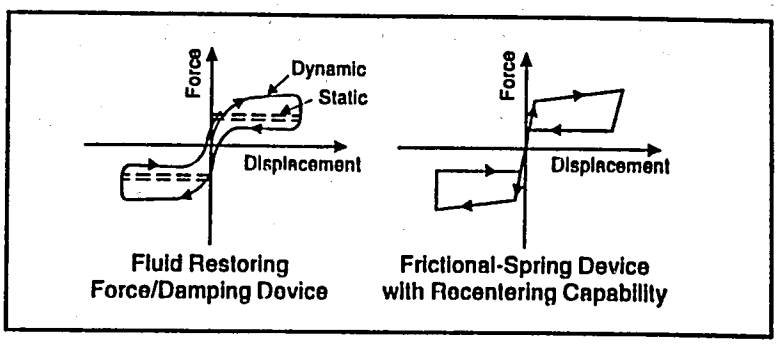

Figure 1.3. Idealized force-displacement loops of other energy dissipation devices

2. MATHEMATICAL MODELING

Passive energy dissipation systems utilize a wide range of materials and technologies as a means to enhance the damping, stiffness and strength characteristics of structures. The dissipation may be achieved either by the conversion of kinetic energy to heat or by tranferring of energy amount vibraiting modes. The first mechanism incorporates both hysteretic devices that dissipate energy with no significant rate dependence and viscoelastic devices that exhibit considerable rate dependence. Included in the former group are devices that operate on principles such as yielding of metals and frictional sliding, while the latter group consists of devices involving deformation of viscoelastic solids or fluids and those employing fluid orificing. A third classification consists of re-centering devices that utilize either a preload generated by fluid pressurization or internal springs, or a phase transformation to produce a modified force-displacement response that includes a natural re-centering component. An idealized single-degree-of-freedom structure is shown in Figure 2.1a with a passive hysteretic, viscoelastic or re-centering device operating in parallel. A macroscopic model defining the stiffness and damping characteristics of the device is needed in order to determine the overall structure response.

The second mechanism mentioned above, pretaining to the transfer of energy modes is utilized in dynamic vibraiton absorbers. In these systems, supplemental oscillators involving mass, stiffness and damping are introduced, as illustrated in Figure 2.1b. In order to significantly enhance performance, the dynamic characteristics of the supplemental oscillators must be tuned to those of the primary structure. Tuned mass dampers and tuned liquid dampers are included in this category.

2.1. Hysteretic Systems

Hysteretic systems, by defination, dissipate energy through a mechanism that is independent of the rate of load application. Included in this group are metallic dampers that utilize the yielding of metals as the dissipative mechanism, and friciton dampers that generate heat through dry sliding friction. Typical force-displacement responses for these devices obtained under constant amplitude, displacement-controlled cyclic conditions are

displayed in Figure 2.2. The quantities F and x represent the overall device force and displacement, respectively. For cyclic loading at displacement amplitude x0 and circular frequency ω, the displacement at the time t can be written

$$x(t) = x_0 \sin \omega t$$

Notice from Figure 2.2 that for both metallic and friction devices, the response remains essentially unchanged at various excitation frequencies, thus demonstrating rate independence. It should be noted that in all cases, energy dissipation occurs only after a certain thresfold froce is exceeded. Consequently, hysteretic dampers are intended primarily for seismic applicaitons.

2.1.1. Metallic Dampers

One of the most effective mechanisms available for the dissipation of energy, input to a structure during an earthquake, is through the inelastic deformation of metallic substances. In trading steel structures, aseismic desing relies upon the post-yield ductility of structural members to provide the required dissipation. However, the idea of utilizing suplemental metallic hysteretic dampers within the superstructure to absorb a portion of the seismic energy began with the conceptual and experimental work. During the ensuing years, considerable progress has been made in the development of metallic dampers and many new designs have been proposed.

Examples of metallic dampers that have received significant attention in recent years include the X-shaped and triangular plate dampers illustrated in Figure 2.3. These parallel plate devices are typically installed within a frame bay between a chevron brace and the overlying beam. As a result, the dampers primarily resist the horizontal forces associated with interstory drift via flexural deformation of the individual plates. Beyond a certain level of force, the plates yield and thus provide a supplemental amount of energy dissipation. The tapered shape of the plates promotes nearly uniform yielding throughout their length.

Despite differences in the geometric configuration of various metallic devices, the underlying dissipative mechanism in all cases results from the inelastic deformation of a metal. Usually that metal is mild steel, although sometimes lead is employed. In any case, in order to effectively employ a metallic damper for improved aseismic structural design, one must construct a reasonable mathematical model of its relevant froce-deformation characteristics.

The response of an annealed mild steel specimen, subjected to monotonic uniaxial loading, is illustrated in Figure 2.4a. This is a very familiar picture which includes the appearance of upper and lower yield stresses, a stress-strain plateau, and then a strain hardening regime. However, under constant amplitude strain-controlled cycling, the response depicted in Figure 2.4b results. At any given amplitude, a stabilized curve is eventually obtained that is independent of the prior loading history. Notice in Figure 2.4b that the knee is now rounded and that the plateau has disappeared.

There are at least two different approaches that can be taken to construct a force-displacement damper model. The first approach involves the direct use of experimental data obtained from component testing of the metallic damper. The basic form of the force-displacement model is selected, usually based upon an analogy with plasticity theory, and then the model parameters are determined via a curve fitting procedure. In the second approach, the force-displacement model is instead constructed from an appropriate constitutive relationship for the metal by applying the principles of mechanics. This latter approach can often devide additional insight into the behavior of the device, while reducing the requirements for component testing.

2.1.2. Friction Dampers

The mechanism involved in energy dissipation in metallic dampers can be categorized as one form of internal friction. On the other hand, attention will now shift to dampers that utilize the mechanism of friction between two solid bodies sliding relative to one another to provide the desired energy dissipation. An examination of the effects of frictional damping on the response of building structures was conducted by Mayes and Mowbray (1975), however it appears that Keightley (1977) was the first to consider

frictional devices for building applications. Subsequently, based primarily upon an anology to automotive brake, the development of passive frictional dampers (1980) then continued to improve the seismic response of structures. The objective is to slow down the motion of buildings "by braking rather than breaking".

There has been considerable progress during the intervening years, and a number of devices have been developed. Two representative types of friction dampers are illustrated in Figure 2.5. Figure 2.5a displays a design proposed by Pall and Marsh (1982) for application in conjunction with cross-bracing in framed structures. Brake lining pads are utilized for the sliding surfaces. Another friction device, based upon an industrial damper, is shown in Figure 2. 5b. In thisuniaxial device, which was recently tested by Aiken and Kelly (1990), copper alloy friction pads slide along the inner surface of the cylindrical steel casing. The required normal force is provided through the action of the spring against the inner and outer wedges.

On the other hand, there are numerous froms of friction that can be effectively used to mitigate damage to structures during environmental disturbances, in friction dampers, irrecoverable work is done by the tangential force required to slide one solid body across the surface of another. It is naturally of paramount importance that a consistent, predictable frictional response be maintained throughout the life of the damper. However, this response depends to a considerable extent on surface conditions, which may in turn be affected by environmental factors.

The scientific study of dry friction has a long history dating to the illustirous work of da Vinci, Amontons, and Coulomb. The basic theory is founded upon the following hypotheses, which were initially inferred from physical experiments involving planar sliding of rectilinear blocks:

- The total frictional that can be developed is independent of the apparent surface area of contact.
- The total frictional force that can be developed is proportional to the total normal force acting across the interface.

- For the case of sliding with low relative velocities, the total frictional force is independent of that velocity.

As a result of these assumptions, at the instant of impending slipage or during sliding itself, one can write

$$F_t=\mu F_n \tag{2.1}$$

where F_t and F_n represent the frictional and normal forces, respectively and μ is the coefficient of friction. Since it is frequently observed that the coefficient of friction is somewhat higher when slippage is imminent than it is during sliding, separate static μ_s and kinetic μ_k coefficients are often introduced. In either case, the frictional force F_t acts tangentially within the interfacial plane in the direction opposing the motion or impending motion.

In order to extent the theory to more general conditions, involving non-uniform distributions or non planar surfaces, these basic assumptions are often abstracted to the infinitesimal limit. Thus, total forces are replaced by surface tractions, and the generalization of Equation 2.1 becomes

$$\tau_t=\mu\tau_n \tag{2.2}$$

in tems of the tangential τ_t and normal τ_n tractions. This from is also useful for determining the nominal contact stresses that are often required for proper design. Note that an integration of Equation 2.2 over a planer contact area recovers Equation 2.1.

The concept of Coulomb friction, as described above, provides the theoretical basis for most of the work that has appeared concerning friction dampers. However, it should be emphasized that frictional processes are seldom that simple. In practice, the Coulomb theory is only approximately true. Furthermore, the coefficient of friction μ, which appears in Equations 2.1 and 2.2, must not be viewed as a constant. Instead, μ is a variable parameter that depends not only upon the selection of sliding materials, but also on the

present condition of the sliding interface. This latter dependency greatly increases the complexity of the modeling problem, since surfaces are often the site of numerous ongoing physical and chemical processes. These processes may change the physical and chemical character of the surfaces, and consequently produce a significant impact on the frictional response through a change in the true area of contact. In particular, the use of galvanic couples (e.g., mild steel and brass) must be avoided, and additional protective measures must be employed in aggressive environments to prevent corrosion.

Considerable effort had been directed toward the development of a modern mechanistic approach to solid friction, which had led to an improved qualitative understanding of the process, however a quantitative asessment of frictional response from first principles is not yet possible. More importantly, since there is still no theory for sliding friction comparable to the well-established theory of metal plasticity, there is a need for much more reliance on physical testing. With that in mind (1980) development of friction dampers was begun by conducting static and dynamic tests on a variety of simple sliding elements having different surface treatments. The goal was not necessarily to obtain maximum energy dissipation, but rather to identify a system that possesses a consistent, predictable response. For the tests, contact was maintained between the faying surfaces by pretensioning high strength bolts.

Of the surface considered, the systems containing heavy duty break lining pads inserted between steel plates did provide a consistent, predictable response. Based upon the behavior, characterization of their simple brake lining frictional system in terms of an elastic-perfectly plastic model is quite appropriate. In some friction dampers, however, a stiff bearing stage occurs for displacements beyond a given slip length. The model, which assumes zero stiffness during slipage, is specified in rate form in order to properly address arbitrary loading-unloading histories. A typical result for displacement controlled cycling at two different amplitudes is displayed in Figure 2.6, where all of the model parameters are detailed.

2.2. Viscoelastic Systems

A range of passive systems that dissipate energy in a rate dependent manner here. This group includes viscoelastic solid dampers and viscoelastic fluid dampers, with the latterexpanded to incorporate devices based uponboth fluid deformation and orificing. Typical force-displacement responses obtained for these devices under constant amplitude, displacement controlled cyclic conditions are provided in Figure 2.7a. In general, the devices exhibit both damping and stiffness, although the important case of a purely viscous damper in which force and displacement are 908 out-of-phase is illustrated in Figure 2.7b. Notice that for viscoelastic devices, the response is dependent upon frequency. However, in Figure 2.7 and in many applicaitions, the behavior is confined to linear range. This often greatly simplifies the required analysis procedures. Furthermore, since energy dissipation occurs even for infinitesimal deformations, viscoelastic devices have potential application for both wind and seismic protection.

2.2.1. Viscoelastic Solid Dampers

Viscoelastic solid materials used in civil engineering structural applications are usually copolymers or glassy substancesthat dissipate energy when subjected to shear deformatoin. A typical viscoelastic damper, which consists of viscoelastic layers bonded with steel plates, is shown in Figure 2.8. When mounted in a structure, shear deformation and hence energy dissipation takes place when the structural vibration induces relaitve motion between the outer steel flanges and the center plate.

The response of these viscoelastic materials under dynamic loading depends upon the frequency of vibration, the level of strain, and the ambient tempature. Under infinitesimal harmonic excitation with frequency ω, the relationship between shear stress $\tau(t)$ and shear strain $\gamma(t)$ can be expressed.

$$\tau(t) = G'(\omega)\gamma(t) + \frac{G''(t)}{\omega}\dot{\gamma}(t) \tag{2.3}$$

where G′(ω) and G″(ω) are the shear storage and loss moduli, respectively. The loss factor is then defined by η(ω) = G″(ω) / G′(ω). For more general excitation, Boltzmann's superposition principle can be invoked to provide the following constitutive relation for polymetric metarials:

$$\tau(t) = \int_{0+}^{t} G(\xi)\dot{\gamma}(t-\xi)d\xi + G(t)\gamma(0) \tag{2.4}$$

For the usual case of zero initial strain γ(0), this reduced to simply

$$\tau(t) = \int_{0}^{t} G(\xi)\dot{\gamma}(t-\xi)d\zeta \tag{2.5}$$

In the above, G(t) represents relaxation modulus, which is defined as the ratio of stress to strain at constant deformation. Thus, G(t) can be determined experimentally for a given material. Results for one particular copoplymer are shown in Figure 2.9. Many different expressions can be assumed for the stress relaxation modulus, including those associated with the classical Kelvin and Maxwell models. However, in order to capture the viscoelastic behavior over a sufficiently broad frequency range, more sophistication is often required. The following four- parameter model originally developed by Williams (1964) has proved to be particularly effective for representing viscoelastic materials in passive energy dissipation systems:

$$G(t) = G_e + \frac{G_g - G_e}{\left[1 + t/t_0\right]^{\alpha}} \tag{2.6}$$

where Ge is the rubbery modulus, Gg is the glassy modulus, t0 is the relaxation time, and α is a real constant giving the slope of the relaxation curve through the transition region between glassy and rubbery behavior. The stress relaxation modulus G(t) as given in Equation 2.6 predicts a bounded modulus for all non-negative time and has been found to be reasonably accurate for most VE material. Initailly, G(t) coincides with the glassy modulus, but then smoothly approaches the rubbery modulus with increasing time.

2.2.2. Viscoelastic Fluid Dampers

All af the passive devices described to this point utilize the action of the solids to enchance the performance of structures subjected to transient environmental disturbances. However, fluides can also be effectively employed in order to achieve the desired level of passive control. Significant effort has been directed in recent years toward the development of viscous fluid dampers for structural applications, primarily through the conversion of technology from the military and heavy industry. Several examples of fluid dampers are shown in Figure 2.10.

One straightforward desing approach is patterned directly after the classical dashpot. In this case, dissipation occurs via conversion of mechanical energy to heat as a piston deforms a thick, higly viscous substance, such as a silicone gel. Figure 2.10a depicts one such damper, which has found application as a component in seismic base isolation systems. While these devices could also be deployed within the superstructure, an alternative, and perhaps more effective, desing concept involves the development of the viscous damping wall (VDW) illustrated in Figure 2.10b. In this design, the piston is simply a steel plate constrained to move in its plane within a norrow rectangular steel container filled with viscous fluid. For typical installation in a frame bay, the piston is attached to the upper floor, while the container is fixed to the lower floor. Relative interstory motion shears the fluid and thus provides energy dissipation.

Both of the devices discussed above accomplish their objective through the deformation of a viscous fluid residing in an open container. In order to maximize the energy dissipation density of these devices, one must employ materials with large viscosities. Typically, this leads to the selection of materials that exhibit both frequency and tempature dependent behavior.

There is, however, another class of fluid dampers that rely instead upon the flow of fluids within a closed container. In these designs, the piston acts now, not simply to deform the fluid locally, but rather, to force the fluid pass through small orifices. As a result, extremely high levels of energy dissipation density are possible. However, a

correspondingly high level of sophistication is required for proper internal design of the damper unit.

A typical orificed fluid damper for seismic application is illustrated in Figure 2.10c. This cyclindrical device contains a compressable silicone oil which is forced to flow via the action of a stainless steel piston rod with a bronze head. The head includes a fluidic control orifice design. In addition, an accumulator is provided to compensate for the change in volume due to rod positioning. Alternatively, the device may be designed with a run-through piston rod to prevent volume changes. High strength seals are required to maintain closure over the design life of the damper. These uniaxial devices, which were originally developed for military and harsh industrial environments, have recently found application in seismic base isolation systems as well as for supplemental damping during seismic and wind-induced vibration.

While viscoelastic fluid damper construction vaires considerably from each other and from the viscoelastic solid damper counterparts, mathematical models suitable for overall force-displacement response have a similar form. In general, the devices are both frequency and tempature dependent, and in some cases amplitude dependence is also evident. Over years, numerous constitutive models have been proposed for such viscoelastic fluids. A particularly effective class is based upon the generalization of classical models to incorporate fractional derivative operators. This was first suggested by Gemant (1936). More recently, Makris and Constantinou (1991) applied fractional derivative Maxwell models to represent the behavior of viscoelastic fluid dampers, and then extended those models by incorporating complex other derivatives.

Consider, for example, the complex-derivative Maxwell constitutive model that has been used to characterize a particular polybutane fluid over a broad frequency and tempature range. At some reference temperature T_0 , under the assumption of infinitesimal incompressable deformation, the proposed model can be written in terms of shear stress τ and shear strain γ as:

$$\tau + [\lambda(T_0)]^{\nu} \frac{d^{\nu}\tau}{dt^{\nu}} = \mu(T_0)\frac{d\gamma}{dt} \tag{2.7}$$

where $\lambda = \lambda 1 + i\lambda 2$, $\psi = \psi 1 + i\psi 2$, and $\mu = \mu 1 + i\mu 1$ are complex-valued material parameters. As indicated, both λ and μ are functions pf temperature. The symbol $d\psi / dt\psi$ denotes a generalized derivative of order ψ with respect to time. For ψ=1, Equation 2.7 reduces to the classical Maxwell model. By Makris and Contantinou (1991), the following fractional derivative Maxwell force-displacement model was utilized to model overall damper response:

$$F(t) + \lambda^{\nu} \frac{d^{\nu}F(t)}{dt^{\nu}} = C_0 \frac{dx(t)}{dt} \tag{2.8}$$

with F as the force applied to the piston and x as the resulting piston displacement. Furthermore, the damper parameters Co, λ, and ψ represent the zero-frequency damping coefficient, the relaxation time and the order of frictional derivative, respectively.

2.3. Re-Centering Systems

Re-centering devices possess distinctly different force-displacement characteristics. Included in this grouping are pressurized fluid dampers, preloaded spring friction dampers, and phase transformation dampers. The first of these displays some rate-depndence due to the presence of the fluid, while the response of the remaining devices tends to be rate independent. All of these devices retain very little residual deformation upon removal of the applied load, and thus provide an inherent re-centering capability.

2.3.1. Pressurized Fluid Dampers

A pressurized fluid restoring device was recently employed by Tsopelas and Constantinou (1994) to provide both damping and re-centering capability for a base isolation system. This double-acting preloaded device is illustrated in Figure 2.11 The resistance is provided by several different physical phenomena, including the preloaded

due to initial pressurization, the device stiffness associated with the compressibility of the silicone oil, seal friction, and damping due to the passage of fluid through the orifices.

2.3.2. Preloaded Spring- Friction Dampers

A similar force-displacement response has also been obtained in a cylindrical device that employs frictional wedges, along with a preloaded internal spring. A schematic of the damper is shown in Figure 2.12.

2.3.3. Phase Transformation Dampers

In recent years, a new class of materials referred to as shape memory alloys have been considered for application in passive dampers. These metals collectively exhibit somewhat counter-intuitive behavior as a result of reversible temperature or stress induced transformations between martensitic and austenitic crystalline phases. Consider, for example, the shape memory effect. A shape memory alloy specimen in its low temperature martensitic phase is first distorted in an apparently manner. The temperature of the specimen is then elevated above a critical level, inducing a transformation to authentic phase. As a consequence, the specimen returns to its original undistorted shape.

2.4. Dynamic Vibration Absorbers

The final class of passive systems to be considered involves the use of dynamic vibration absorbers in a structure. The objective of incorporating a dynamic vibration absorber into a structure is basically the same as that associated with all of the other passive devices discussed previously, namely, to reduce energy dissipation demand on the primary structural members under the action of external forces. The reduction, in this case, is accomplished by transferring some of the structural vibrational energy to the absorber. Two basic types of dynamic vibration absorbers are prevalent in practice. The first is the tuned mass damper which, in its simplest from, consists of an auxiliary mass-spring-dashpot system anchored or attached to the main structure. The second type is labeled tuned liquid dampers, and generally involves the dissipation of energy either through the sloshing of liquids in a container or via the passage of liquids through orifices. Although

tuned mass dampers and tuned liquid dampers have been proposed for aseismic design, the primary applications to date have been for alleviation of vibrations due to wind loading. The present limitations for seismic application include detuning that occurs as the primary structure yields, the high level of damping that are normally required, and an inability to effectively control higher mode response often associated with transient or impulsive excitations.

2.4.1. Tuned Mass Dampers

The modern concept of tuned mass dampers for structural applications has its roots in dynamic vibration absorbers studied as early as 1909 by Frahm. A shematic representation of Frahm's absober is shown in Figure 2.13 which consists of a small mass m and a spring with spring stiffness k attached to the main mass M with spring stiffnes K. Under a simple harmonic load, one can show that the main mass M can be kept completely stationary when the natural frequency ($\sqrt{k/m}$) of the attached absorber is chosen to be (or tuned to) the excitation frequency.

Much of the early development as described above has been limited to the use of dynamic absorbers in mechanical engineering systems in which one operating frequency is in resonance with the fundamental frequency of a machine. Building structures, however, are subjected to environmental loads, such as wind and earthquakes, which possess many frequency components. The performance of a dynamic vibration absorber, frequently referred to as a tuned mass damper, in complex multi-degree-of-freedom damped building structures, is expected to be different.

Consider fist the response of a single-degree-of-freedom structural system subjected to a vibratory force f(t) as shown in Figure 2.14a The response of the structural system can be reduced in some circumstances by adding a secondary mass, or a tuned mass damper, which has motion relative to the system as shown in Figure 2.14b. The Equations of motion for the structure-tuned mass damper system:

$$M\ddot{y}_1(t) + C\dot{y}_1(t) + Ky_1(t) = c\dot{z}(t) + kz(t) + f(t) \qquad (2.9)$$

$$m\ddot{z}(t) + c\dot{z}(t) + kz(t) = -m\ddot{y}_1(t) + g(t) \tag{2.10}$$

where y1(t) is the displacement of the structural system and z(t) is the relative displacement of the added mass with respect to the structure. The damping coefficients and stiffness are denoted by c and k for the added mass and C and K for the structural system, respectively. The external force on the structure is represented by f(t), while g(t) equals zero for wind excitation and equals μf(t) for earthquake loading, μ = m / M being the mass ratio.

Summation of Equations (2.9) and (2.10) leads to

$$(M+m)\ddot{y}_1(t) = C\dot{y}_1(t) + Ky_1(t) = f(t) + g(t) - m\ddot{z}(t) \tag{2.11}$$

It is seen that the net effect of the added small mass (m) one the structure, aside from a slight decrease in natural frequency and a slight increase in external force from f(t) to f(t) + g(t), is the addtion of a 'force term' ✓mz□(t)✓.

2.4.2. Tuned Liquid Dampers

The basic principles involved in applying a tuned liquid damper to reduce the dynamic response of structures is quite similar to that discussed for the tuned mass damper. In particular, a secondary mass is introduced into the structural system and tuned to act as a dynamic vibration absorber. In the caseof tuned liquid dampers, generally the response of the secondary system is highly nonlinear due either to liquid sloshing or the presence of orifices. As a consequence of this inherent nonlinearity, most of the work related to characterizing response ıf tuned liquid dampers has been based upon physical experiments. However, some mathematical modelshave been developed for tuned liquid dampers, under the assumption of moderate amplitude sloshing with no wave breaking. All of these efforts utilize extensions of the classical theories by Airy and Boussinesq for shollow water gravity waves of finite amplitude.

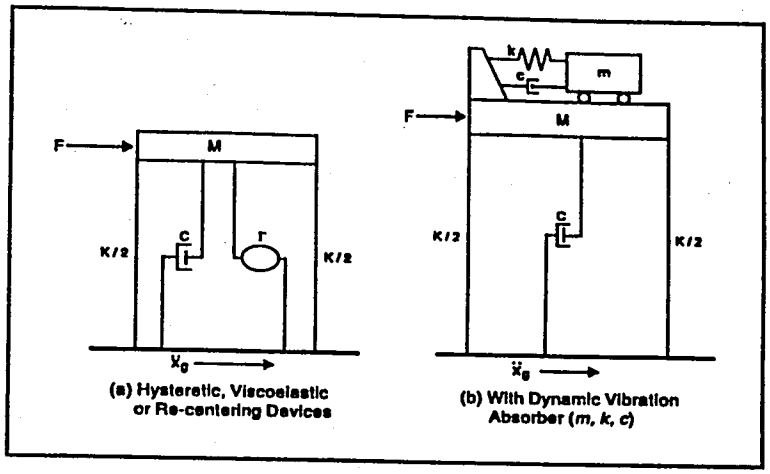

Figure 2.1. Idealizations for passively damped structures (M, K, C)

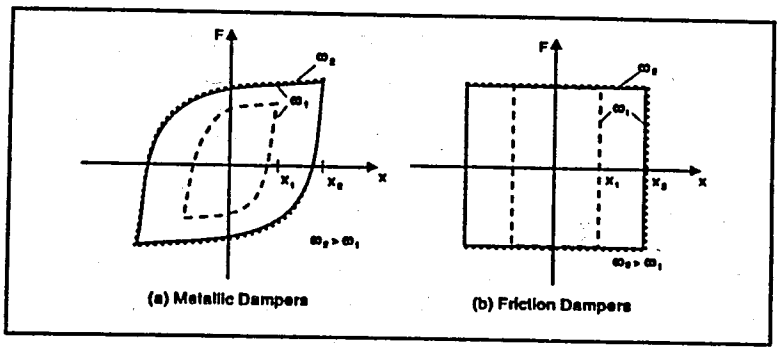

Figure 2.2. Idealized force-displacement response of hysteretic devices

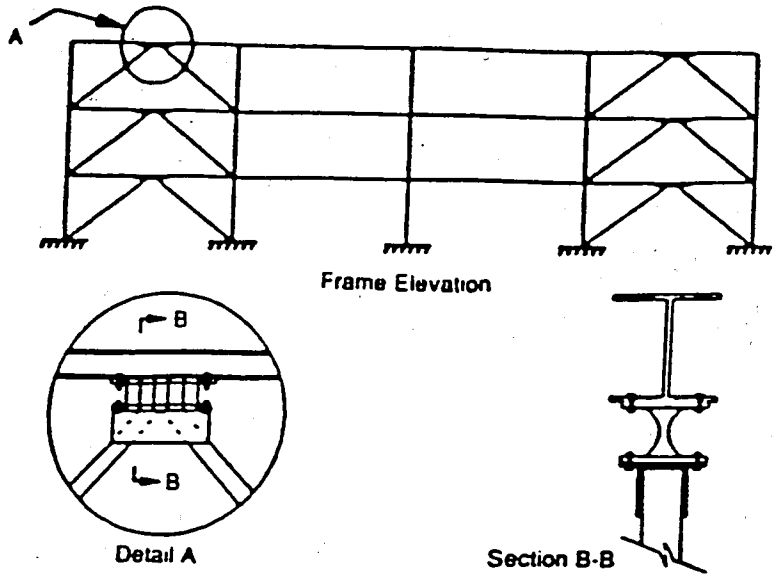

Figure 2.3. Metallic damper geometries

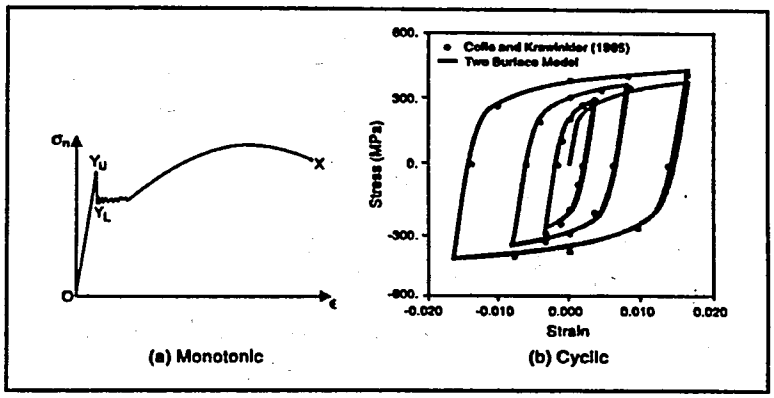

Figure 2.4. Stress-strain response of structural steel

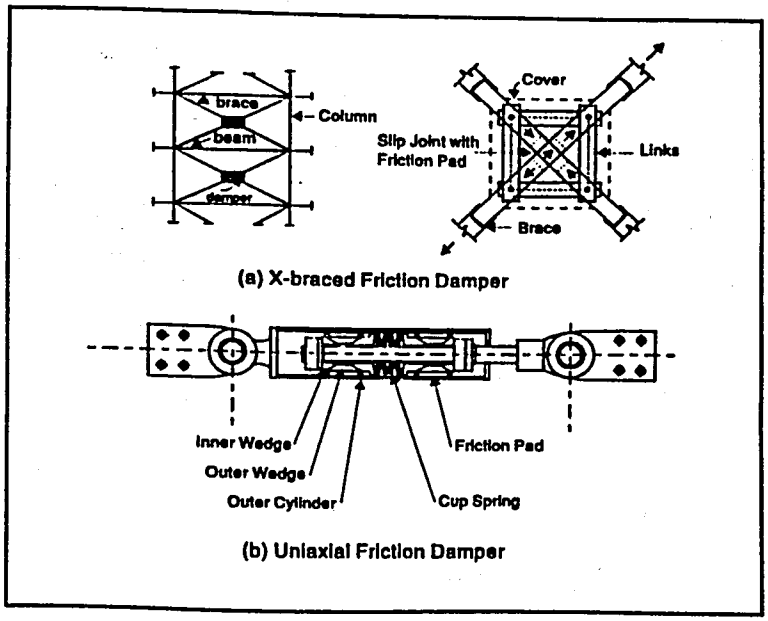

Figure 2.5. Representative friction dampers

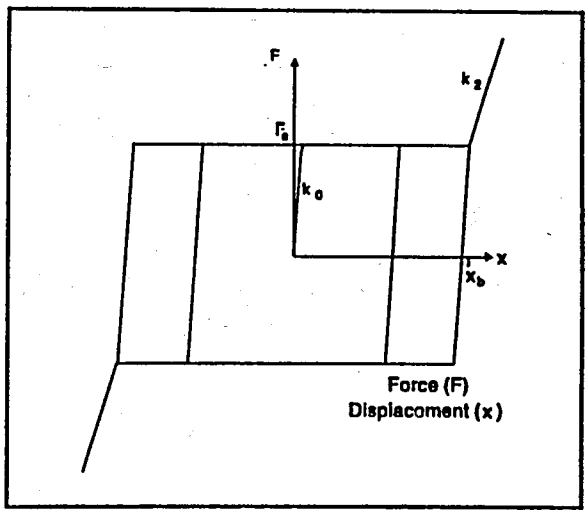

Figure 2.6. Coulomb friction element

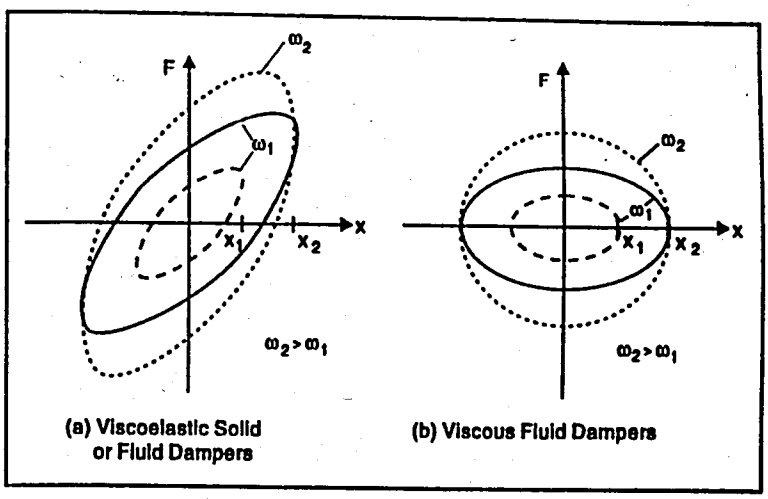

Figure 2.7. Idealized force-displacement responce of viscoelastic devices

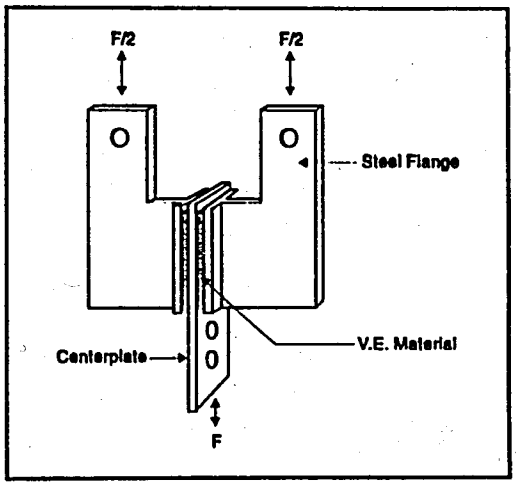

Figure 2.8. Typical viscoelastic solid damper configuration

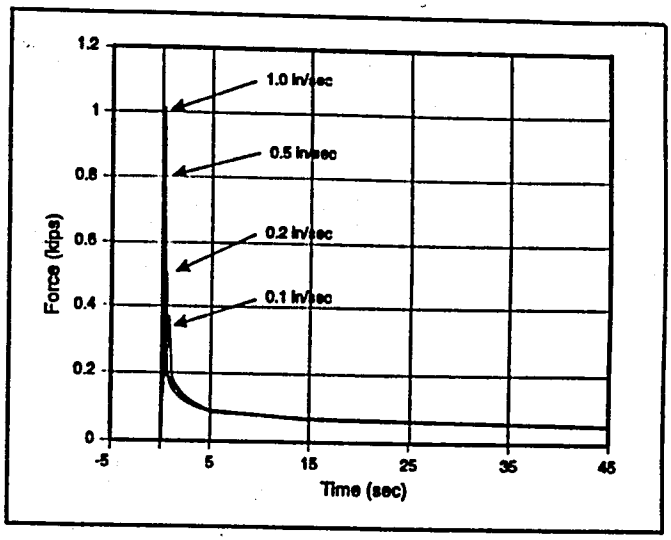

Figure 2.9. Stress relaxation tests at different strain rates

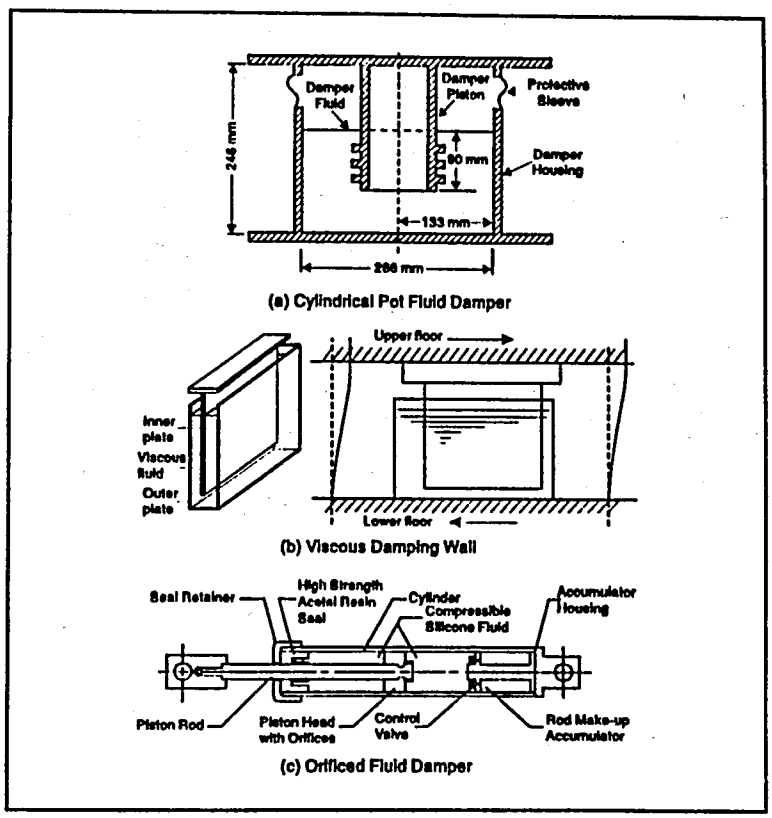

Figure 2.10. Viscoelastic fluid dampers

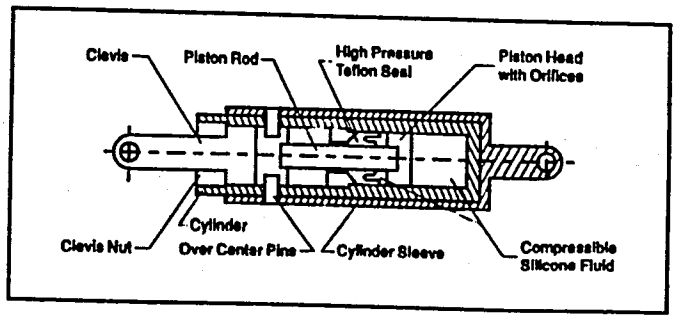

Figure 2.11. Pressurized fluid restoring device

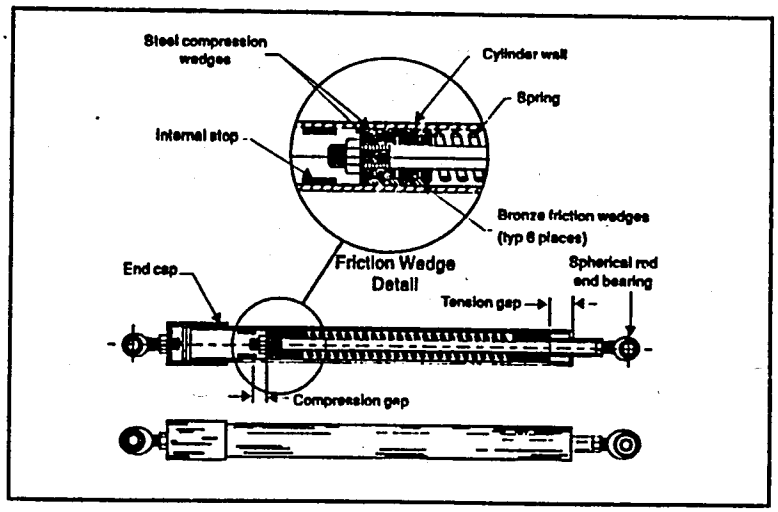

Figure 2.12. Spring-friction damper

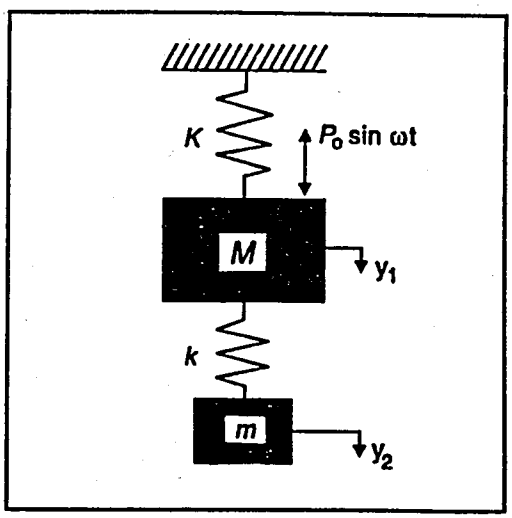

Figure 2.13. Undamped absorber and main mass subject to harmonic excitation

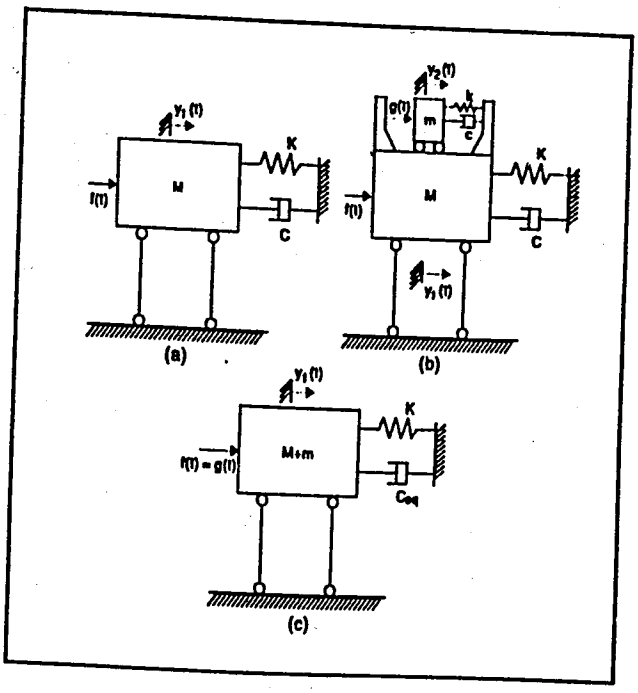

Figure 2.14. Models of single-degree-of-freedom structure and tuned mass damper

3. PHILOSOPHY OF BASE ISOLATION

J. A. Calantarients, a medical doctor from the northern English city of Scarborough, wrote a letter to the Director of the Seismological Service of the of Chile in Santiago calling his attention to a method of building construction that he had developed whereby "substantial buildings can be put up in earthquake countries on this principle with perfect safety since the degree of severity of an earthquake loses its significance through the existence of the lubricated free joint. What the doctor was prescribing was an early example of an earthquake resistant design strategy known as *base isolation* or *seismic isolation.* Many mechanisms have been invented over the last century to try to achieve the goal of uncoupling the building from the damaging action of an earthquake, for example, rollers, balls, cables, rocking columns, as well as sand.

The concept of seismic isolation has become a practical reality with in the last 20 years with the development of multilayer elastomeric bearings, which are made by vulcanization bonding of sheets of rubber to thin reinforcing plates. These bearings are very stiff in the vertical direction and can carry the vertical load of the building but are very flexible horizontally, thereby enabling the building to move laterally under strong ground motion. Their development was an extension of the use of elastomeric bridge bearings and bearings for the vibration isolation of buildings. In recent years, other systems have been developed that are modifications of the sliding approach. The concept of base isolation is now widely accepted in earthquake-prone regions of the world for protecting important structures from strong ground motion, and there are now many examples in the United States and Japan.

Seismic isolation involves introducing to a structure a plane of lateral flexibility that is intended to significantly lengthen the structure's fundamental period, shifting it away from the destructive frequency range of typical ground motions. In buildings, the lateral flexibility is often achieved through the use of elastomeric bearings, usually near the base of the structure. The accelerations transmitted to the superstructure can be greatly reduced trough the damping mechanism provided in the isolators. Thus, high-energy seismic ground motions can be transformed into low-frequency, low energy harmonic motions on

the structure, and the structural accelerations acting on the isolated building are significantly reduced. Several key assumptions influence the design of seismically isolated structures:

- A significant increase in both fundamental mode period and damping accompanies the addition of isolators to the structure's lateral force resisting system. Fundamental period increases of 1.5-3 times are typical, while damping increases from a few percent to greater than 10% are common.
- Lateral deformations are concentrated in the isolators, and in many cases the reminder of the structure is assumed to behave relatively stiffly (perhaps even rigidly), thus providing no significant dynamic amplification over the height of the building.
- The dependence of isolator response on its deformation history is neglected, the fully developed isolator flexibility and damping is assumed to act during the entire duration of strong ground shaking.

Figure 3.1 shows a typical acceleration response spectrum of an earthquake together with the possible ranges of the natural periods of vibration of medium rise buildings with and without isolation elements installed at the base. Figure 3.2 shows the behavior of base-isolated and non-isolated structures.

The first dynamic mode of the isolated structure involves deformation only in the isolation system, the structure above being to all intents and purposes rigid. The higher modes that produce deformation in the structure are orthogonal to the first mode and, consequently, to the ground motion. These higher modes do not participate in the motion, so that the high energy in the ground motion at these higher frequencies can not be transmitted into the structure. The isolation system does not absorb the earthquake energy, but rather deflects it through the dynamics of the system; this effect does not depend on damping, but a certain level of damping is beneficial to suppress possible resonance at the isolation frequency.

Most recent examples of isolated buildings use multilayered laminated rubber bearings with steel reinforcing layers as the load-carrying component of the system.

Because of the reinforcing steel plates, these bearings are very stiff in the vertical direction but are very soft in the horizontal direction, thereby producing the isolation effect. Easy to manufacture, these bearings have no moving parts, are unaffected by time and are very resistant to environmental degradation.

In the United Stated the most commonly used isolation system is the lead plug rubber bearing. These bearings are multilayered, laminated elastomeric bearings that have one or more circular holes. Lead plugs are inserted into these holes to add damping to the isolation system. Although some projects are isolated solely with lead-plug rubber bearings, they are generally used in combination with multilayered elastomeric bearings without lead plugs.

3.1. Isolation System Components

Now, base isolation is a mature technology and is used in many countries and there a number of acceptable isolation systems, the construction of which is well understood. Nevertheless, the concept appears to have an irresistible attraction to inventors, and many new and different systems of isolators are proposed and patented each year.

Most systems used today incorporate either elastomeric bearings, with the elastomer being either natural rubber or neoprene, or sliding bearings, with the sliding surface being Teflon and stainless steel although other sliding surfaces have been used. Systems that combine elastomeric bearings and sliding bearings have also been proposed and implemented.

3.2. Elastomeric-Based Systems

Natural rubber bearings are large rubber blocks without the steel reinforcing plates used today and compress by about 25% under the weight of the building. The bearings have a vertical stiffness that is only a few times the horizontal stiffness and the rubber is relatively undamped. Characteristic of isolation system of this kind, the horizontal motion is strongly coupled to rocking motion, so that purely horizontal ground motion induces vertical accelerations in the rocking mode. The system also has foam-glass on either side

of a rubber bearing that are intended to act as fuses to prevent movement in the building under wind, internal foot traffic, or low seismic input.

Many other buildings have been built on natural rubber bearings but with internal steel reinforcing plates that reduce the lateral bulging of the bearings and increase the vertical stiffness. The internal steel plates, referred to as shims, provide a vertical stiffness that is several hundred times the horizontal stiffness. These multilayered elastomer bearings provide vibration isolation for apartment blocks, hospitals, and concert halls built over subway lines or mainline railroads.

3.2.1. Low Damping Natural and Synthetic Rubber Bearings

Low damping natural bearings and synthetic rubber bearings have been widely used in Japan in conjunction with supplementary damping devices, such as viscous dampers, steel bars, lead bars, frictional devices and so on. The elastomer used in Japan comprises natural rubber, while in France neoprene has been used in several projects. The isolators have two thick steel endplates and many thin steel shims. The rubber is vulcanized and bonded to the steel in a single operation under heat and pressure in a mold. The steel shims prevent bulging of the rubber and provide a high vertical stiffness but have no effect on the horizontal stiffness, which is controlled by the low shear modulus of the elastomer. The material behavior in shear is quite linear up to shear strains above 100%, with the damping in the range of 2-3% of critical. The material is not subject to creep and the long-term stability of the modulus is good.

The advantages of the low damping elastomeric laminated bearings are many: They are simple to manufacture because the compounding and bonding process to steel is well understood, easy to model and their mechanical response is unaffected by rate, temperature, history, or aging. The single disadvantage is a supplementary damping system is generally needed. These supplementary systems require elaborate connections and, in the case of metallic dampers, are prone to low-cycle fatigue.

3.2.2. Lead Plug Bearings

The lead bearing was invented in New Zealand in 1975 and has been used extensively in New Zealand, Japan and the United States. Lead-plug bearings are laminated rubber bearings similar to low damping bearings but contain one or more lead plugs that are inserted into holes as shown in Figure 3.3. The steel plates in the bearing force the lead plug to deform in shear. The lead in the bearing deforms physically at a flow stress of around 10 Mpa, providing the bearing with a bilinear response. The lead must fit tightly in the elastomeric bearing, and this is achieved by making the lead plug slightly larger than the hole and forcing it in. Because the effective stiffness and effective damping of the lead plug bearing is dependent on the displacement, it is important to state the displacement at which a specific damping value is required. Lead-plug isolators are also shown in Figure 3.9 and Figure 3.10.

3.2.3. High Damping Natural Rubber Systems

The development of a natural rubber compound with enough inherent damping to eliminate the need for supplementary damping elements was achieved in 1982 by the Malaysian Rubber Producers' Research Association of the United Kingdom. The damping is increased by adding extrafine carbon block, oils or resins and other proprietary fillers. The damping is increased to levels between 10 and 20% at 100% shear strains, with the lower levels corresponding to low hardness (50-55 durometer) and a shear modulus around 0.34 Mpa and the high levels to high hardness (70-75 durometer) and a high shear modulus

The material is nonlinear at shear strains less than 20% and is characterized by higher stiffness and damping, which tends to minimize response under wind and low-level seismic load. Over the range of 20-120% shear strain, the modulus is low and constant. At large strains the modulus increases due to a strain crystallization process in the rubber that is accompanied by an increase in the energy dissipation. This increase in stiffness and damping at large strains can be exploited to produce a system that is stiff for small input, is fairly linear and flexible at design level input, and can limit displacements under unanticipated input levels that exceed design levels.

Another serendipitous advantage of the high damping rubber system is that it provides a degree of ambient vibration reduction. The isolators will act to filter out high frequency vertical vibrations caused by traffic or adjacent underground railways.

3.3. Isolation Systems Based On Sliding

A purely sliding system is the earliest and simplest isolation system to be proposed. As mentioned before, a system using pure sliding was proposed in 1909 by Johannes Avetican Calantarients. He suggested separating the structure from the foundation by a layer of talc. It was the method of decoupling the building and the foundation.

3.3.1. Friction Pendulum System

The friction pendulum system is a frictional isolation system that combines a sliding action and a restoring force by geometry. The friction pendulum system isolator has an articulated slider that moves on a stainless steel spherical surface. The side of the articulated slider in contact with the spherical surface is coated with a low-friction composite material. The other side of the material is also spherical, coated with stainless steel, and sits in a spherical cavity, also coated with the low-friction composite material. As the slider moves over the spherical surface, it causes the supported mass to rise and provides the restoring force for the system. Friction between the articulated slider and the spherical surface generates damping in the isolators. The effective stiffness of the isolator and the isolation period of the structure are controlled by the radius of curvature of the concave surface.

3.3.2. Resilient-Friction Base Isolation System

The resilient-friction base isolation bearing attempts to overcome the problem of the high friction coefficient of Teflon on stainless steel at high velocities by using many sliding interfaces in a single bearing. Thus the velocity between the top and bottom of the bearing is divided by the number of layers so that the velocity at each face is small, maintaining a low friction coefficient Figure 3.4. In addition to the sliding elements, there is a central core of rubber that carries no vertical load but provides a restoring force. Tests

of this system found that the rubber core did not prevent the displacement from being concentrated at a single interface; therefore, a central steel rod was inserted in the rubber core that improved the distribution of displacement among the sliding layers.

3.4. Helical Springs and Viscodampers

The vibration isolation provided by the rubber pads is limited to the horizontal direction only. Rubber elements, although very flexible in the horizontal direction, are very stiff in the vertical direction. Therefore, it is not possible to eliminate the amplification of the vertical accelerations in the superstructure, due to very high rigidity of these elements in the vertical direction.

The secondary structural elements, piping systems, machinery and other equipment would be subject to the excessive amount of the vertical component of the response. Thus, although the horizontal response is significantly reduced, the overall safety of the structure would be hindered on account of the existence of such large vertical amplifications. In addition, due to lack of sufficient damping in the rubber elements, horizontal displacements also become unacceptably large.

Earthquakes excite the structures not only horizontally, but also vertically in a three dimensional way. This fact further increases the importance of the flexibility of the isolation elements in the vertical direction. In order to achieve vibration isolation in all three directions, a number of new isolation systems with appropriate elastic properties in all directions have been introduced. Helical springs and velocity proportional dampers proved to be very efficient in providing vibration isolation practically in all possible directions of motion. Figure 3.5, 3.6 and 3.7 show samples of helical springs used for vibration isolation and its application in a building.

The helical springs are very suitable for isolation of earthquake excitations since the ratio between their vertical and horizontal stiffnesses may be easily varied to meet the requirements of three-dimensional isolation. The necessary damping is supplied by means of viscodampers so that both the acceleration and displacement response are reduced to any desired level. In Figure 3.8 non-prestressable spring unit with visco damper is shown.

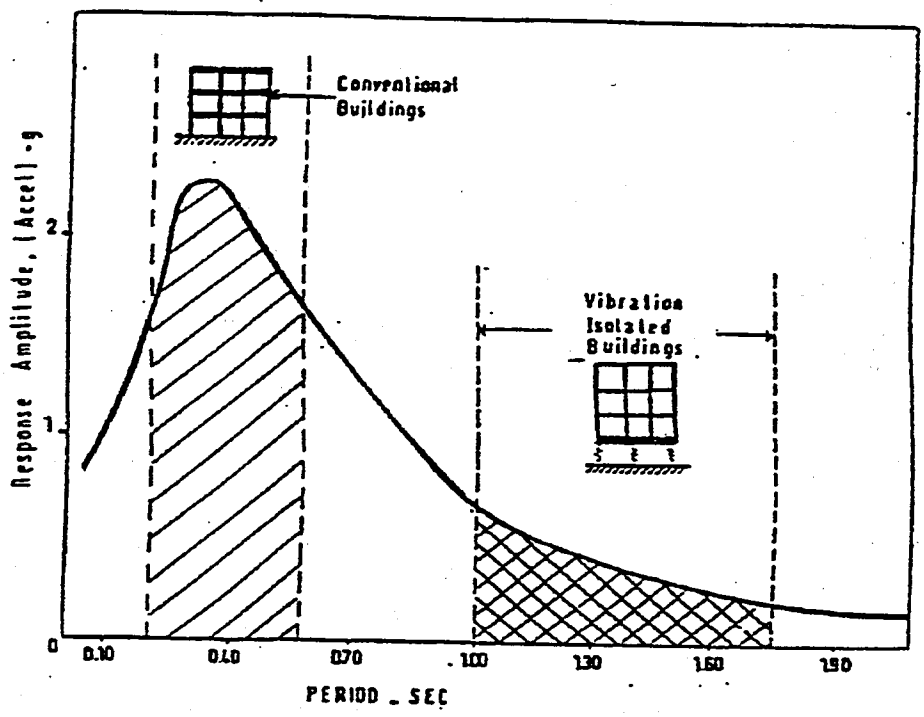

Figure 3.1. Influence of vibration isolation on structures

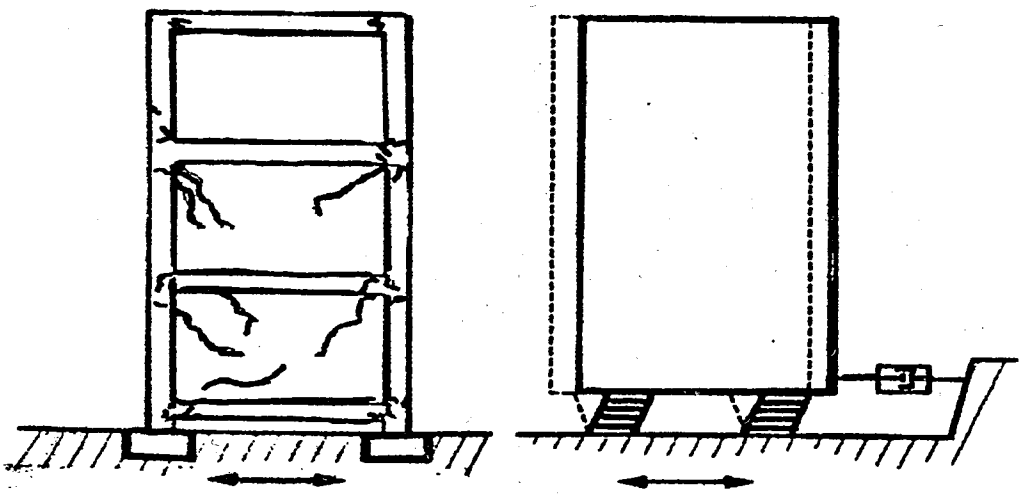

Figure 3.2. Schematic seismic response of isolated and non-isolated buildings

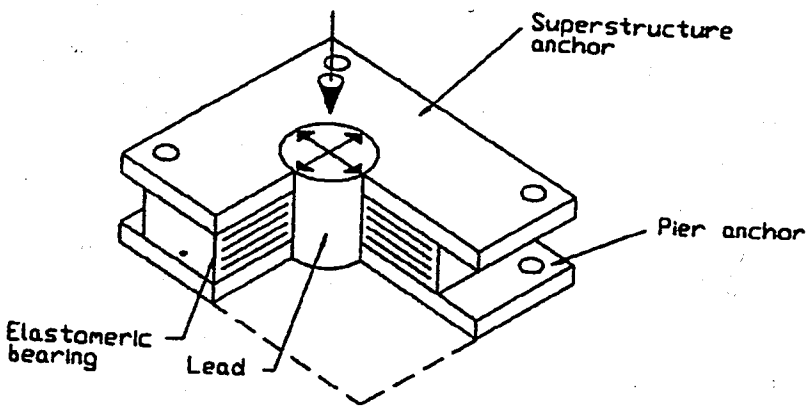

Figure 3.3. Lead-plug isolator

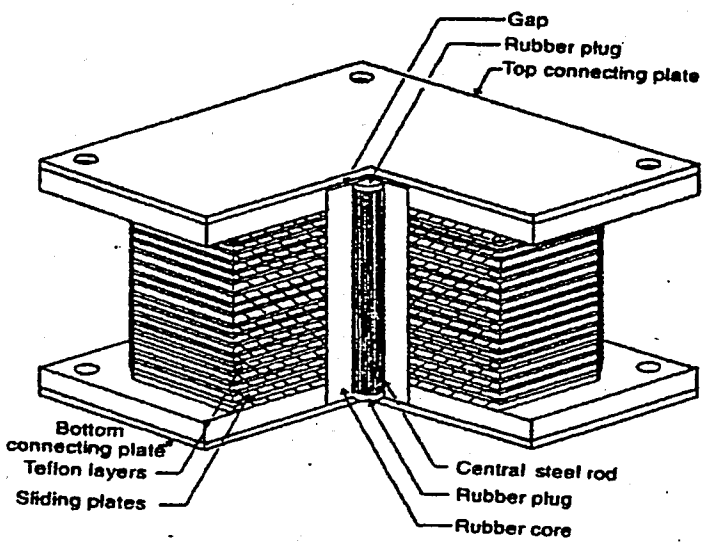

Figure 3.4. Resilient-friction base isolation system

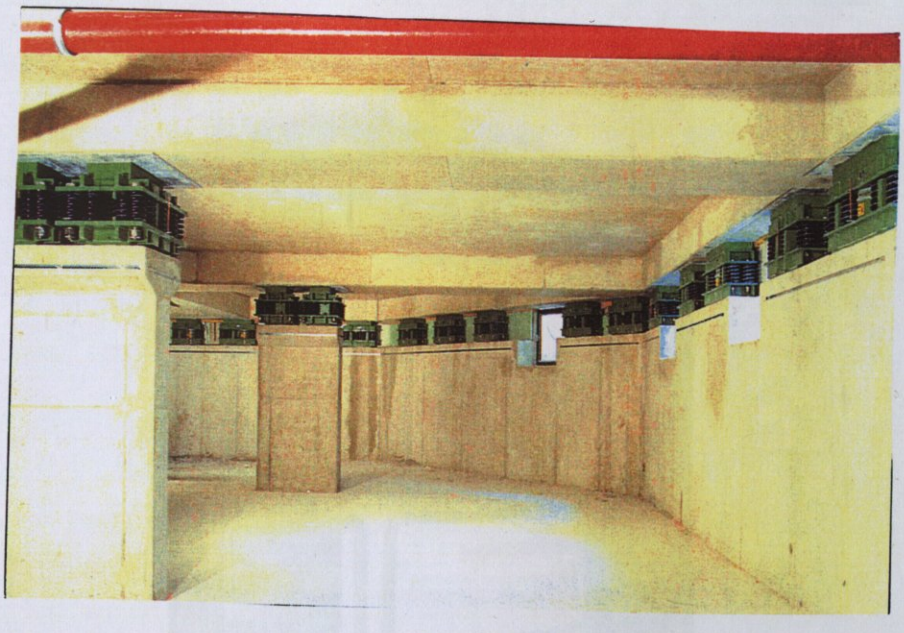

Figure 3.5. An application of helical springs and viscodampers at the basement floor

Figure 3.6. Spring units in a staircase

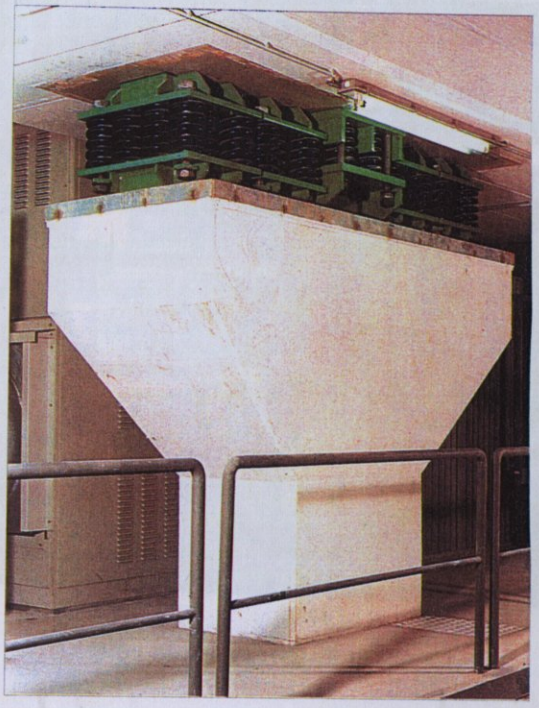

Figure 3.7. Elastic support of a turbine deck

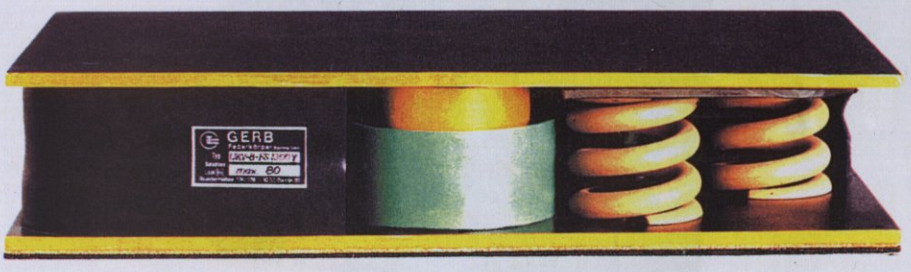

Figures 3.8. Non-prestressable spring unit with viscodamper

Figure 3.9. Lead-plug isolators

Figure 3.10. An application of a lead-plug isolator

4. MODELLING WITH SAP2000n PROGRAM

4.1. Overview

In SAP2000n program there are options named as 'Nllink Element' and 'Nlprop Properties' that are used to model local structural nonlinearities. The first one is the name of the element that is used to model:

- Viscoelastic damping
- Gap (compression only) and hook (tension only)
- Uniaxial plasticity
- Biaxial-plasticity base isolator
- Friction-pendulum base isolator

The second one is the place where the properties of the element is given. Nonlinear behavior is only exhibited during nonlinear time-history analyses. For all other analyses, the 'Nllink element' behaves linearly. Each element is assumed to be composed of six separate springs, one for each of six deformational degrees of freedom (axial,shear, torsion, and pure bending).Each of these springs possesses a dual set of properties:

- Linear effective stiffness and effective damping properties used for all linear analyses
- An optional nonlinear force-deformation relationship used only for nonlinear time-history analyses

If the optional nonlinear properties are not specified for a given degree of freedom, the linear stiffness (but not the damping) properties are used for nonlinear time-history analysis. The linear effective damping property is only used for response-spectrum analyses and linear time-history analyses. The nonlinear force-deformation relationships of these springs may be coupled or uncoupled, depending on the type of behavior modeled.

A set of properties for all six degrees of freedom is called an 'Nlprop'. Each Nlprop consists of mass, weight, and up to six linear and nonlinear force-deformation relationships that may be used by one or more Nllink elements. Each element has its own local coordinate system for defining the force-deformation properties and for interpreting output.

4.2. Nlprop Properties

A Nlprop is a set of structural properties that can be used to define the behavior of one or more Nllink elements. Nlprops are defined independently of the Nllink elements and are referenced during the definition of the elements.

Each Nlprop specifies the optional nonlinear force-deformation relationships for the six internal deformations. These nonlinear properties are used only during a nonlinear time-history analysis. Effective stiffness and effective damping properties may also be specified. These properties are used for all linear analyses, which include; static analysis, P-delta analysis, modal analysis, moving-load analysis, response-spectrum analysis, harmonic steady-state analysis, and linear or periodic time-history analysis.

The effective stiffness is also used during nonlinear time-history analyses for all degrees of freedom for which nonlinear properties are not specified. The effective damping is never used for nonlinear time-history analysis. Mass and weight properties may also be specified.

4.2.1. Internal Nonlinear Springs

Each Nlprop is assumed to be composed of six internal nonlinear springs, one for each of six internal deformations. Each spring may actually consist of several components, including springs and dashpots. The force-deformation relationships of these springs may be coupled or independent of each other.

Figure 4.3 shows the springs for three of the deformations: axial, shear in the 1-2 plane, and pure bending in the 1-2 plane. It is important to note that the shear spring is located a distance dj2 from joint j. All shear deformation is assumed to occur in this spring;

located a distance dj2 from joint j. All shear deformation is assumed to occur in this spring; the links connecting this springs to the joints (or ground) are rigid in shear. Deformation of the shear spring can be caused by rotations as well as translations at the joints. The force in this spring will produce a linearly-varying moment along the length. This moment is taken to be zero at the shear spring, which acts as a moment hinge.

4.2.2. Spring Force-Deformation Relationships

There are six force-deformation relationships that govern the behavior of the element, one for each of the internal springs.

Axial:	f_{u1} vs. d_{u1}
Shear:	f_{u2} vs. d_{u2}, f_{u3} vs. d_{u3}
Torsional:	f_{r1} vs. d_{r1}
Pure bending:	f_{r2} vs. d_{r2}, f_{r3} vs. d_{r3}

where fu1, fu2, and fu3 are the internal-spring forces; and fr1, fr2, and fr3 are the internal-spring moments.

4.2.3. Linear Force-Deformation Relationships

If each of the internal springs behaves linearly, the spring force-deformation relationships can be expressed in matrix form as:

$$\begin{Bmatrix} f_{u1} \\ f_{u2} \\ f_{u3} \\ f_{r1} \\ f_{r2} \\ f_{r3} \end{Bmatrix} = \begin{bmatrix} k_{u1} & 0 & 0 & 0 & 0 & 0 \\ & k_{u2} & 0 & 0 & 0 & 0 \\ & & k_{u3} & 0 & 0 & 0 \\ & & & k_{r1} & 0 & 0 \\ & \text{sym.} & & & k_{r2} & 0 \\ & & & & & k_{r3} \end{bmatrix} \begin{Bmatrix} d_{u1} \\ d_{u2} \\ d_{u3} \\ d_{r1} \\ d_{r2} \\ d_{r3} \end{Bmatrix} \qquad (5.1)$$

where ku1, ku2 , ku3 , kr1 , kr2 , kr3 are the linear stiffness coefficients of the internal springs.

Similar relationships hold for linear damping behavior, except that the stiffness terms are replaced with damping coefficients, and the displacements are replaced with the corresponding velocities. Consider an example where the equivalent shear and bending springs are to be computed for a prismatic beam with a section bending stiffness of EI in the 1-2 plane. The stiffness matrix at joint j for the 1-2 bending plane is:

$$\begin{Bmatrix} V2 \\ M3 \end{Bmatrix}_J = \frac{EI}{L^3}\begin{bmatrix} 12 & -6L \\ -6L & 4L^2 \end{bmatrix}\begin{Bmatrix} u_2 \\ r_3 \end{Bmatrix}_J \qquad (5.2)$$

From this it can be determined that the equivalent shear spring has a stiffness of $k_{u2} = 12\frac{EI}{L^3}$ located at $dj2 = \frac{L}{2}$, and the equivalent pure-bending spring has a stiffness of $k_{r3} = \frac{EI}{L}$. For an element that possesses a true moment hinge in the 1-2 bending plane, the pure-bending stiffness is zero, and *dj2* is the distance to the hinge.

4.2.4. Linear Effective Stiffness

For each Nlprop you may specify six linear effective-stiffness coefficients, ke, one for each of the internal springs. The linear effective stiffness represents the total elastic stiffness for the Nllink element that is used for all linear analyses: static analysis, P-delta analysis, modal analysis, moving-load analysis, response-spectrum analysis, harmonic steady-state analysis, and linear or periodic time-history analysis. The actual nonlinear properties are ignored for these types of analysis.The linear effective stiffness is also used for all degrees of freedom during a nonlinear time-history analysis.

The effective stiffness properties are not directly used for nonlinear degrees of freedom during nonlinear time-history analysis. However, these analyses do make use of the vibration modes that are computed based on the effective stiffness. During time integration, the behaviour of these modes is modified so that the structural response reflects the actual stiffness and other nonlinear parameters specified.

Some of the basic rules in the way of choosing k_e (effective stiffness), and k (nonlinear stiffness) in the analysis are given as:

For gap and hook elements the effective stiffness should usually be zero or k depending on whether the element is likely to be open or closed, respectively, in normal service. For damper elements, the effective stiffness should usually be zero. If an artificially large value for k is chosen, a much more smaller value for ke must be chosen to help avoid numerical problems in nonlinear time-history analyses.

4.2.5. Linear Effective Damping

For each Nlprop six linear effective-damping coefficients, ce, may be specified, one for each of the internal springs. By default, each coefficient ce is equal to zero. The linear effective damping represents the total viscous damping for the Nllink element that is used for response-spectrum analyses, and for linear and periodic time-history analyses. The actual nonlinear properties are ignored for these types of analysis. Effective damping can be used to represent energy dissipation due to nonlinear damping, plasticity or friction.

The effective force-deformation rate relationships for the Nlprops are given by Equation (5.1) above with the appropriate values of ce substituted for ku1, ku2 , ku3 , kr1 , kr2, kr3 , and deformation rates substituted for the corresponding deformations.

The effective damping values are converted to modal damping ratios assuming proportional damping, i.e., the modal cross-coupling damping terms are ignored. These effective modal-damping values are added to any other modal damping that is specified directly. Model cross-coupling damping terms can be very significant for some structures. A linear analysis based on effective damping properties may grossly overestimate the amount of damping present in the structure.Nonlinear time-history analysis is strongly recommended to determine the effect of added energy dissipation devices. Nonlinear time history analysis does not use the effective damping values since it accounts for energy dissipation in the elements directly, and correctly accounts for the effects of modal cross-coupling.

4.2.6. Nonlinear Properties

The nonlinear properties for each Nlprop must be of one of the six types which are; damper property, gap property, hook property, plastic1 property, isolator1 property, and isolator2 property. Damper property option is studied in the modelling of viscoelastic dampers in this master thesis. The type chosen from the above list determines which degrees of freedom may be nonlinear and the kinds of nonlinear force-deformation relationships available for those degrees of freedom.

Every degree of freedom may have linear effective-stiffness and effective-damping properties specified. During nonlinear time history analysis, the nonlinear force-deformation relationships are used at all degrees of freedom for which nonlinear properties were specified. For all other degrees of freedom, the linear effective stiffnesses are used during nonlinear time-history analysis.

Each nonlinear force-deformation relationship includes a stiffness coefficient, k. This represents the linear stiffness when the nonlinear effect is negligible, e.g., for rapid loading of the Damper. If k is zero, no nonlinear force can be generated for that degree of freedom. It is usually tempted to specify very large values of k, particularly for Damper, but this may cause numerical difficulties during solution. If to limit elastic deformations in a particular internal spring is important, it is usually sufficient to use a value of k that is from 102 to 104 times as large as the corresponding stiffness in any connected elements.

4.2.7. Damper Property

For each deformational degree of freedom, independent damping properties may be specified. The damping properties are based on the Maxwell model of viscoelasticity (Malvern, 1969) having a nonlinear damper in series with a spring. See Figure 4.1.

If nonlinear properties are not specified for a degree of freedom, that degree of freedom is linear using the effective stiffness, which may be zero. The nonlinear force-deformation relation is given by:

$$f = k * d_k = c * \dot{d}_c^{\,cexp} \tag{5.3}$$

where k is the spring constant, c is the damping coefficient, cexp is the damping exponent, dk is the deformation across the spring, and $\dot{d}_c$ is the deformation rate across the damper. The damping exponent must be positive; the practical range is between 0.2 and 2.0. The spring and damping deformations sum to the total internal deformation:

$$d = d_k + d_c \tag{5.4}$$

If pure damping behavior is desired, the effect of the spring can be made negligible by making it sufficiently stiff. The spring stiffness should be large enough so that the characteristic time of the spring-dashpot system, given by $\tau = c/k$ (when cexp=1), is an order of magnitude smaller than the size of the load steps. The load steps are the time intervals over which the load is changing. The stiffness should not be made excessively large or else numerical sensitivity may result.

4.2.8. Isolator Property

This is a biaxial hysteretic isolator that has coupled plasticity properties for the two shear deformations, and linear effective-stiffness properties for the remaining four deformations. The plasticity model is based on the hysteretic behaviour proposed by Wen (1976), and Park, Wen and Ang (1986), and recommended for base-isolation analysis by Nagarajaiah, Reinhorn and Constantinou (1991). See Figure 4.2.

For each shear deformation degree of freedom you may independently specify either linear or nonlinear behaviour:

If both shear degrees of freedom are nonlinear, the coupled force-deformation relationship is given by:

$$f_{u2} = \text{ratio2 k2 } d_{u2} + (1\text{- ratio2}) \text{ yield2 } z_2$$
$$f_{u3} = \text{ratio3 k3 } d_{u3} + (1\text{- ratio3}) \text{ yield3 } z_3$$

where k2 and k3 are elastic spring constants, yield2 and yield3 are the yield forces, ratio2 and ratio3 are the ratios of post-yield stiffness to elastic stiffness (k2 and k3), and z2 and z3 are internal hysteretic variables.

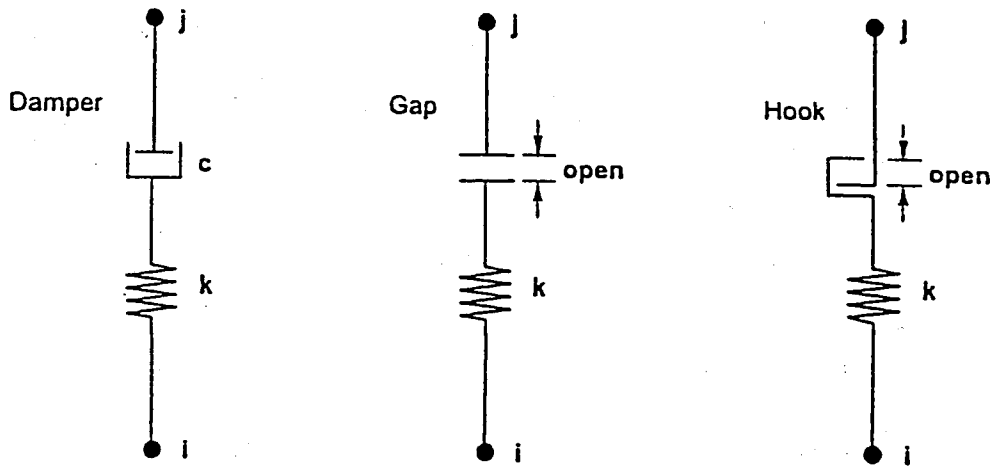

Figure 4.1. Three of the six independent nonlinear springs in an Nnlink Element

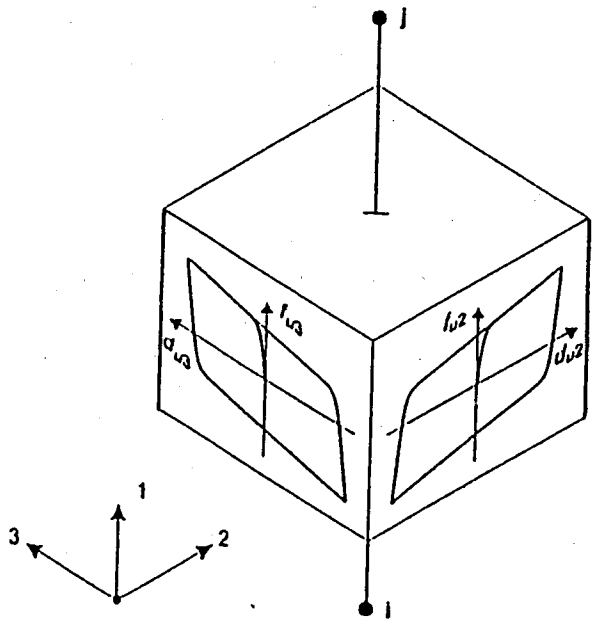

Figure 4.2. Location of shear spring at a moment hinge or point of inflection

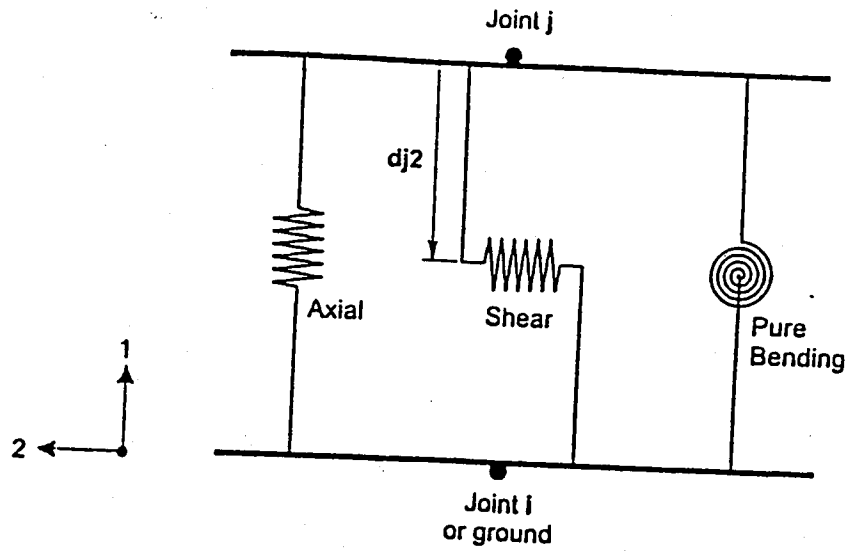

Figure 4.3. Damper, Gap and Hook Property types, shown for axial deformations

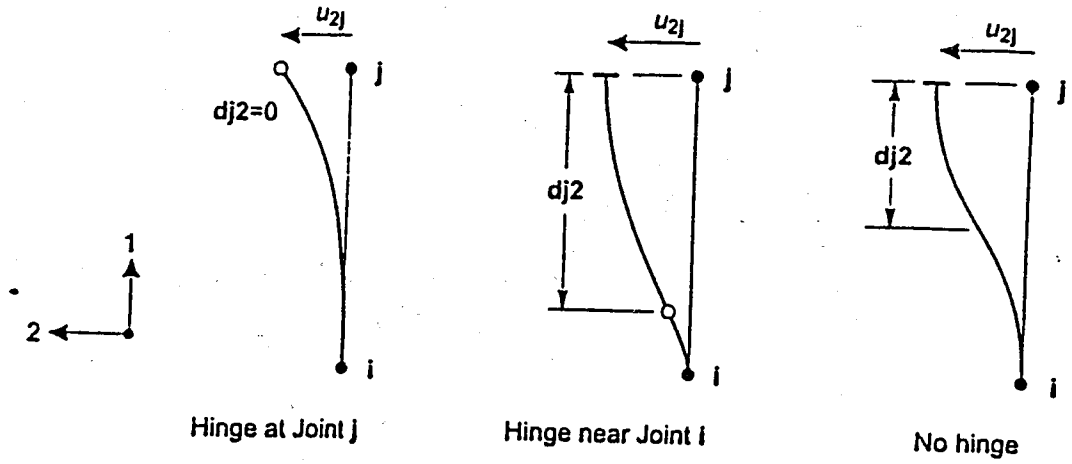

Figure 4.4. Isolator1 property for biaxial shear deformation

5. BASE ISOLATION DESIGN PROCEDURE

First, the Seismic Zone Factor is found. It is determined by establishing the seismic zone of the project's site from the UBC-97 Table 16-2 and the corresponding seismic zone factor Z from the UBC-97 Table 16-I The Site Soil Profile is determined from the UBC-97 Table 16-J. The seismic source is determined for each controlling seismic hazard source from the UBC-97 Table 16-S.

For each seismic source type, corresponding near source factors Na and Nv are determined from the UBC-97 Table 16-T. By multiplying Z and N_v, the ZN_v value is obtained. M_M is read from the UBC-97, Table A-16-D. With the seismic zone factor and the site soil profile, appropriate seismic coefficients C_V and C_V are obtained from the UBC-97 Table 16-R and 16-Q. These are then called C_{VD} and C_{AD}.

Using the soil profile type, M_M, Z and N_v are multiplied to obtain M_MZN_V. C_{VM} is read from the UBC-97, Table A-16-G. Similarly after calculating M_MZN_V and using the UBC-97, Table A-16-F, the above value of coefficient C_{VM} is obtained. Reduction factor R_i is obtained corresponding to the structural system from the UBC-97, Table A-16-E. An appropriate conservative estimate of the damping level is provided.

An initial estimate for the fundamental period of vibration at the design basis displacement level is decided. An isolated period between 2.0 and 3.0sec is desirable. Equation 5.1 and Equation 5.2 are used to estimate the design earthquake level stiffness and maximum capable earthquake level stiffness of the isolation system for the isolated period established before.

$$k_{D,min} = \frac{4\pi^2}{T_D^2}\frac{W}{g} \tag{5.1}$$

$$k_{M,min} = \frac{4\pi^2}{T_M^2}\frac{W}{g} \tag{5.2}$$

where, $k_{D,min}$ and $k_{M,min}$ are minimum stiffness that correspond to the Design Based Earthquake and Maximum Capable Earthquake response respectively, W is the weight of the building, g is gravity, and T_D and T_M are periods that correspond to the Design Based Earthquake and Maximum Capable Earthquake response respectively.

According to Equation 5.3 and Equation 5.4 the initial estimate of the minimum and maximum design displacements are calculated. If the minimum design displacement value is larger than what is acceptable for the project, a stiffer system is needed. Therefore, a smaller estimate of the vibration period should be chosen.

$$d_D = \frac{gc_{VD}T_D}{B4\pi^2} \tag{5.3}$$

$$d_M = \frac{gc_{VM}T_M}{B4\pi^2} \tag{5.4}$$

where B is the reduction factor, A_0 is the effective ground acceleration coefficient, and T_b is the spectrum characteristic period.

Minimum lateral displacement values can also be calculated according to the TDY-98. according to Equation 5.5.

$$V = A_o SW$$

$$d = \frac{V}{k}$$

$$k = \frac{4\pi^2}{T^2}\frac{V}{g}$$

$$d = A_o(2.50)\left(\frac{T_b}{T}\right)^{0.8}\frac{gT^2}{4\pi^2}$$

$$d_D = \frac{0.063}{B} A_0 g T_b^{0.8} T_D^{1.2} \tag{5.5}$$

Using Equation 5.6 and Equation 5.7, the minimum design lateral forces V_D and V_{SD} are calculated.

$$V_D = \Sigma k_D \times d_D \tag{5.6}$$

$$V_{SD} = \frac{V_D}{R_i} = \frac{642.6}{2} = 321.3\text{kN} \tag{5.7}$$

With V_{SD}, static lateral forces are calculated at each level of the building. Using the preliminary displacement, stiffness force and damping properties that were established, the isolator units to resist the gravity load and lateral load are designed.

According to Equation 5.8 and Equation 5.9, thickness of the isolator pad and stiffness of the isolator pad are calculated. The area and the diameter of the disk of the isolator are calculated based on the Equation 5.10 and Equation 5.11.

$$t\gamma_{max} = d_D$$

$$t = \frac{d_D}{\gamma_{max}} \tag{5.8}$$

where t is the thickness of the isolator pad and A and D are the area and the diameter of the disc respectively and G is the shear modulus at large strains.

$$k_D = \frac{AG}{t} \Rightarrow A = \frac{K_D t}{G} \tag{5.9}$$

$$A = \frac{K_D t}{G} \tag{5.10}$$

$$D = \sqrt{\frac{4A}{\pi}} \tag{5.11}$$

The base shear of the fixed-based building is found by Equation 5.12 and is compared with the base shear of the isolated building satisfying Equation 5.13.

$$V_{fixed} = \frac{c_V I}{RT_D} W \geq 0.11 c_a I W \tag{5.12}$$

$$V_{SD} > V_{fixed} \tag{5.13}$$

The thickness of the rubber layers is calculated, and should be between D/40 and D/80 according to Equation 5.14. The shape factor of the rubber layers and the effective vertical modulus of the isolators are calculated based on Equation 5.15 and Equation 5.16.

$$t_o = \left(\frac{D}{40}; \frac{D}{80}\right) \tag{5.14}$$

$$S = \frac{D}{4t_o} \tag{5.15}$$

where, S is the shape factor of rubber layers, to. $E_{eff,v}$ is the effective vertical modulus of the isolators and E_c is the composite compression modulus.

$$E_{eff.v} = \frac{6GS^2 E_c}{6GS^2 + E_c} \tag{5.16}$$

The vertical stiffness and vertical displacement and the vertical period T_v for the system are calculated according to Equation 5.17, Equation 5.18, Equation 5.19 and Equation 5.20.

$$\Sigma k_V = \frac{AE_{eff}}{t} \tag{5.17}$$

$$\Delta t = \frac{Wt}{AE_{eff}} = \frac{W}{k_v} \tag{5.18}$$

$$T_h = T_v\sqrt{6}S \tag{5.19}$$

$$T_v = \frac{T_h}{\sqrt{6}S} \tag{5.20}$$

The shear strain due to vertical load is calculated according to Equation 5.21 and Equation 5.22. A' Common area is calculated according to Equation 5.23.

$$\varepsilon_z = \frac{\Delta t}{t} \tag{5.21}$$

$$\gamma_v = 6S\varepsilon_z \tag{5.22}$$

$$A' = A\left[1 - \frac{2}{\pi}(\theta + \sin\theta\cos\theta)\right] \tag{5.23}$$

$$\sin\theta = \frac{d_D}{D}$$

where A' is common area and γ_v is strain due to vertical load.

The maximum load that an isolator can carry is calculated based on Equation 5.24. The shear strain due to vertical load is calculated according to Equation 5.25 and Equation 5.26. Maximum shear strain is found by the sum of strains due to vertical load and lateral load as shown in Equation 5.27.

$$W = A'GS\gamma_V \tag{5.24}$$

$$\gamma_s = \frac{\tau}{G} \tag{5.25}$$

$$\gamma_S = \frac{V_D}{AG} = \frac{k_D d_D}{AG_a} \tag{5.26}$$

$$\gamma_{max} = \gamma_V + \gamma_S \tag{5.27}$$

where γ_s is strain due to lateral load and γ_{max} is maximum shear strain.

Buckling load is calculated according to Equation 5.28.

$$P_{cr} = \sqrt{\frac{AG\pi^2 EI}{3t^2}} \tag{5.28}$$

The design of the lead plug bearing system that provides the same period and global damping at the design displacement is obtained for the high-damping rubber system and is a straightforward procedure. The design philosophy for lead plugs is that they should not be too slender or too squat.

Firstly, the plug diameter is selected and the lead area is calculated according to Equation 5.29 and Equation 5.30. The first estimation of yield force Q_y is made based on Equation 5.31 or alternatively Equation 5.32.

$$d_l \leq \frac{t}{1.5} \tag{5.29}$$

$$A_{lead} = \frac{\pi d_l^2}{4} \tag{5.30}$$

$$Q_y \cong \frac{A_{loop}}{4d_D} \tag{5.31}$$

$$Q_y = \tau_y A_{lead}$$

where Q_y is yield force of the lead plug.

The elasto-plastic stiffness k_2 of rubber is calculated assuming $k_1=10k_2$ as shown in Equation 5.33. Then the lead area, the diameter of the lead and V_d are calculated according to Equation 5.34, Equation 5.35 and Equation 5.36.

$$A_{lead} = \frac{Q_y}{\tau_y} \tag{5.33}$$

$$k_{eff} = \frac{Q_y}{d_D} + k_2 \Rightarrow k_2 = k_{eff} - \frac{Q_y}{d_D} \tag{5.34}$$

$$\phi_{lead} = \sqrt{\frac{4 \times A_{lead}}{\pi}} \tag{5.35}$$

$$V_d = Q_y\left(1 - \frac{k_2}{k_1}\right) + k_2 d_D \tag{5.36}$$

6. CASE STUDY

6.1 Analytical Investigation

By using SAP2000n program, a control theoretical four-story frame building was modeled without any passive energy dissipation systems. In a second model, isolators were used at the base level of the building. In a third, viscoelastic dampers are fixed at each storey. In the fourth model isolators are at the base level together with viscoelastic dampers at each storey. The intent of this study is to document the seismic behavior of these systems from their recorded response for two earthquakes producing different durations of shakings and predominant periods. The efficiency of passive energy dissipation devices under different earthquake frequencies is studied. The results are used to verify key assumptions made in the design of the buildings and to shed new light on the actual earthquake response of these kinds of buildings.

Two artificial earthquakes are created. This is done first by taking 9000 time records of the Bursa Tofaş Factory Record of the Kocaeli Earthquake and changing the time interval Δt of the earthquake; therefore the duration is shortened or lengthened without changing the number of time steps N. The maximum acceleration of the earthquake is also changed by multiplying by a scale factor. In this way, two artificial earthquakes; Earthquake-A and Earthquake-B are produced. The record and the response spectrum of Earthquake-A are shown in Figure 6.1 and Figure 6.2 and the record and the response spectrum of Earthquake-B is shown in Figure 6.3 and Figure 6.4. These earthquakes have predominant periods of 0.13sec. and 1.43sec. respectively and a maximum acceleration of $3.96 m/sn^2$. $\Delta t = 0.001$sec. and $\Delta t = 0.01$sec. time intervals are used to obtain 0.13sec. and 1.43sec. predominant periods. By decreasing Δt, the durations have been decreased causing a reduction in the fundamental period of earthquake and this situation represents the stiff soil situation. The change in the building responses at different Δt values are studied by structural analyses and compared with each other.

Two time history analyses and equivalent seismic load method have been conducted using Sap2000n program. Time history analyses have been performed using the two

artificial records. For fixed-based buildings, equivalent seismic loads are calculated according to the Turkish Building Code-1997 and for base-isolated buildings; these loads are calculated based on the Uniform Building Code-1997.

The viscoelastic dampers and lead-plug bearings were modeled by the "NLPROP" and "NLLINK" tools of Sap2000n program. Linear time history analyses have been performed for the linear behavior of the viscoelastic dampers and lead-plug bearings. During linear time history analyses, the linear force-deformation relationships are used at all degrees of freedom.

Storey displacements, moments at the top of the columns and storey drift ratios are chosen as seismic response parameters and compared. Damper and isolator properties are activated by introducing effective stiffness and effective damping for linear degrees of freedom.

The damping ratio supplied by the viscoelastic devices is obtained by an analogy of a logarithmic decrement curve for a one-degree of freedom system. The displacement versus time graph of a one-degree of freedom system is a decreasing sine curve from which the damping ratio is calculated by the formula

$$\ln \frac{u_1}{u_2} = \frac{2\pi\nu}{\sqrt{1-\nu^2}}$$

where u_1, is the displacement at time t, and u_2 is the displacement at time t_2, ν is the damping ratio and is easily obtained if u_1 and u_2 are read from graph.

In the same manner, if u_1 is the maximum top displacement at time t for the undamped system and u_2 is the maximum top displacement at time t for the damped frame, then the damping ratio supplied by the devices is ν.

6.2. The Fixed-based Case

A four-storey two-bay reinforced concrete frame is designed with identical columns of dimension 40 / 70 and beams of dimension 40 / 50. Concrete type C25 and StI is used as the construction elements. The weight of one floor is 735.75kN. The storey height is 3.0m. and the building height is 12m. The section along the height of the proposed building is shown in Figure 6.5.

The building is exposed to the two artificial earthquake ground motion acceleration records for 9sec. and 90sec. Time history traces of the proposed building are recorded as 'top floor displacement' and 'moment at top column at top floor'.

6.3. The Rubber Base-isolated Case

A four-storey two-bay reinforced concrete frame is designed with identical columns of dimension 40 / 70 and beams of dimension 40 / 50. Concrete type C25 and StI is used as the construction elements. The weight of one floor is 735.75kN. The storey height is 3.0m. and the building height is 12m. Lead-plug bearings have been used at the base level of the frame. The exterior and interior isolators are designed with different stiffness because of the weight of the building, which the isolators carry. The section along the height of the proposed building is shown in Figure 6.5.

6.4. The Viscodampers Case

A four-storey two-bay reinforced concrete frame is designed with identical columns of dimension 40 / 70 and beams of dimension 40 / 50. Concrete type C25 and StI is used as the construction elements. The weight of one floor is 735.75kN. The storey height is 3.0m. and the building height is 12m. The system is equipped with the viscoelastic damping devices at each storey level. All the dampers chosen are the same. Due to the dampers, 21.30 per cent damping is obtained over the structure. The section along the height of the proposed building is shown in Figure 6.6.

6.5. The Rubber Base Isolation Combined with Viscoelastic Dampers Case

A four-storey two-bay reinforced concrete frame is designed with identical columns of dimension 40 / 70 and beams of dimension 40 / 50. Concrete type C25 and StI is used as the construction elements. The weight of one floor is 735.75kN. The storey height is 3.0m. and the building height is 12m. While modeling this system, both lead-plug bearings have been used at the base level of the frame and the viscoelastic damping devices have been set at each storey level. The exterior and interior isolators are designed with different stiffness because of the weight of the building, which the isolators carry. All the dampers chosen are the same. The section along the height of the proposed building is shown in Figure 6.6.

6.6. Base Isolation Calculations

As a design example for this study, a representative frame building is considered as described above. The building and bearing loads are as follows:

Wbuilding	= 2943 kN	
Wa	= 735.75 kN	Exterior Isolators
Wb	= 1471.5 kN	Interior Isolators

The selection strategy for the bearings is to use one bearing size to save the cost of an extra mold and to use two different high damping compounds, which will be denoted by A (soft) and B (hard).

Using the value M≥7.0 and Slip Rate = SR≥5mm/year, for the controlling seismic hazard source, then the corresponding seismic source type is determined from the UBC-97 Table 16-U as A Type.

The site is assumed as zone 4 with S_D soil type and it is assumed that the site is not less than 15km from a known active fault. Using the requirements given in the 1997-UBC Appendix, Chapter 16, the parameters associated with the location are Z=0.40, S=S_D, N_a=1, N_v=1, and M_M=1.25 where Z is the seismic zone factor from the UBC-97, Table 16-I. It is determined by establishing the seismic zone of the project's site from the UBC-97,

Fig. 16-2. S_D is Site Soil Profile Type from the UBC-97, Table 16-J. N_a and N_v are seismic source and near source factors respectively specified from the UBC-97, Tables 16-S and 16-T.

$$ZN_v = 0.40 \times 1 = 0.40 \tag{6.1}$$

$$M_M = 1.25 \tag{6.2}$$

In Equation 6.1 and 6.2, by multiplying Z and N_v, ZN_v is obtained and the maximum capable earthquake response coefficient M_M is read from the UBC-97, Table A-16-D

$$C_V = 0.64 \rightarrow C_{VD} = 0.64 \tag{6.3}$$

$$C_A = 0.44 \rightarrow C_{AD} = 0.44 \tag{6.4}$$

where C_V and C_A are Seismic Coefficients obtained from UBC-97 Tables 16-R and 16-Q and called C_{VD} and C_{AD} with seismic zone factor and site soil profile respectively.

$$\alpha = M_M Z N_A \tag{6.5}$$

$$\alpha = 1.25 \times 0.40 \times 1 = 0.50 \rightarrow C_{AM} = 1.1\,\alpha = 1.1 \times 0.5 = 0.55$$

$$\alpha' = M_M Z N_V \tag{6.6}$$

$$\alpha' = 1.25 \times 0.40 \times 1 = 0.50 \rightarrow C_{VM} = 1.6\,\alpha' = 1.6 \times 0.5 = 0.80$$

Using the soil profile type determined above, M_M, Z and N_a are multiplied and using the UBC-97, Table A-16-F, CAM is obtained. Similarly, after calculating $M_M Z N_v$ and using the UBC-97, Table A-16-G, the value of coefficient C_{VM} is obtained.

$$R_i = 2$$

The structural system can be taken as a reinforced-concrete shear wall building, which allows a value R_i of 2.

$$T_f = 0.575 \text{ sec.}$$

T_f is the Fixed Based Elastic Period of the building.

$$\beta_{eff} = 0.15$$

The isolators consist of lead plug and laminated rubber so according to the value of 0.15 of β_{eff}, B is obtained as 1.35 from the UBC-97, Table A-16-C.

$T_D = 2.30$ sec.	Target Design Level Period
$T_M = 2.70$ sec.	Target Maximum Capable Period
Shear Modulus	
Large Strains	Small Strains
Ga = 500 kN/m2	Ga = 700 kN/m2
Gb = 1000 kN/m2	Gb = 1400 kN/m2
$\gamma_{max} = 1.50$	

Elastic Modulus

$E_c = 2000000$ kN/m2

It is assumed that the target design level period is 2.5sec, the target maximum capable period is 2.70sec and the target maximum shear strain is 1.5. It should be noted that it would be possible to use only a single bearing design, for this study, since the system is small.

6.6.1. Calculation of Lateral Stiffness

Design earthquake level stiffness

$$k_{D,min} = \frac{4\pi^2}{T_D^2}\frac{W}{g} = \frac{4\pi^2}{2.30^2}\frac{735.75}{9.81} = 559.7 kN/m, type-a$$

$$k_{D,min} = \frac{4\pi^2}{T_D^2}\frac{W}{g} = \frac{4\pi^2}{2.30^2}\frac{1471.5}{9.81} = 1119.4 kN/m, type-b$$

Maximum capable earthquake level stiffness

$$k_{M,min} = \frac{4\pi^2}{T_M^2}\frac{W}{g} = \frac{4\pi^2}{2.70^2}\frac{735.75}{9.81} = 406.2kN/m, type-a$$

$$k_{M,min} = \frac{4\pi^2}{T_M^2}\frac{W}{g} = \frac{4\pi^2}{2.70^2}\frac{1471.5}{9.81} = 812.3kN/m, type-b$$

where $k_{D,min}$ and $k_{M,min}$ are the minimum stiffness that correspond to the Design Based Earthquake and the Maximum Capable Earthquake response respectively, W is the weight of the building, g is gravity, and T_D and T_M are periods that correspond to the Design Based Earthquake and the Maximum Capable Earthquake responses respectively.

6.6.2 Calculation of Minimum Lateral Displacement dDmin and dMmin

According to the UBC-97;

$$d_D = \frac{gc_{VD}T_D}{B4\pi^2} = \frac{9.81\times0.64\times2.3}{1.35\times4\pi^2} = 0.270m$$

$$d_M = \frac{gc_{VM}T_M}{B4\pi^2} = \frac{9.81\times0.80\times2.7}{1.35\times4\pi^2} = 0.397m$$

The value d_D is minimum displacement value according to the TDY-98:

$$d_D = \frac{0.063}{B}A_0 g T_b^{0.8} T_D^{1.2}$$

where B is the reduction factor, A0 is the effective ground acceleration coefficient, and T_b is the spectrum characteristic period.

Assuming A_{0D}=0.40 and A_{0M}=0.50, according to the design level earthquake and the maximum capable earthquake, displacements are calculated.

$$d_D = \frac{0.063}{1.35} \times 0.40 \times 9.81 \times 0.40^{0.8} \times 2.30^{1.2} = 0.239\text{m}$$

$$d_M = \frac{0.063}{1.35} \times 0.50 \times 9.81 \times 0.40^{0.8} \times 2.70^{1.2} = 0.362\text{m}$$

It is noted that the Turkish code TDY-98 gives slightly smaller results.

6.6.3. Estimation of Disc Diameter, D

$$t\gamma_{max}=d_D$$

$$t = \frac{d_D}{\gamma_{max}} = \frac{0.27}{1.5} = 0.18\text{cm}$$

where t is the thickness of the isolator pad and $\gamma_{max} = 1.50$ and t = 20cm can be used.

$$k_D = \frac{AG}{t} \Rightarrow A = \frac{K_D t}{G}$$

$$A_a = \frac{k_D t}{G} = \frac{597.7 \times 0.20}{500} = 0.2245\text{m}^2, \text{type} - \text{a}$$

$$D_a = \sqrt{\frac{4A}{\pi}} = \sqrt{\frac{4 \times 0.224}{\pi}} = 0.53\text{m}, \text{type} - \text{a}$$

$$\Phi_a = 0.55\text{m}$$

$$A_b = \frac{k_D t}{G} = \frac{1119.4 \times 0.20}{1000} = 0.224\text{m}^2, \text{type} - \text{b}$$

$$D_b = \sqrt{\frac{4A}{\pi}} = \sqrt{\frac{4 \times 0.224}{\pi}} = 0.53\text{m}, \text{type} - \text{b}$$

$$\Phi_b = 0.55m$$

According to equation 5.10, A and D are calculated and they are the area and the diameter of the disc respectively and G is the shear modulus at large strains.

$$A_a = A_b = \frac{\pi D^2}{4} = \frac{\pi 0.55^2}{4} = 0.238m^2$$

6.6.4 Base Shear of the Isolated Building

According to the chosen height and the diameter of the bearing, stiffness for elements are calculated.

$$k_D = \frac{AG}{t} = \frac{0.238 \times 500}{0.2} = 595kN/m, type-a$$

$$k_D = \frac{AG}{t} = \frac{0.238 \times 1000}{0.2} = 1190kN/m, type-b$$

Stiffness for the frame is;

$$\Sigma k_D = 2 \times 595 + 1190 = 2380 \text{ kN/m}$$

If the period is checked;

$$T_D = 2\pi\sqrt{\frac{W}{k_D g}} = 2\pi\sqrt{\frac{2943}{2380 \times 9.81}} = 2.23 \sec.$$

It is seen that the value of 2.23sec. is close to 2.30 sec. which has been chosen at the beginning of the design. The base shear V_D is calculated as follows and devided by the reduction factor.

$$V_D = \Sigma k_D \times d_D = 2380 \times 0.27 = 642.6 \text{ kN}$$

$$V_{SD} = \frac{V_D}{R_i} = \frac{642.6}{2} = 321.3kN$$

Fixed-based shear is determined with $T_D = 2.23$ sec.

$$V_{fixed} = \frac{c_V I}{RT_D} W \geq 0.11 c_a IW$$

$$V_{fixed} = \frac{0.64 \times 1}{8 \times 2.23} 2943 = 105.6kN$$

The value of 142.4kN governs! If it is checked;

$$V_{fixed} = 0.11 c_a IW = 0.11 \times 0.44 \times 1 \times 2943 = 142.4kN$$

$$V_{SD}=321.3 > 142.4kN$$

6.6.5 Vertical Stiffness

For compressive stresses under vertical loads, the isolators undergo relatively smaller shear strains on the order of $\gamma = 0.20$ Therefore, Ga=700kN and Gb=1400kN are used.

S is the shape factor of rubber layers, to. to should be between D/40 and D/80. $E_{eff.v}$ is effective vertical modulus of the isolators and Ec is composite compression modulus of the isolators.

$$t_o = \frac{0.55}{40} = 0.01375m$$

$$S = \frac{D}{4t_o} = \frac{0.55}{4 \times 0.013} = 10.58$$

$$E_c = 2 \times 10^6 \text{ kN/m}^2$$

$$E_{eff.v} = \frac{6GS^2E_c}{6GS^2 + E_c}$$

$$E_{eff,v} = \frac{6 \times 700 \times 10.58^2 \times 2 \times 10^6}{6 \times 700 \times 10.58^2 + 2 \times 10^6} = 380654 \text{kN/m}^2, \text{type} - \text{a}$$

$$E_{eff,v} = \frac{6 \times 1400 \times 10.58^2 \times 2 \times 10^6}{6 \times 1400 \times 10.58^2 + 2 \times 10^6} = 639579 \text{kN/m}^2, \text{type} - \text{b}$$

Vertical stiffness for the full plane frame taking into account of the composite action of type-a and type-b isolators;

$$\sum k_V = \frac{[2 \times 380654 + 639579] \times 0.238}{0.20} = 1667055 \text{kN/m}$$

According to Equation 5.19 Vertical Displacement Δt wil be as follows;

$$\Delta t = \frac{Wt}{AE_{eff}} = \frac{W}{k_V} = \frac{2943}{1667055} = 0.00177\text{m} = 1.77\text{mm}$$

Using Equations 5.19 and 5.20, T_v will be as follows

$$\frac{T_h}{T_v} = \sqrt{6}S = \sqrt{6} \times 10.58 = 25.9$$

$$T_v = \frac{T_h}{25.9} = 0.086 \text{sec.}$$

6.6.6. Shear Strains and Vertical Load

Shear strain due to vertical load is calculated.

$$\varepsilon_z = \frac{\Delta t}{t} = \frac{0.00177}{0.20} = 0.0089$$

$$\gamma_v = 6 \times 10.58 \times 0.0089 = 0.565$$

A' Common Area

$$A' = A\left[1 - \frac{2}{\pi}(\theta + \sin\theta\cos\theta)\right]$$

$$\sin\theta = \frac{d_D}{D} = \frac{0.27}{0.55} = 0.4909 \Rightarrow \theta = 29.40^\circ \ldots\ldots \cos\theta = 0.8712$$

$$A' = 0.238\left[1 - \frac{2}{\pi}(0.5131 + 0.4909 \times 0.8712)\right] = 0.0955 m^2$$

Max Load;

$W_a = A'GS\gamma v = 0.0955 \times 700 \times 10.58 \times 0.565 = 400kN < 735.75kN$

$W_b = A'GS\gamma v = 0.0955 \times 1400 \times 10.58 \times 0.565 = 800kN < 1471.5kN$ No Good!

Shear strain due to lateral load is calculated;

$$\gamma_s = \frac{\tau}{G} = \frac{V_D}{AG} = \frac{k_D d_D}{AG_a}$$

$$\gamma_s = \frac{595 \times 0.27}{0.238 \times 500} = 1.35, \text{type} - a$$

$$\gamma_s = \frac{1190 \times 0.27}{0.238 \times 1000} = 1.35, \text{type} - b$$

Max shear strain will be;

$$\gamma_{max} = \gamma_s + \gamma_v = 1.35 + 0.565 = 1.915$$

6.6.7. Calculation of Buckling Load

Buckling load for the isolators is;

$$P_{cr} = \sqrt{\frac{AG\pi^2 EI}{3t^2}} = \sqrt{\frac{0.238 \times 500 \times \pi^2 \times 347000 \times \pi \times 0.270^4 \times 0.25}{3 \times 0.20^2}}$$

where E is the effective compressive modulus in Equation 6.19.

$$P_{cr} = 3765\text{kN} > 735.75\text{kN}, \text{good!}$$

6.6.8. Lead Plug Design

Firstly, plug diameter is selected;

$$d_1 \leq \frac{t}{1.5} = \frac{0.20}{1.5} = 0.133\text{m}$$

dl = 0.20m can used and lead plug area is

$$A_{lead} = \frac{\pi d_1^2}{4} = \frac{\pi \times 0.2^2}{4} = 0.031\text{m}^2$$

Yield force Q_y first estimation is made in Equation 6.20 where τ_y is yield stress.

$$Q_y = \tau_y A_{lead} = 10500 \times 0.031 = 326\text{kN}$$

Alternate method to determine Q_y is written in Equation 6.21

$$A_{loop} = 4Q_y(d_D - d_y) \cong 4Q_y d_D \Rightarrow Q_y \cong \frac{A_{loop}}{4d_D}$$

By definition,

$$\beta = \frac{A_1}{2\pi k_D d_D^2} = 0.15, \text{given}$$

$$k_D = \frac{4\pi^2}{T_M^2}\frac{W}{g} = \frac{4\pi^2}{2.23^2}\frac{2943}{9.81} = 5311 kN/m$$

$$d_D = 0.27m$$

$$A_{loop} = \beta\left[2\pi k_D d_D^2\right] = 0.15 \times 2\pi \times 5.311 \times 0.27^2 = 365$$

$$Q_y \cong \frac{365}{4 \times 0.27} \cong 338kN$$

Elasto-plastic Stiffness k2 of Rubber is calculated assuming $k_1 = 10k_2$.

$$k_{eff} = \frac{Q_y}{d_D} + k_2 \Rightarrow k_2 = k_{eff} - \frac{Q_y}{d_D} = 5311 - \frac{338}{0.27} = 4059 kN/m$$

$$d_y = \frac{Q_y}{k_1 - k_2} = \frac{Q_y}{k_2\left(\frac{k_1}{k_2} - 1\right)} = \frac{338}{4059 \times 9} = 0.0093m$$

$$A_{lead} = \frac{Q_y}{\tau_y} = \frac{338}{10500} = 0.0322m^2 \Rightarrow \phi_{lead} = \sqrt{\frac{4 \times 0.322}{\pi}} = 0.20m$$

$\Phi = 0.20$m. can be used.

$$V_d = Q_y\left(1-\frac{k_2}{k_1}\right)+k_2 d_D = 338(1-0.1)+4059(0.27)^2 = 600kN$$

6.7. The Calculation of Equivalent Static Forces

In order to calculate the equivalent static earthquake forces over the structure, Turkish Earthquake Code is followed.

6.7.1. Isolated Structure

$V_{sd} = 321.3kN$

Force loaded to each storey is F = 321.3 / 4 = 80.33kN

6.7.2. Fixed-based Structure

T1 = 0.575sec.

A(T) = Ao I S(T)

where A(T) is the spectral acceleration coefficient, Ao is effective ground acceleration coefficient, I is building importance factor, and S(T) is spectral design acceleration Spectra.

$A_o = 0.4$ determined by looking at the Seismic Zone1 from TDY-98, Table 6.2 I = 1 Assuming that the structure is residential building, the value is read from TDY-98, Table 6.3.

T_A = 0.15sec. T_B = 0.40sec. According to local site class Z_2 from TDY-Table 6.4 spectrum characteristic periods are obtained.

S(T) = 2.5(TB/T)0.8 = 2.5(0.40/0.575)0.8 = 1.87

A(T) = 0.4×1×1.87 = 0.748

Total equivalent seismic load:

$Vt = W\ A(T1) / Ra(T1) \geq 0.10\ Ao\ I\ W$

$T > TA \Rightarrow Ra(T1) = 8$

$Vt = 2943 \times 0.748 / 8 = 275.2$ kN

$0.10\ Ao\ I\ W = 0.10 \times 0.40 \times 1 \times 2943 = 117.72$kN

117.72kN < 275.2kN

Table 6.1. Calculation of the Forces Acting at Floor Levels

Story	W_i (kN)	H_i (m)	W_iH_i	$Vt/\Sigma W_iH_i$	$F_i=V_iH_iVt/\Sigma W_iH_i$ (kN)
4	735.75	12	8829.00	0.01246	110.08
3	735.75	9	6621.75	0.01246	82.56
2	735.75	6	4414.50	0.01246	55.04
1	735.75	3	2207.25	0.01246	27.52

6.7.3. Structure with Viscodampers

$T1 = 0.474$sec.

$A(T) = Ao\ I\ S(T)$

where A(T) is the spectral acceleration coefficient, A_o is effective ground acceleration coefficient, I is building importance factor, and S(T) is spectral design acceleration Spectra.

$Ao = 0.4$ determined by looking at the Seismic Zone1 from TDY-98, Table 6.2 $I = 1$ Assuming that the structure is residential building, the value is read from TDY-98, Table 6.3.

$T_A = 0.15$sec. $T_B = 0.40$sec. According to local site class Z_2 from TDY-Table 6.4 spectrum characteristic periods are obtained.

$S(T) = 2.5(TB/T)0.8 = 2.5(0.40/0.474)0.8 = 2.18$

$A(T) = 0.4 \times 1 \times 2.18 = 0.872$

Total equivalent seismic load:

$Vt = W\ A(T1) / Ra(T1) \geq 0.10\ Ao\ I\ W$

$T > TA \Rightarrow Ra(T1) = 8$

$Vt = 2943 \times 0.872 / 8 = 320.79$ kN

$0.10\ Ao\ I\ W = 0.10 \times 0.40 \times 1 \times 2943 = 117.72$kN

$117.72\text{kN} < 320.79\text{kN}$

Table 6.2. Calculation of the forces acting at floor levels

Story	W_i (kN)	H_i (m)	W_iH_i	$Vt/\Sigma W_iH_i$	$F_i=V_iH_iVt/\Sigma W_iH_i$ (kN)
4	735.75	12	8829.00	0.01453	128.31
3	735.75	9	6621.75	0.014533	96.24
2	735.75	6	4414.50	0.014533	64.16
1	735.75	3	2207.25	0.014533	32.08

Lateral sway at each story, bending moment values at the top of the columns, and story drift ratios are graphically illustrated on fixed-based, base-isolated, viscodamped, and viscodamped and isolated structures as shown in Figure 6.7 through 6.10.

In addition, top displacement time histories and top column upper part moment time histories are shown comparatively in Figures 6.11 through 6.14.

6.8. Comments About UBC-97 Requirements

The large minimum displacements imposed by the UBC-97 requirements make the designing and implementation of a seismic isolation for this building extremely difficult. UBC-97 requirements are so harsh and stringent. For instance, to assume reduction factor as 2 in the design of base-isolated structures is an injustice compared with design of principal used for fixed-based structures in which R=8.

The design example highlights the UBC-97 inherent bias in the performance requirements for fixed-based versus isolated structures. While fixed-based buildings are

routinely designed to a life safety objective, isolated buildings are expected to perform with uninterrupted operation during and immediate occupancy after the design earthquake. The code does not allow seismically isolated structures the same limited life safety objectives accorded to fixed-based buildings. Given the fact that seismic-isolated structures, even when they fail, provide a much more enhanced protection of life and limb for their occupants compared to their fixed-base counterparts, restriction of isolated designs to immediate occupancy objectives is not reasonable and must be changed.

6.9. Effects of Earthquake Predominant Period on the Performances of Buildings

Buildings have performed well under low predominant period, which means on stiff soils or rocky ground. On the other hand, soft surface material has behaved similarly to jelly on shaking table and can cause considerable amplification of the ground motion.

Earthquake-A has a peak ground acceleration of 0.4g and has a predominant period of 0.13sec. Earthquake-B has a peak ground acceleration of 0.4g and has a predominant period of 1.43sec. This is obtained by changing equal time intervals Δt. When Δt is increased, the predominant period is increased presenting the weak soil case. When Δt is decreased, the predominant period is lowered presenting the stiff soil case. Also, all the ground acceleration values multiplied by a scale factor to obtain peak ground acceleration as 0.4g.

It is seen that higher moment, displacement and drift ratio values are obtained when the models are conducted with the time history analysis which has higher predominant period. On the other hand, it is observed that lower moment, displacement and drift ratio values are obtained when the models are conducted with the time history analysis which has lower predominant period.

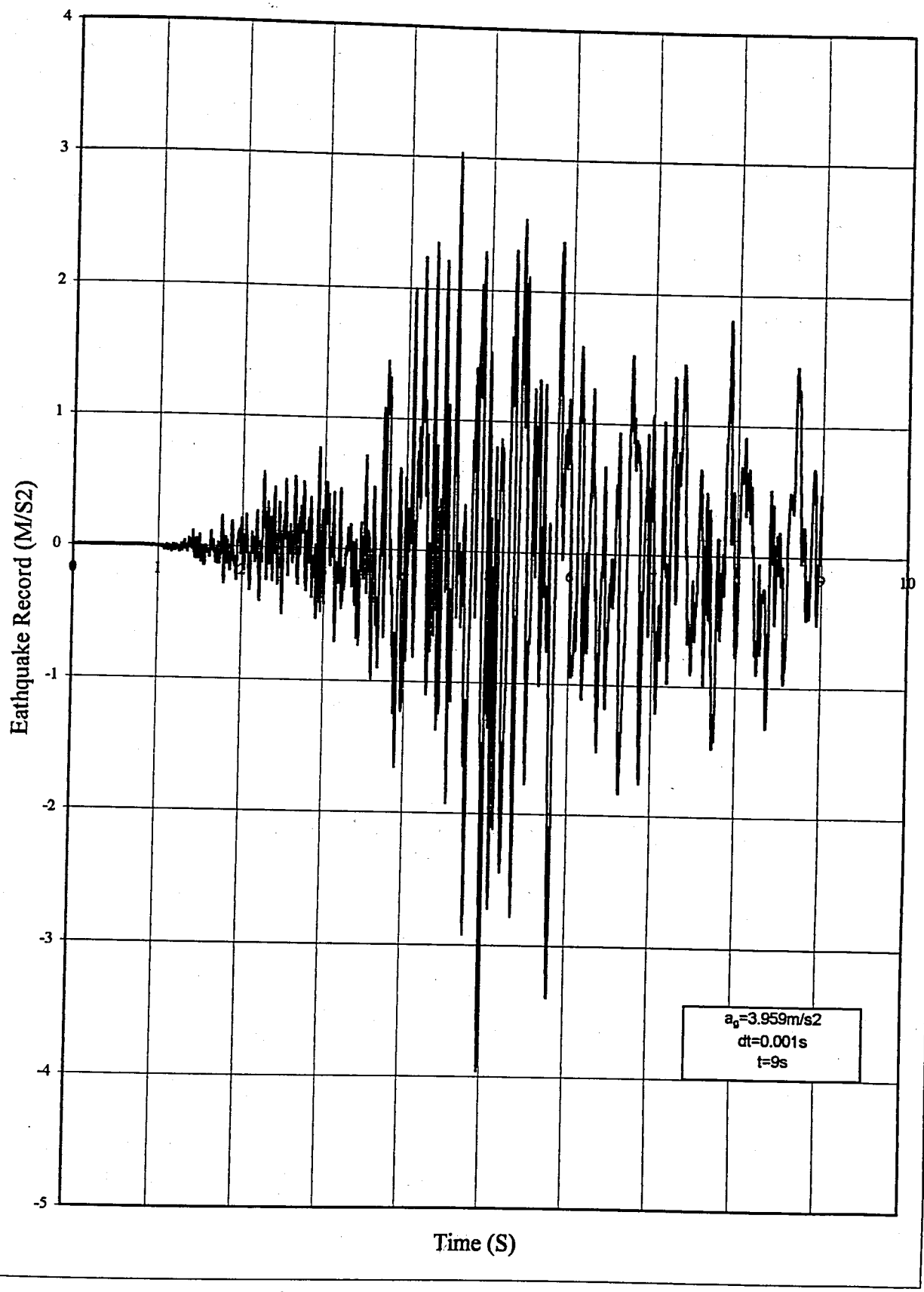

FIGURE 6.1 Record of Eathquake-A

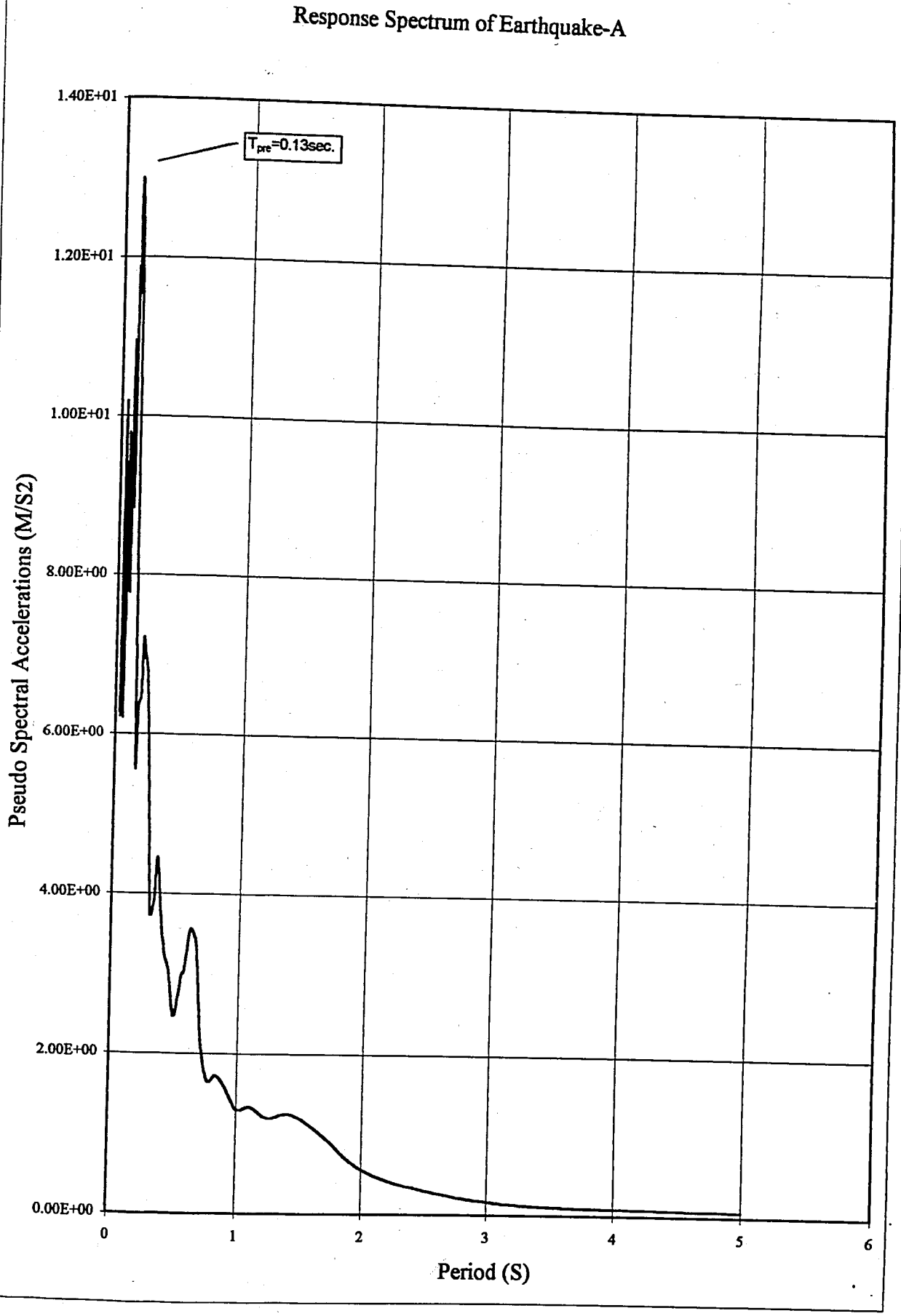

FIGURE 6.2 Response Spectrum of Earthquake-A

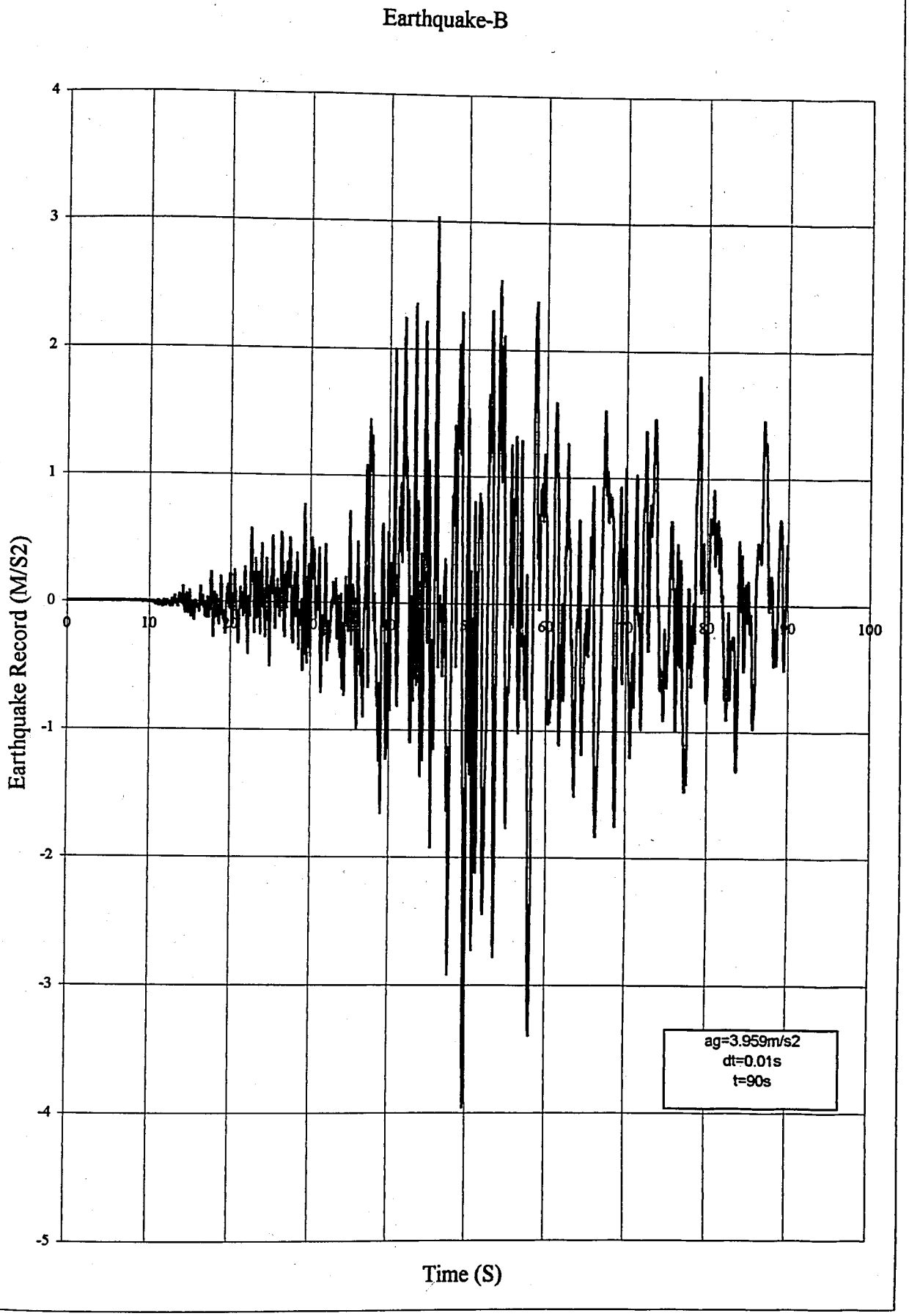

FIGURE 6.3 Record of Earthquake-B

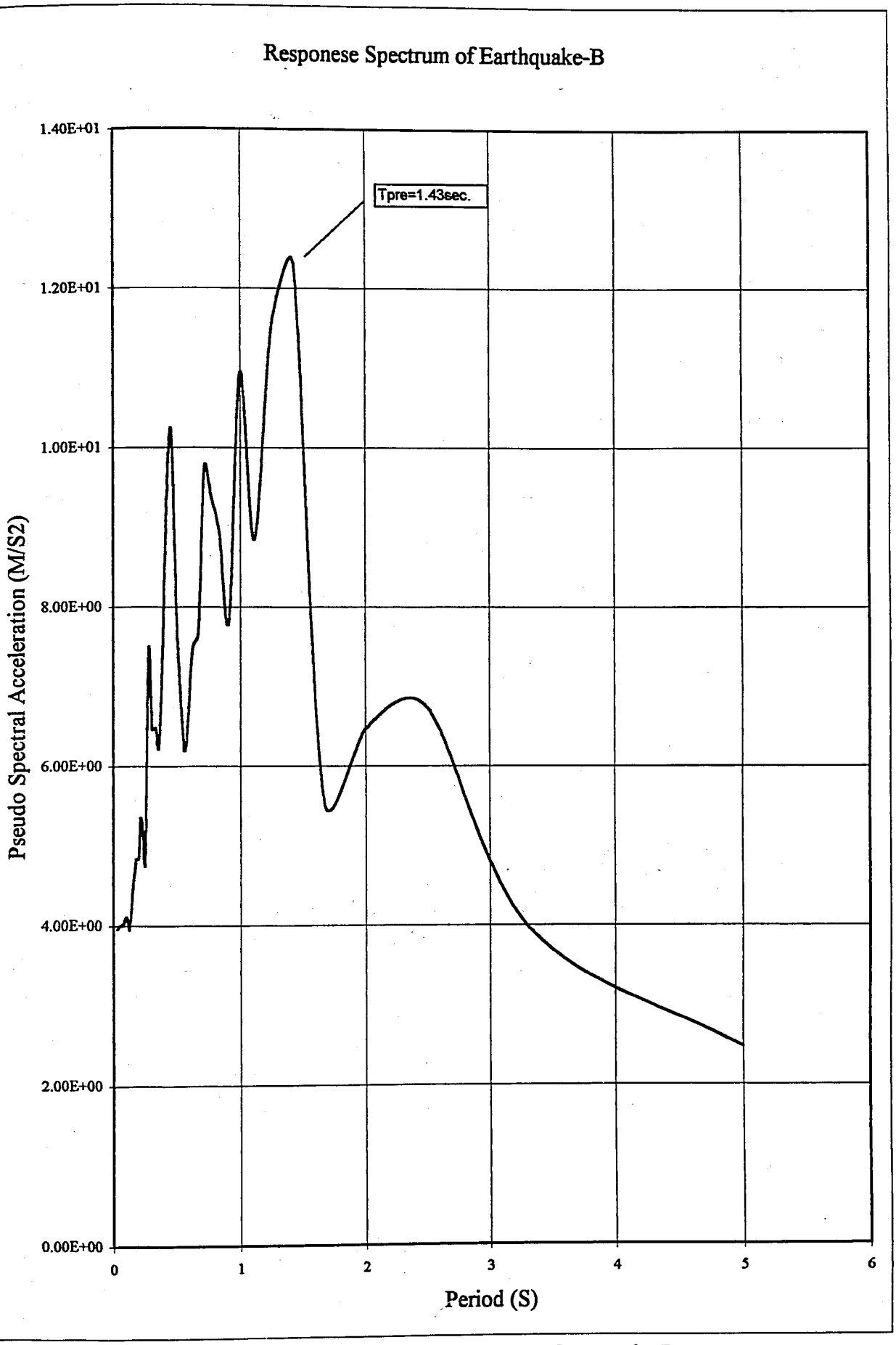

FIGURE 6.4 Response Spectrum of Eartquake-B

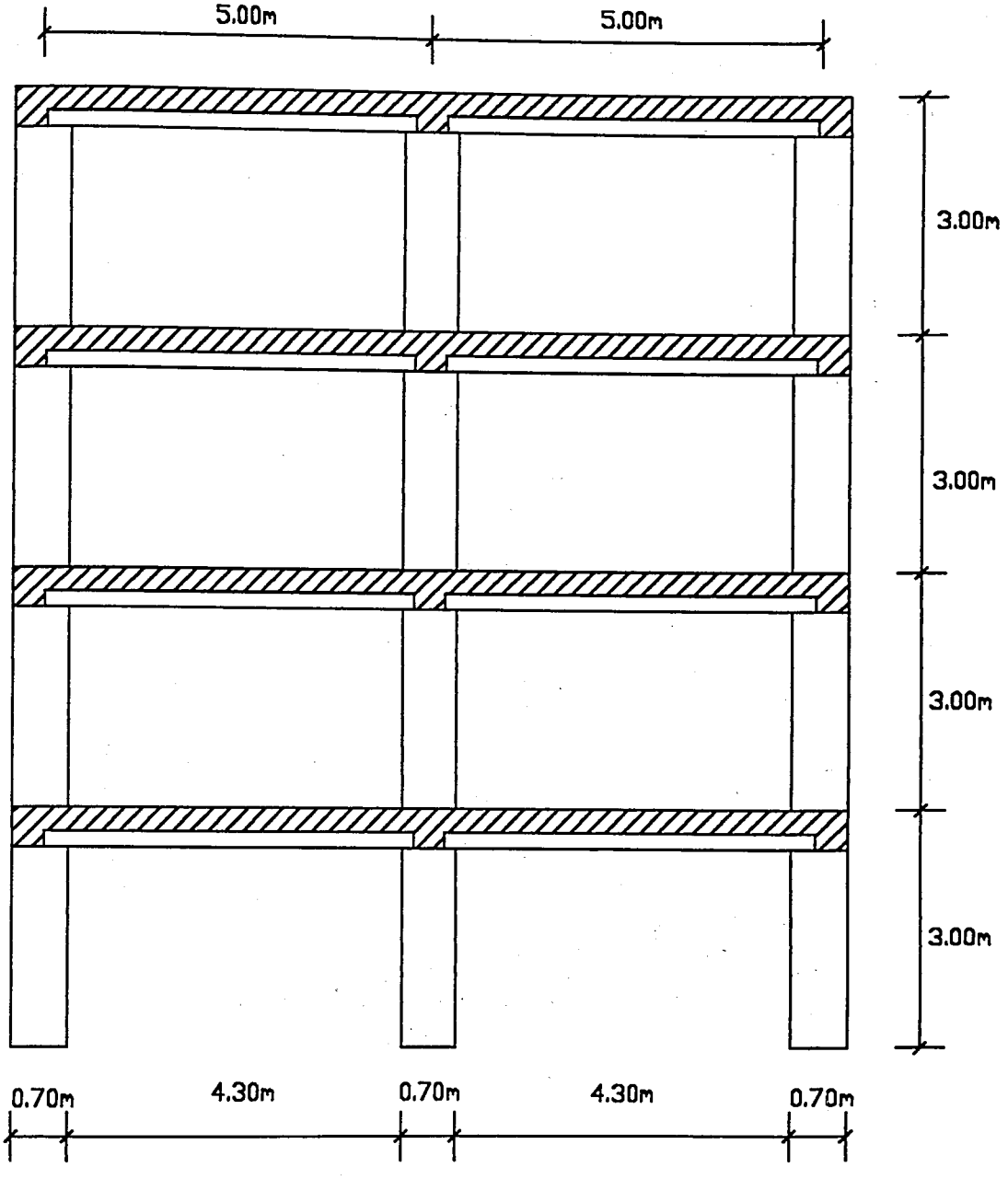

FIGURE 6.5 The Fixed-base Case

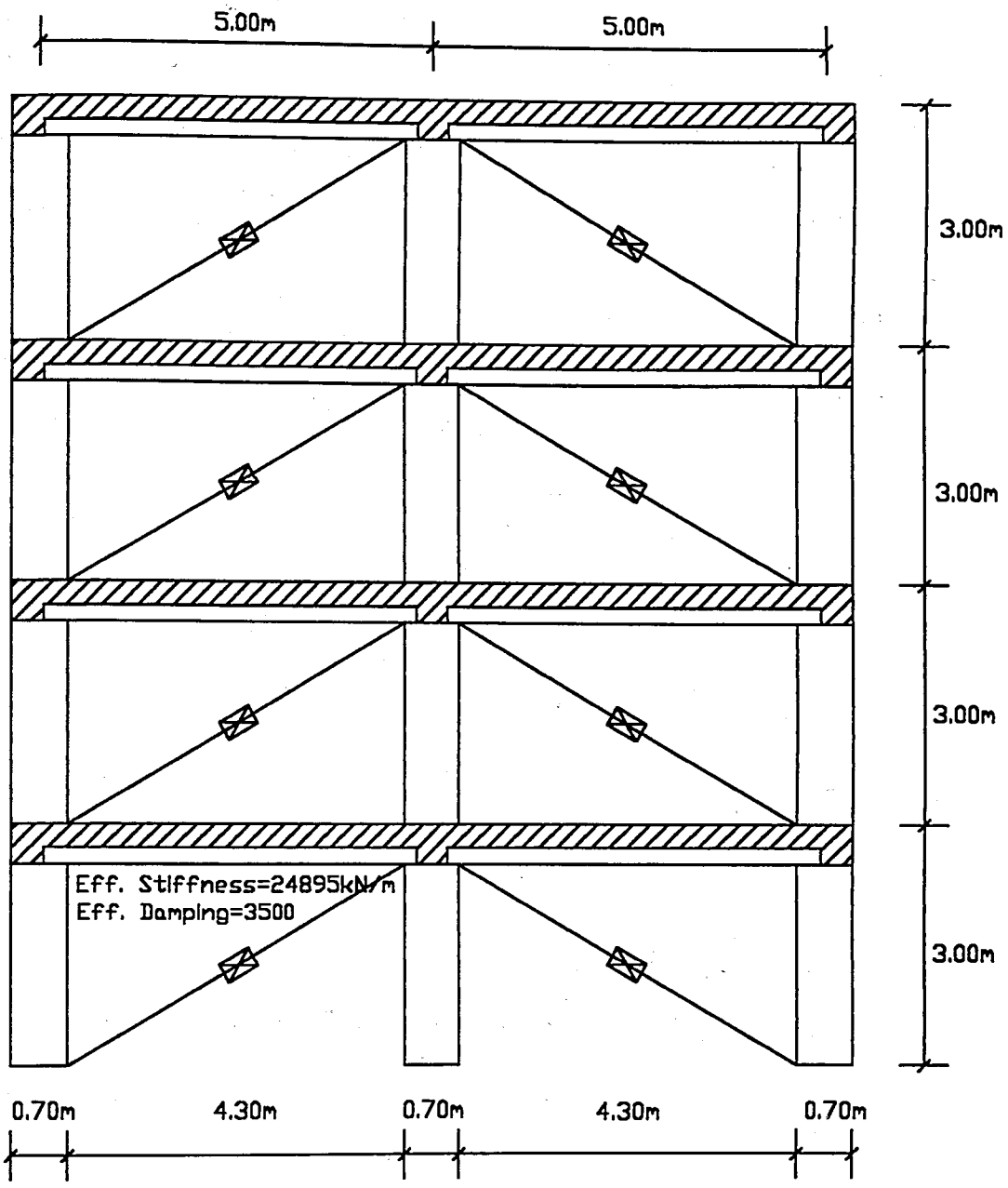

FIGURE 6.6 The Viscodampers Case

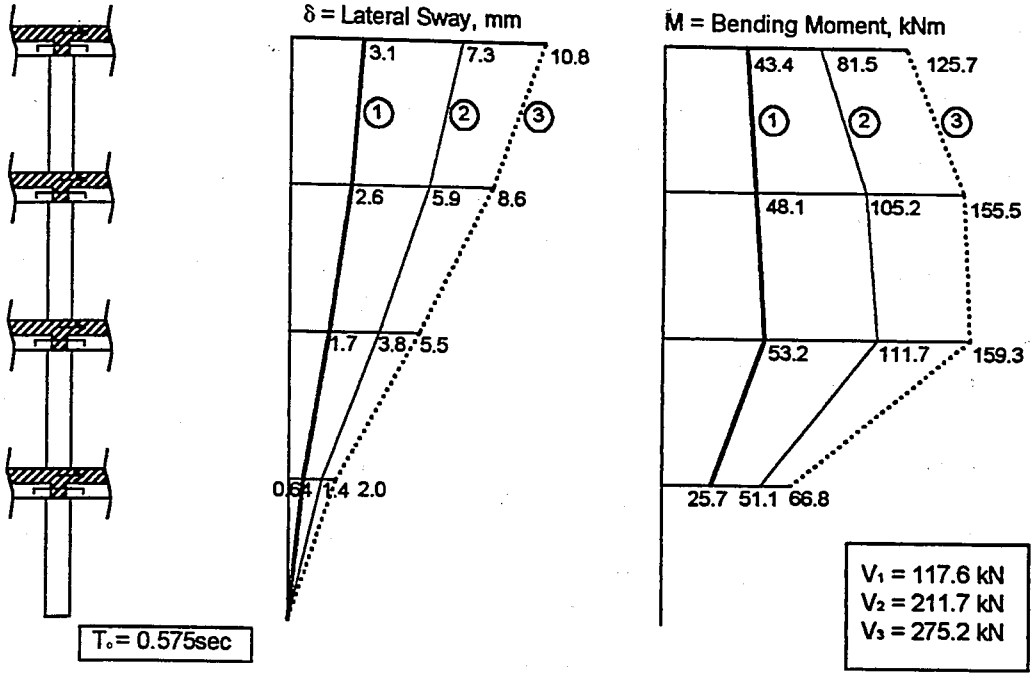

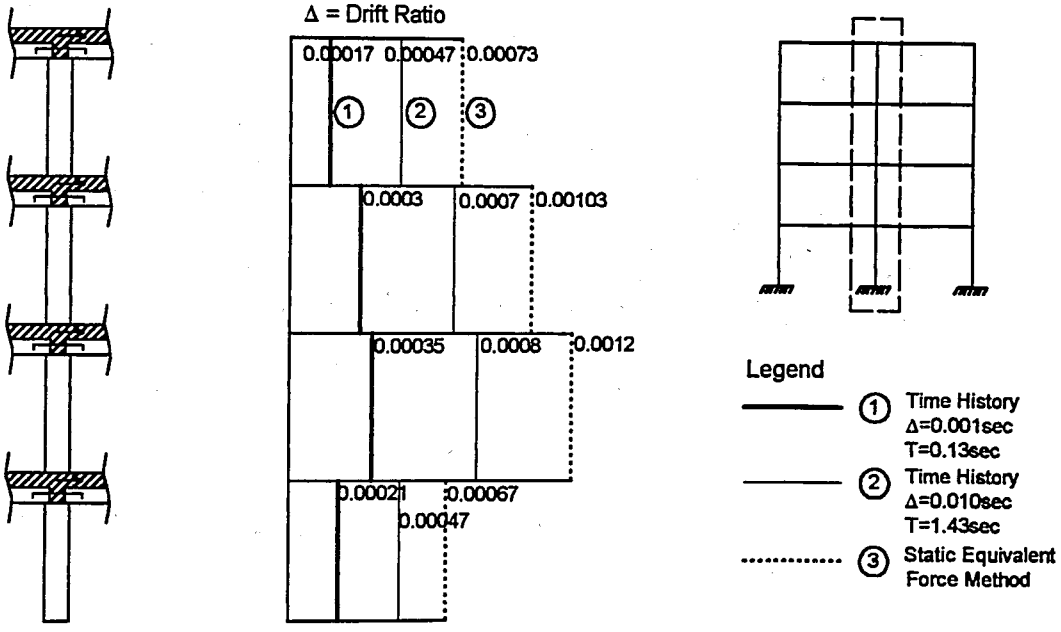

FIGURE 6.7 Response of Fixed-base Case

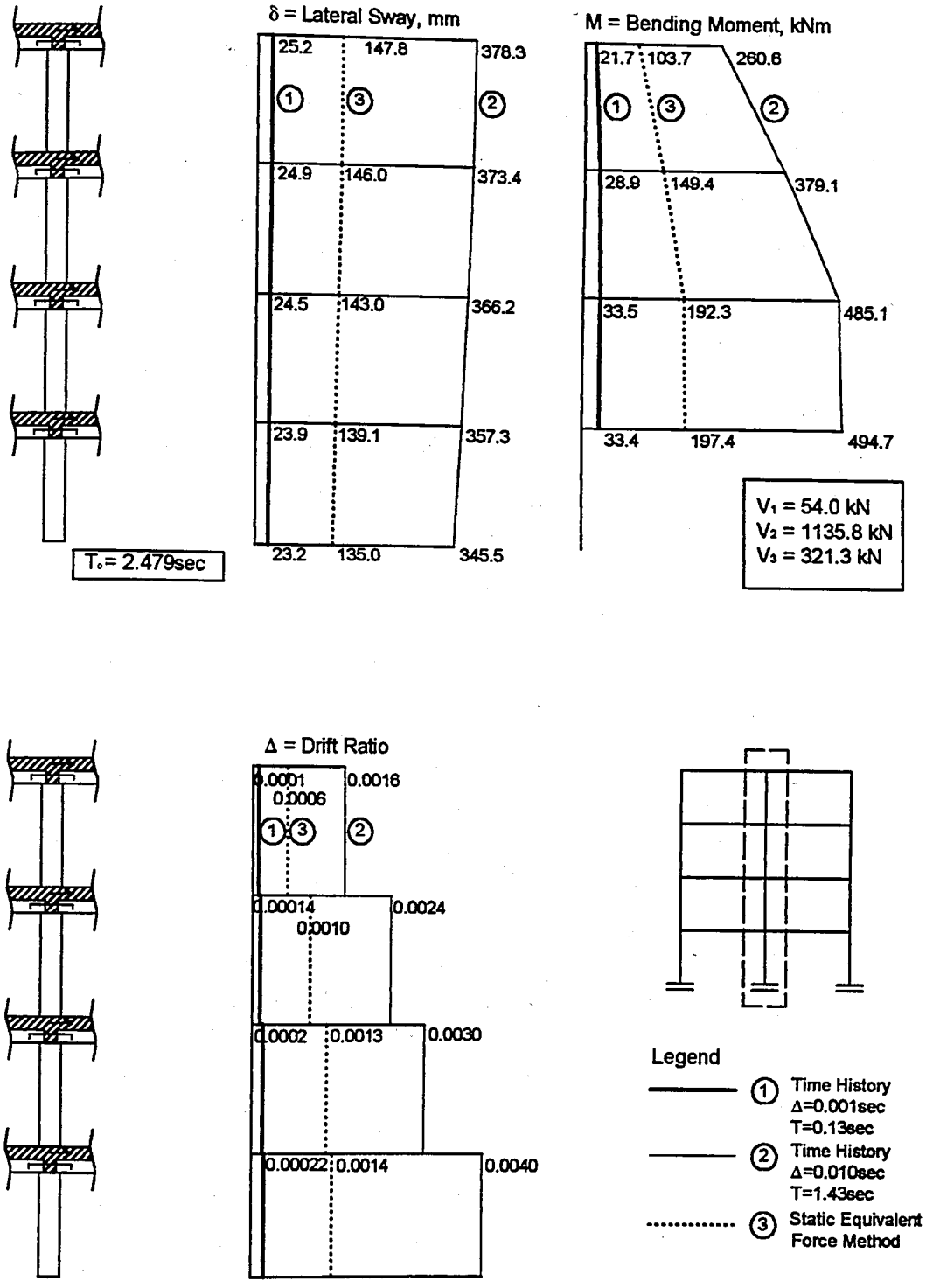

FIGURE 6.8 Response of the Rubber Base-isolated Case

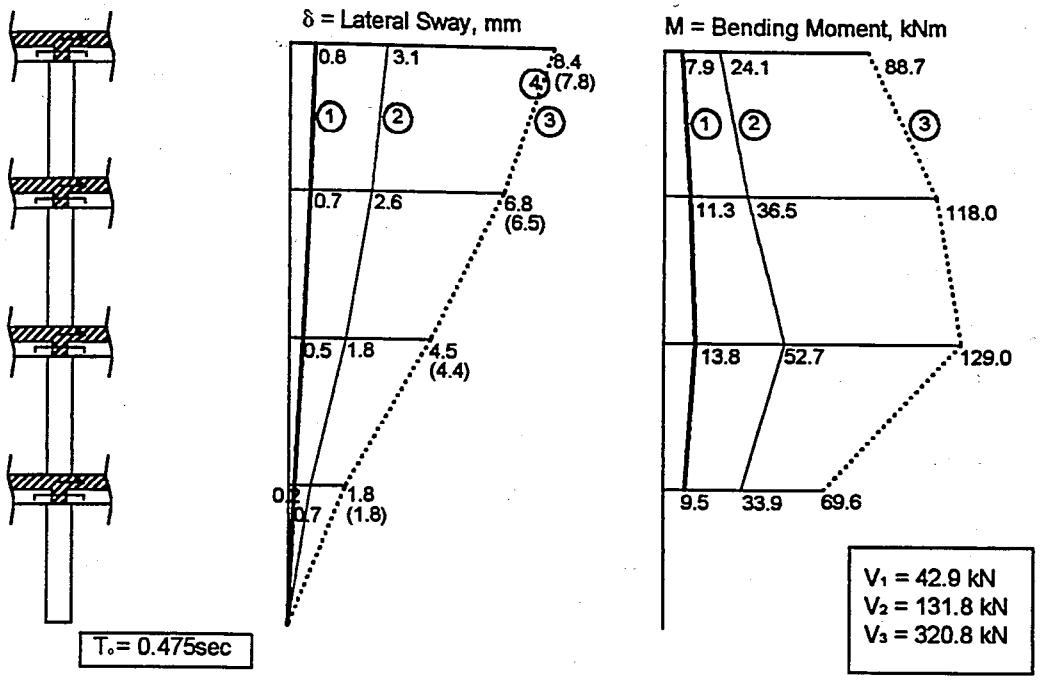

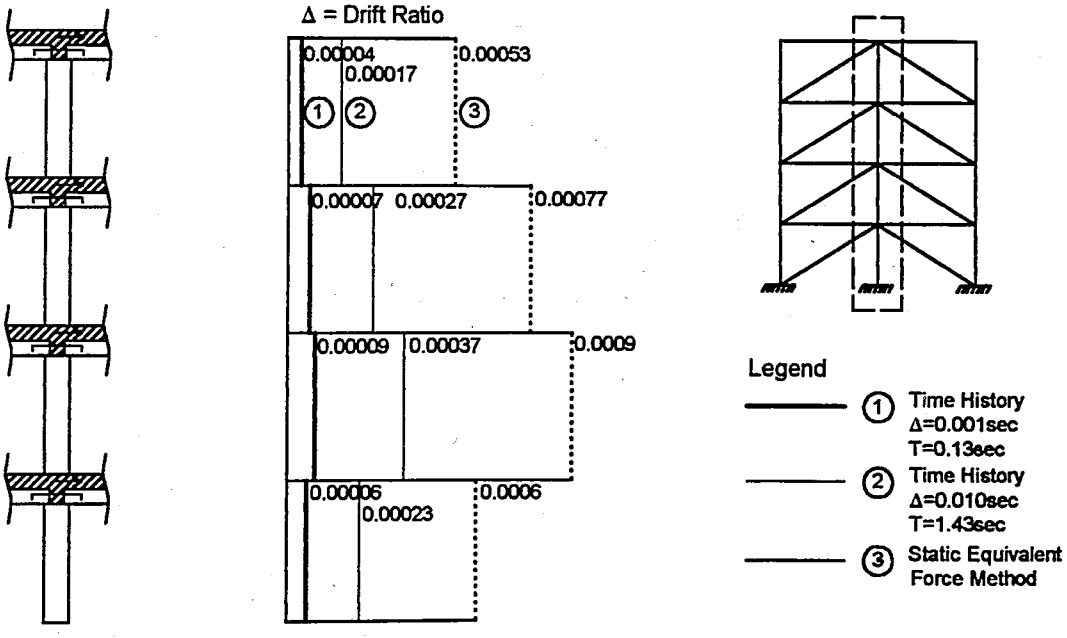

FIGURE 6.9 Response of the Viscodampers Case

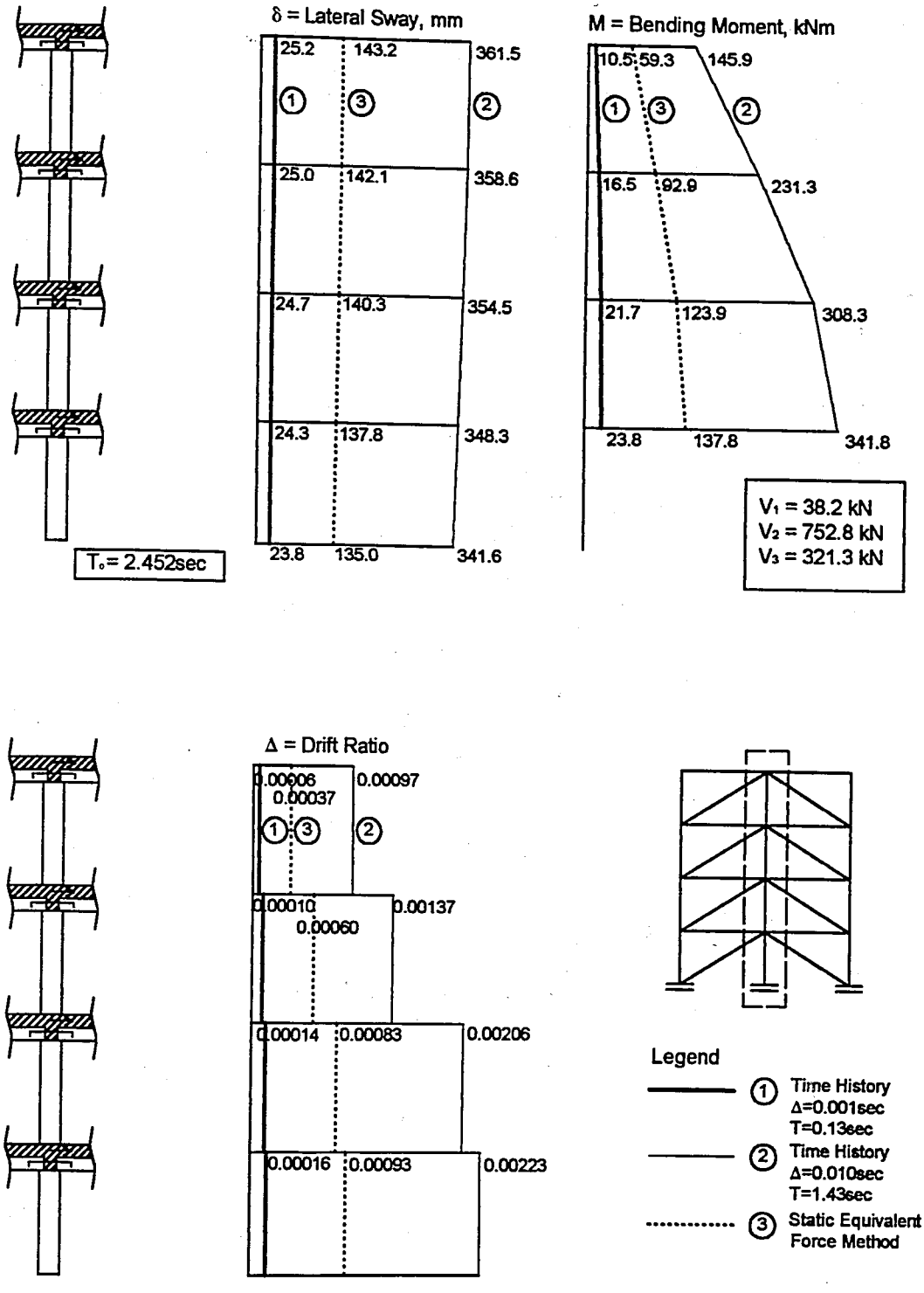

Figure 6.10. Response of the Rubber Base Isolation combined with Viscoelastic Dampers Case

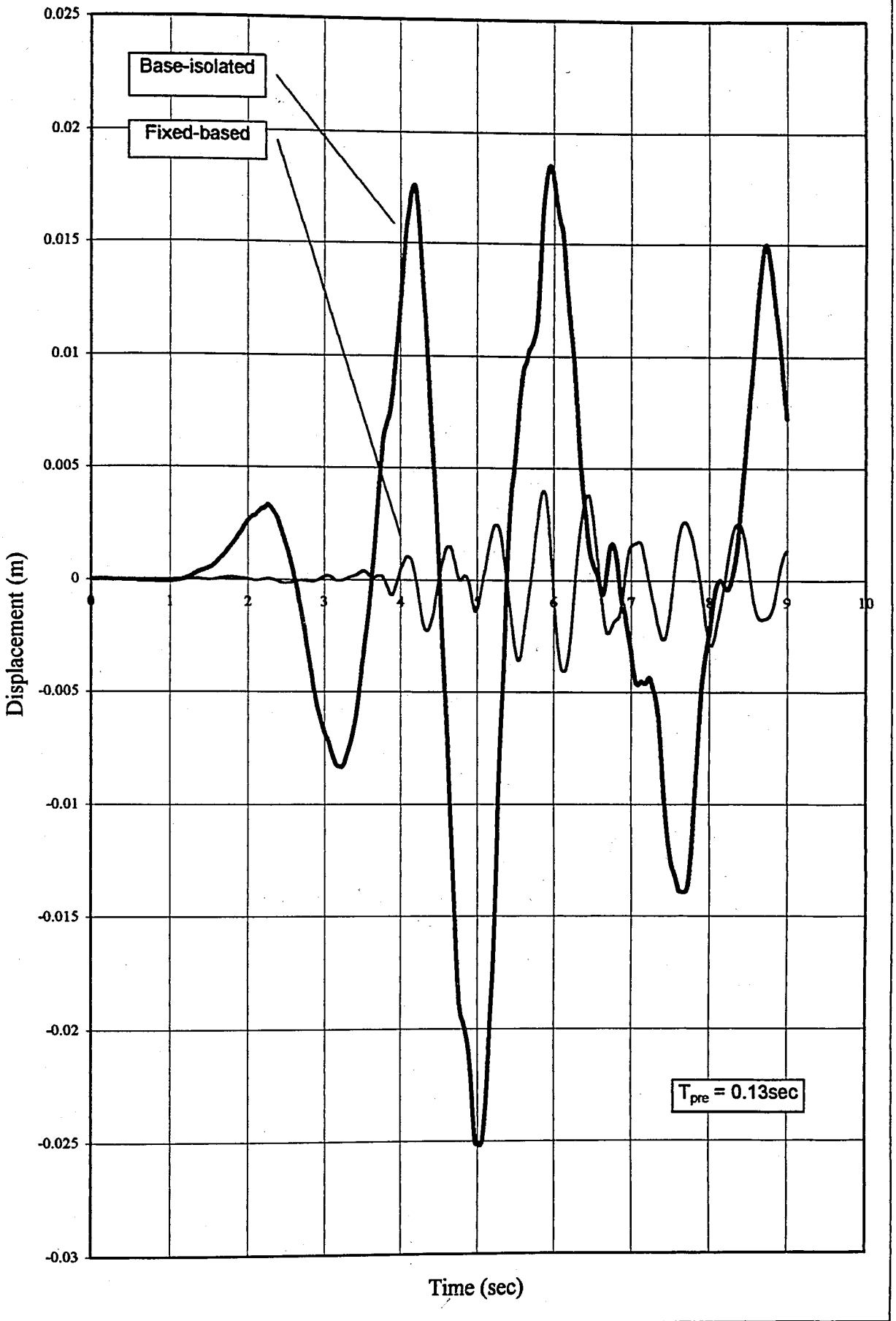

Figure 6.11. Top displacement time histories of the Fixed-based and the Base-isolated Cases

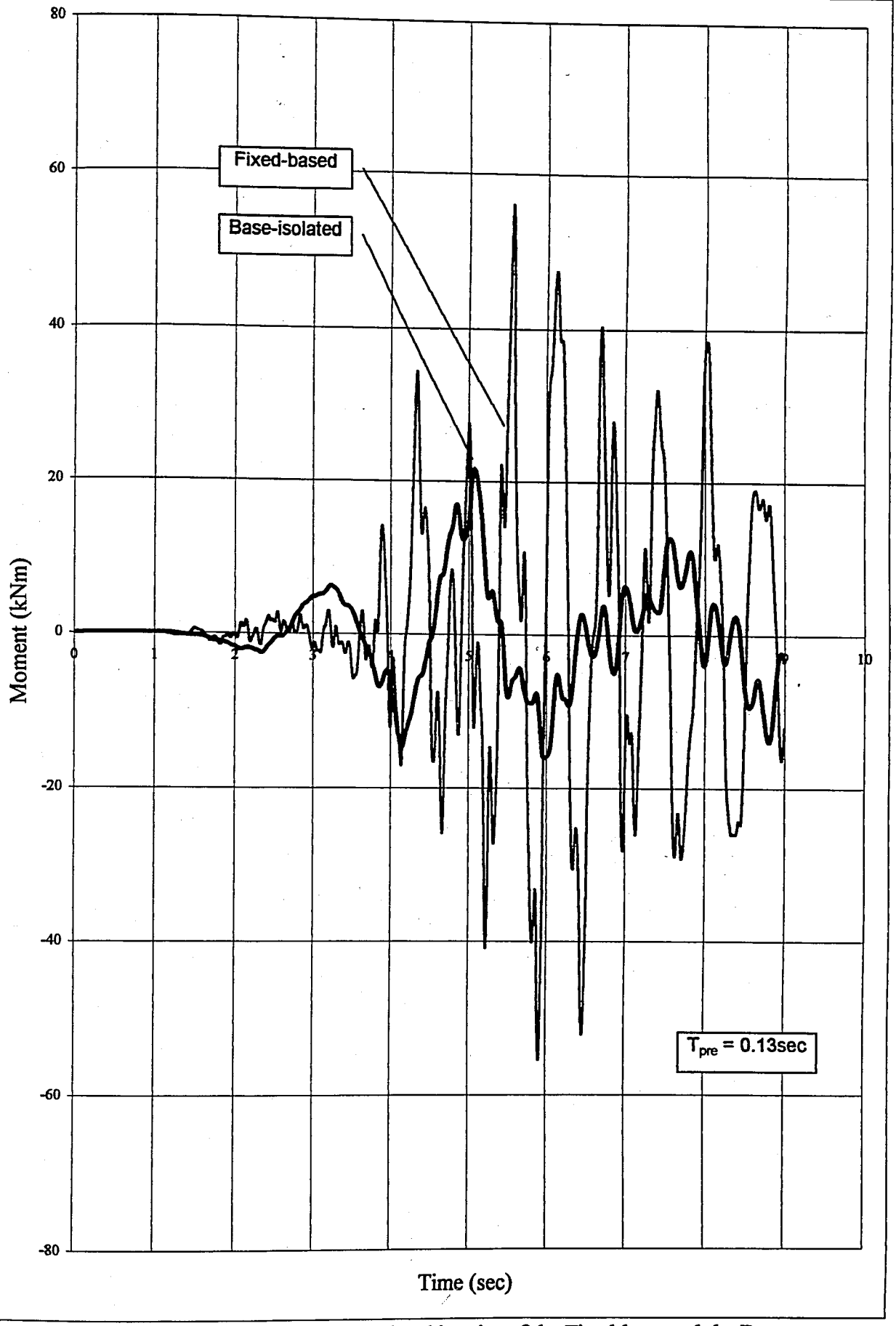

Figure 6.12. Top column upper part time histories of the Fixed-base and the Base-isolated Cases

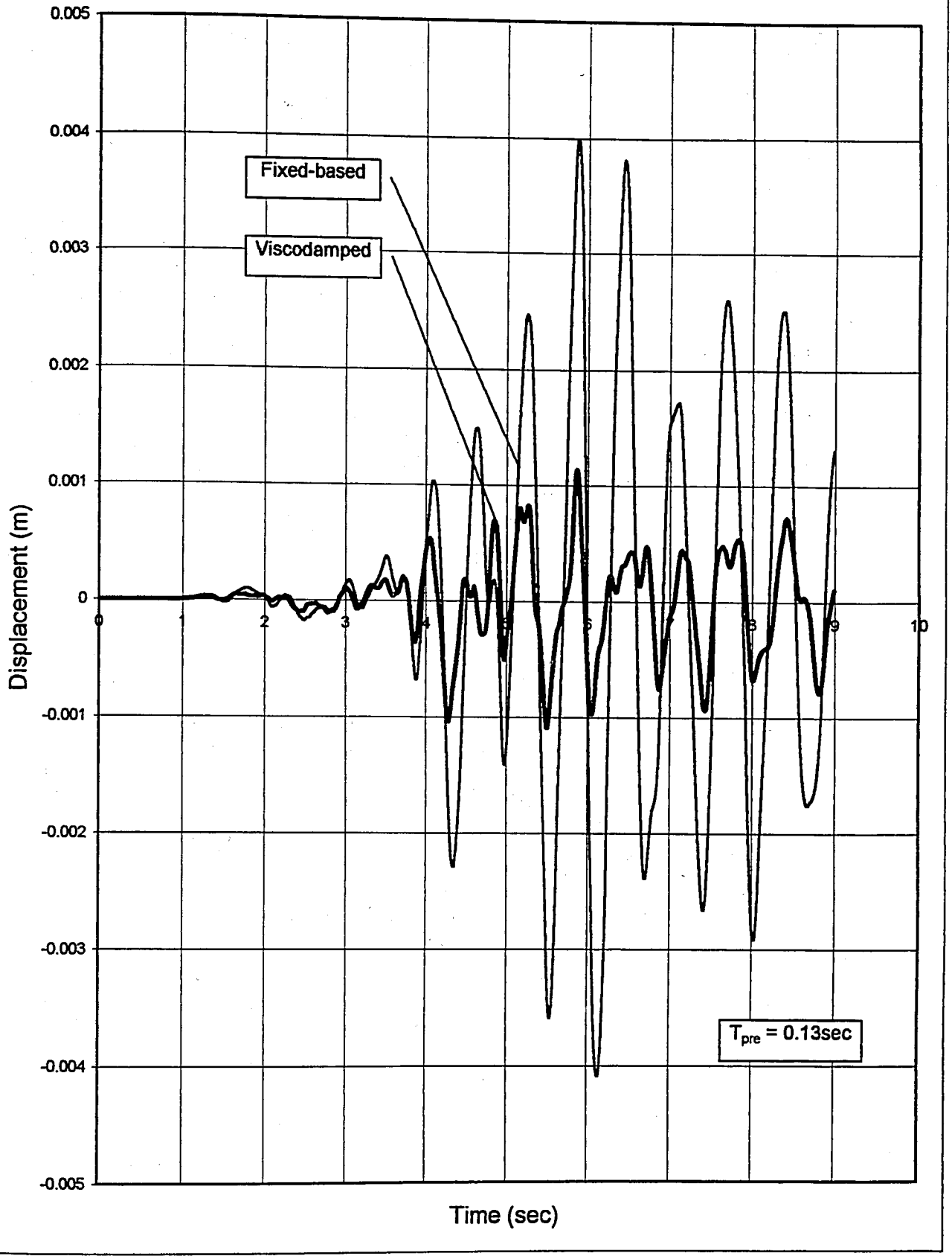

Figure 6.13. Top displacement time histories of the Fixed-base and the Viscodampers Cases

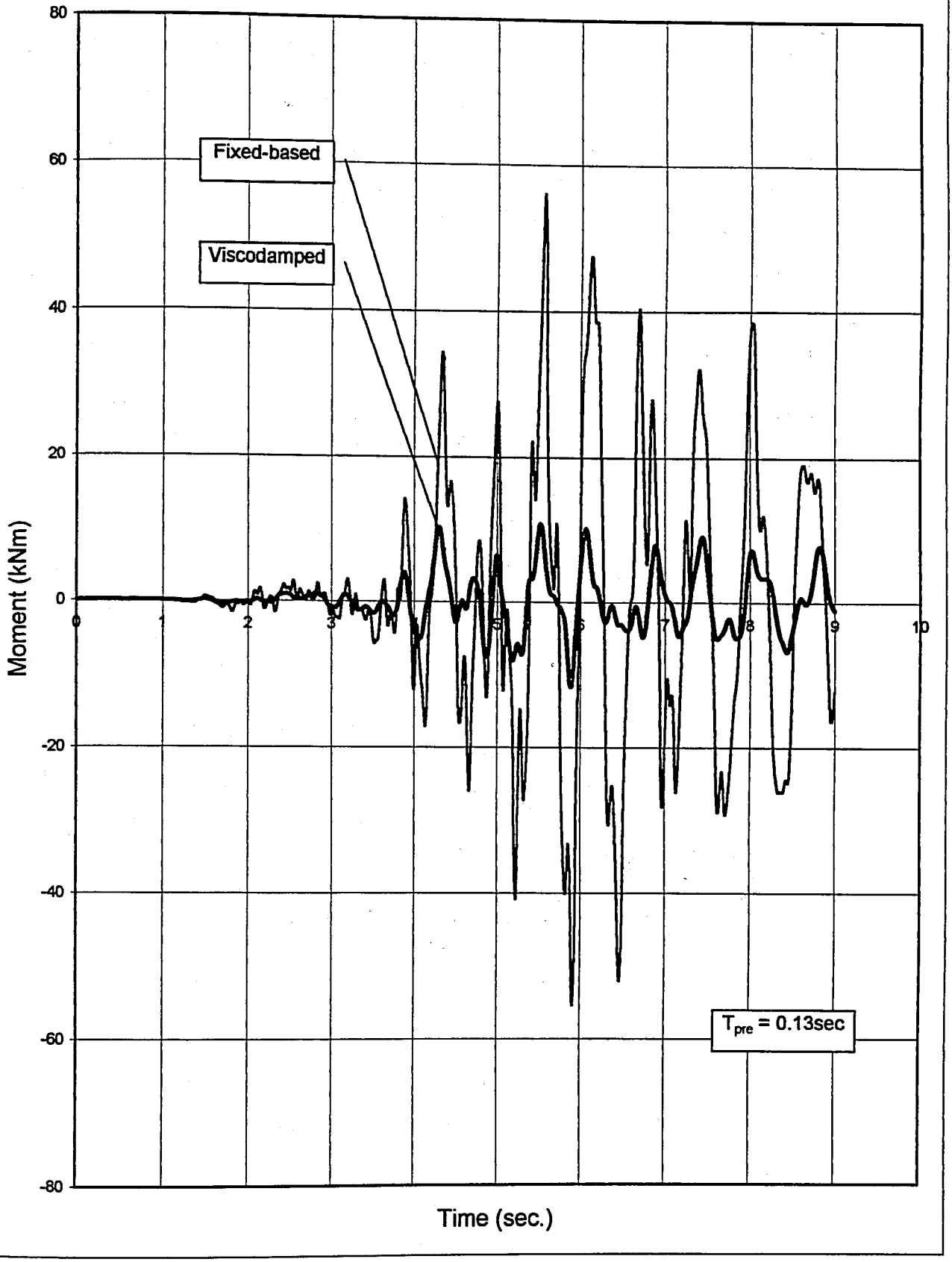

Figure 6.14. Top column upper part time histories of the Fixed-based and the Viscodampers Cases

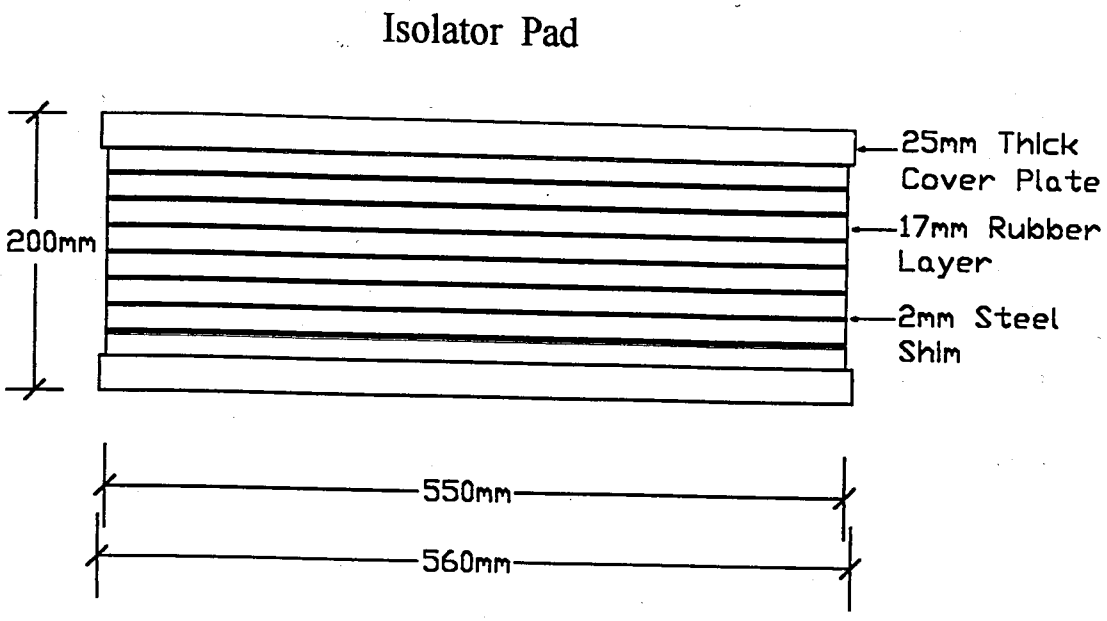

Figure 6.15. The geometry of the Isolator Pad

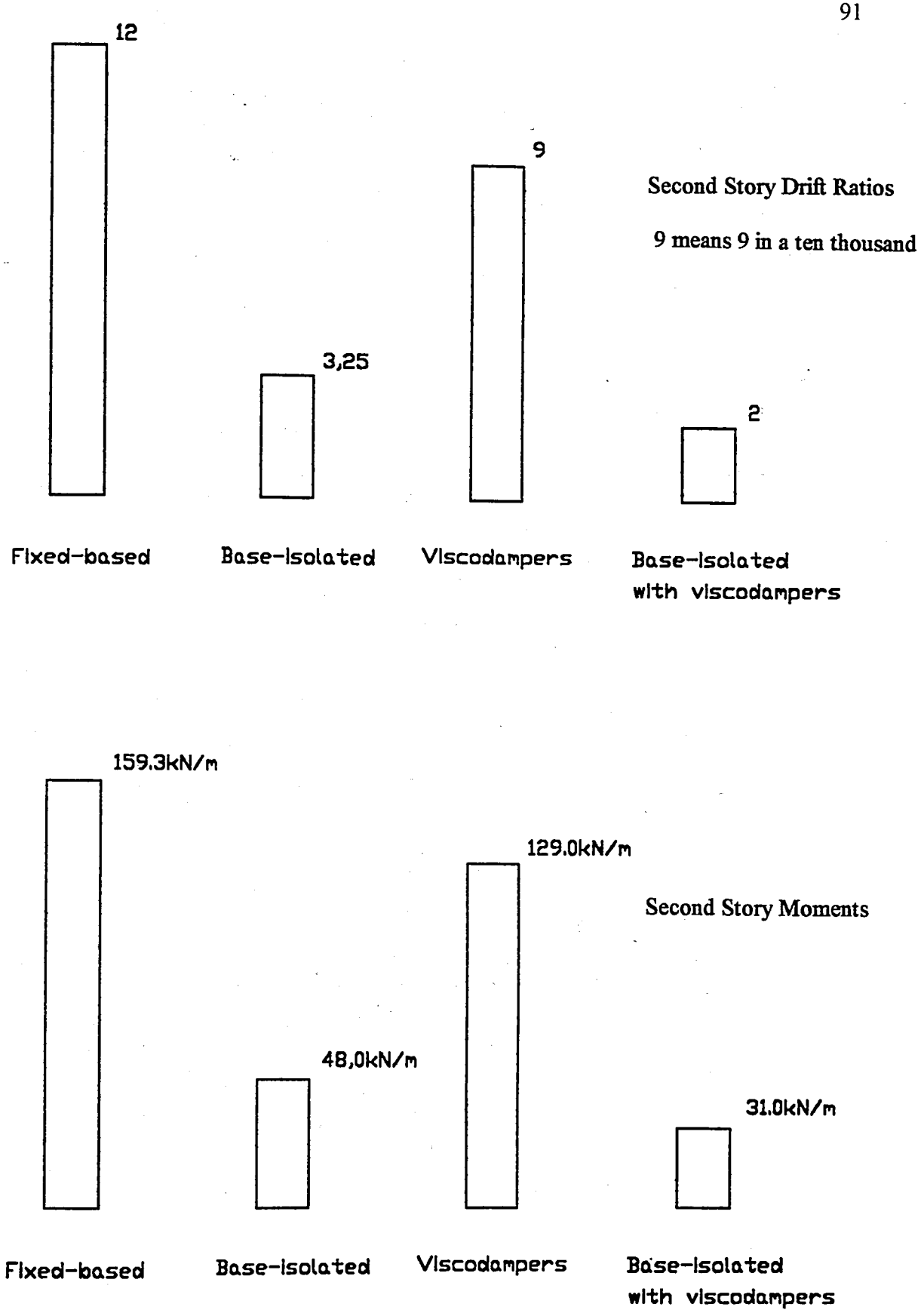

Figure 6.16. Second story nominated drift ratio and moment values

7. CONCLUSIONS

The goal of this study was to study the results of passive energy dissipation devices incorporated into building design and to analyse their effectiveness. Types of passive energy dissipation devices were discussed. Two devices, namely lead-plug bearings and viscoelastic dampers were chosen. The effectiveness of these was analysed after subjection to two differing earthquake simulations.

Lead-plug bearings and viscoelastic dampers were modeled with Sap2000n program and a large analytical study was performed to illustrate the behaviour of the structures under the effects of the passive energy dissipation systems.

Earthquake-A and Earthquake-B, which had a peak ground acceleration of 3.96m/sn^2 and predominant periods of 0.13sec. and 1.43sec. respectively were applied to four models using time history analyses. The models were also analysed by the equivalent seismic load method. The models were;

- fix-based
- with viscodampers
- base-isolated
- base-isolated with viscodampers

In order to understand the effect of ground motion periods on these devices, the results from the time history analyses of Earthquake-A and Earthquake-B were compared. The conclusions may be summarized as follows:

- As base isolation tools, lead-plug bearings isolate the building from the ground motions by increasing the fundamental period of the building and thereby moving the structure to the less energetic region of the spectral curve.

- After the analyses of fix-based and base-isolated models, it has been seen that storey displacements increase when base isolation is applied to a fix-based structure as well

as drift ratios. On the other hand, moment values at the top of columns and base shear values of the structure decrease.

- When the structure is base-isolated, rigid body motion takes place because base isolation introduced a plane lateral flexibility to the structure that lengthened the structure's fundamental period. This shifted it away from the destructive period range of typical ground motions. When the building is fix-based, its fundamental period is 0.575sec. On the other hand, when base isolation is used at the base level of the building, the fundamental period goes up to 2.48sec.

- The cumulative modal participating mass ratio at first mode of base-isolated building is 99.9 per cent while 79.5 per cent for the fix-based building.

- When the building has viscodampers at each storey, moment, displacement and drift ratio values decrease significantly compared to the fix-based building. The viscodampers are therefore shown to be excellent tools to stop a newly started vibration. Another important property is that they can be used in the rehabilitation of existing damaged buildings because they can be installed at any time to an existing building easily.

- The base-isolated building with the viscodampers has almost exactly rigid body motion. While the storey displacements remain almost the same as displacements of the base-isolated building, moment, drift ratio and base shear values decreased remarkably.

- It is found that base isolation was more effective during shorter periods of ground motion and less effective during longer periods of ground motion.

APPENDIX A: INPUT FILE OF ISOLATED BUILDING

```
; File C:\SAP2000N\isolated1.$2k saved 5.2.01 11:26:59 in KN-m

SYSTEM
   DOF=UX,UZ,RY  LENGTH=m  FORCE=KN  LINES=59

JOINT
   1  X=-5  Y=0  Z=0
   2  X=-5  Y=0  Z=3
   3  X=-5  Y=0  Z=6
   4  X=-5  Y=0  Z=9
   5  X=-5  Y=0  Z=12
   6  X=0  Y=0  Z=0
   7  X=0  Y=0  Z=3
   8  X=0  Y=0  Z=6
   9  X=0  Y=0  Z=9
   10  X=0  Y=0  Z=12
   11  X=5  Y=0  Z=0
   12  X=5  Y=0  Z=3
   13  X=5  Y=0  Z=6
   14  X=5  Y=0  Z=9
   15  X=5  Y=0  Z=12

RESTRAINT
   ADD=1  DOF=U3
   ADD=6  DOF=U3
   ADD=11  DOF=U3

CONSTRAINT
   NAME=DIAPH4  TYPE=DIAPH  AXIS=Z  CSYS=0
      ADD=5
      ADD=10
      ADD=15
   NAME=DIAPH3  TYPE=DIAPH  AXIS=Z  CSYS=0
      ADD=4
      ADD=9
      ADD=14
   NAME=DIAPH2  TYPE=DIAPH  AXIS=Z  CSYS=0
      ADD=3
      ADD=8
      ADD=13
   NAME=DIAPH1  TYPE=DIAPH  AXIS=Z  CSYS=0
      ADD=2
      ADD=7
      ADD=12

PATTERN
```

```
  NAME=DEFAULT

MASS
  ADD=7  U1=75
  ADD=8  U1=75
  ADD=9  U1=75
  ADD=10  U1=75

MATERIAL
  NAME=STEEL  IDES=S  M=7.8271  W=76.81954
    T=0  E=1.99948E+08  U=.3  A=.0000117
  NAME=CONC  IDES=C  M=2.4007  W=23.5616
    T=0  E=3.025E+07  U=.2  A=.0000099
  NAME=OTHER  IDES=N  M=2.40068  W=23.56161
    T=0  E=2.482113E+07  U=.2  A=.0000099

FRAME SECTION
  NAME=BEAM MAT=CONC SH=R T=.5,.4 A=.2 J=5.474168E-03 I=4.166667E-03,2.666667E-
03 AS=.1666667,.1666667
  NAME=COLUMN MAT=CONC SH=R T=.7,.4 A=.28 J=.0096051 I=1.143333E-02,3.733333E-03
AS=.2333333,.2333333

NLPROP
  NAME=ISO1E    TYPE=Isolator1
    DOF=U1  KE=380654  CE=.15
    DOF=U2  KE=595  CE=.15
  NAME=ISO1M    TYPE=Isolator1
    DOF=U1  KE=639579  CE=.15
    DOF=U2  KE=1190  CE=.15

FRAME
  1  J=1,2  SEC=COLUMN  NSEG=2  ANG=0
  2  J=2,3  SEC=COLUMN  NSEG=2  ANG=0
  3  J=3,4  SEC=COLUMN  NSEG=2  ANG=0
  4  J=4,5  SEC=COLUMN  NSEG=2  ANG=0
  5  J=6,7  SEC=COLUMN  NSEG=2  ANG=0
  6  J=7,8  SEC=COLUMN  NSEG=2  ANG=0
  7  J=8,9  SEC=COLUMN  NSEG=2  ANG=0
  8  J=9,10  SEC=COLUMN  NSEG=2  ANG=0
  9  J=11,12  SEC=COLUMN  NSEG=2  ANG=0
  10  J=12,13  SEC=COLUMN  NSEG=2  ANG=0
  11  J=13,14  SEC=COLUMN  NSEG=2  ANG=0
  12  J=14,15  SEC=COLUMN  NSEG=2  ANG=0
  13  J=2,7  SEC=BEAM  NSEG=4  ANG=0
  14  J=3,8  SEC=BEAM  NSEG=4  ANG=0
  15  J=4,9  SEC=BEAM  NSEG=4  ANG=0
  16  J=5,10  SEC=BEAM  NSEG=4  ANG=0
  17  J=7,12  SEC=BEAM  NSEG=4  ANG=0
  18  J=8,13  SEC=BEAM  NSEG=4  ANG=0
  19  J=9,14  SEC=BEAM  NSEG=4  ANG=0
  20  J=10,15  SEC=BEAM  NSEG=4  ANG=0
  21  J=1,6  SEC=BEAM  NSEG=4  ANG=0
  22  J=6,11  SEC=BEAM  NSEG=4  ANG=0
```

```
NLLINK
  8  J=1  NLP=ISO1E  ANG=0  AXDIR=+Z
  9  J=6  NLP=ISO1M  ANG=0  AXDIR=+Z
  10  J=11  NLP=ISO1E  ANG=0  AXDIR=+Z

LOAD
  NAME=LOAD1

MODE
  TYPE=EIGEN  N=4  TOL=.00001

FUNCTION
  NAME=FUNCBU DT=.001 NPL=1 PRINT=Y FILE=bukisans.txt

HISTORY
  NAME=HISTBU TYPE=LIN NSTEP=9000 DT=.001 DAMP=.05
    ACC=U1  ANG=0 FUNC=FUNCBU SF=.03924 AT=0

OUTPUT
; No Output Requested

END

; The following data is not required for analysis. It is written here as a
backup.
; This data will be used for graphics and design if this file is imported.
; If changes are made to the analysis data above, then the following data
; should be checked for consistency.
; Any errors in importing the following data are ignored without warning.
SAP2000 V6.11 SUPPLEMENTAL DATA
  GRID GLOBAL  X "1"  -5
  GRID GLOBAL  X "2"  0
  GRID GLOBAL  X "3"  5
  GRID GLOBAL  Y "4"  0
  GRID GLOBAL  Z "5"  0
  GRID GLOBAL  Z "6"  3
  GRID GLOBAL  Z "7"  6
  GRID GLOBAL  Z "8"  9
  GRID GLOBAL  Z "9"  12
  MATERIAL STEEL FY 248211.3
  MATERIAL CONC FYREBAR 413685 FYSHEAR 275790 FC 27579 FCSHEAR 27579
  CONCRETESECTION BEAM COLUMN  COVER .05 REBAR RR-3-3
  CONCRETESECTION COLUMN COLUMN  COVER .04572 REBAR RR-3-3
  STATICLOAD LOAD1 TYPE DEAD
END SUPPLEMENTAL DATA
```

APPENDIX B: OUTPUT FILE OF ISOLATED BUILDING

C O N S T R A I N T C O O R D I N A T E S A N D M A S S E S

CONS DIAPH1 ========== TYPE = DIAPH, NORMAL DIRECTION = U3

LOCAL COORDINATE SYSTEM FOR CONSTRAINT MASTER

GLOBAL	U1	U2	U3	R1	R2	R3
X	.000000	1.000000	.000000	.000000	1.000000	.000000
Y	-1.000000	.000000	.000000	-1.000000	.000000	.000000
Z	.000000	.000000	1.000000	.000000	.000000	1.000000

TRANSLATIONAL MASS AND MASS MOMENTS OF INERTIA

U1	U2	U3	R1	R2	R3
10.851164	85.851164	.000000	.000000	.000000	160.846900

CENTER OF MASS

GLOBAL	U1	U2	U3
X	.000000	.000000	.000000
Y	.000000	.000000	.000000
Z	3.000000	3.000000	3.000000

CONS DIAPH2 ========== TYPE = DIAPH, NORMAL DIRECTION = U3

LOCAL COORDINATE SYSTEM FOR CONSTRAINT MASTER

GLOBAL	U1	U2	U3	R1	R2	R3
X	.000000	1.000000	.000000	.000000	1.000000	.000000
Y	-1.000000	.000000	.000000	-1.000000	.000000	.000000
Z	.000000	.000000	1.000000	.000000	.000000	1.000000

TRANSLATIONAL MASS AND MASS MOMENTS OF INERTIA

U1	U2	U3	R1	R2	R3
10.851164	85.851164	.000000	.000000	.000000	160.846900

CENTER OF MASS

GLOBAL	U1	U2	U3
X	.000000	.000000	.000000
Y	.000000	.000000	.000000
Z	6.000000	6.000000	6.000000

CONS DIAPH3 ========== TYPE = DIAPH, NORMAL DIRECTION = U3

LOCAL COORDINATE SYSTEM FOR CONSTRAINT MASTER

GLOBAL	U1	U2	U3	R1	R2	R3
X	.000000	1.000000	.000000	.000000	1.000000	.000000
Y	-1.000000	.000000	.000000	-1.000000	.000000	.000000
Z	.000000	.000000	1.000000	.000000	.000000	1.000000

TRANSLATIONAL MASS AND MASS MOMENTS OF INERTIA

U1	U2	U3	R1	R2	R3
10.851164	85.851164	.000000	.000000	.000000	160.846900

CENTER OF MASS

GLOBAL	U1	U2	U3
X	.000000	.000000	.000000

Y	.000000	.000000	.000000
Z	9.000000	9.000000	9.000000

CONS DIAPH4 ========== TYPE = DIAPH, NORMAL DIRECTION = U3

LOCAL COORDINATE SYSTEM FOR CONSTRAINT MASTER

GLOBAL	U1	U2	U3	R1	R2	R3
X	.000000	1.000000	.000000	.000000	1.000000	.000000
Y	-1.000000	.000000	.000000	-1.000000	.000000	.000000
Z	.000000	.000000	1.000000	.000000	.000000	1.000000

TRANSLATIONAL MASS AND MASS MOMENTS OF INERTIA

U1	U2	U3	R1	R2	R3
7.826282	82.826282	.000000	.000000	.000000	110.432200

CENTER OF MASS

GLOBAL	U1	U2	U3
X	.000000	.000000	.000000
Y	.000000	.000000	.000000
Z	12.000000	12.000000	12.000000

D I S P L A C E M E N T D E G R E E S O F F R E E D O M

(A) = Active DOF, equilibrium equation
(-) = Restrained DOF, reaction computed
(+) = Constrained DOF
( ) = Null DOF

JOINTS			UX	UY	UZ	RX	RY	RZ
1			A		-		A	
2	TO	5	+		A		A	
6			A		-		A	
7	TO	10	+		A		A	
11			A		-		A	
12	TO	15	+		A		A	

CONSTRAINTS	U1	U2	U3	R1	R2	R3
DIAPH1 TO DIAPH4		A				

A S S E M B L E D J O I N T M A S S E S

IN GLOBAL COORDINATES

JOINT	UX	UY	UZ	RX	RY	RZ
1	2.208644	2.208644	2.208644	.000000	.000000	.000000
2	3.216938	3.216938	3.216938	.000000	.000000	.000000
3	3.216938	3.216938	3.216938	.000000	.000000	.000000
4	3.216938	3.216938	3.216938	.000000	.000000	.000000
5	2.208644	2.208644	2.208644	.000000	.000000	.000000
6	3.408994	3.408994	3.408994	.000000	.000000	.000000
7	79.417288	4.417288	4.417288	.000000	.000000	.000000
8	79.417288	4.417288	4.417288	.000000	.000000	.000000
9	79.417288	4.417288	4.417288	.000000	.000000	.000000
10	78.408994	3.408994	3.408994	.000000	.000000	.000000
11	2.208644	2.208644	2.208644	.000000	.000000	.000000
12	3.216938	3.216938	3.216938	.000000	.000000	.000000

13	3.216938	3.216938	3.216938	.000000	.000000	.000000
14	3.216938	3.216938	3.216938	.000000	.000000	.000000
15	2.208644	2.208644	2.208644	.000000	.000000	.000000

T O T A L A S S E M B L E D J O I N T M A S S E S

IN GLOBAL COORDINATES

	UX	UY	UZ	RX	RY	RZ
TOTAL	348.206056	48.206056	48.206056	.000000	.000000	.000000

T O T A L A C C E L E R A T E D M A S S A N D L O C A T I O N

TOTAL MASS ACTIVATED BY ACCELERATION LOADS, IN GLOBAL COORDINATES

	UX	UY	UZ
MASS	348.206056	.000000	40.379774
X-LOC	1.79E-17	.000000	-2.20E-17
Y-LOC	.000000	.000000	.000000
Z-LOC	7.292338	.000000	7.162901

M O D A L P E R I O D S A N D F R E Q U E N C I E S

MODE	PERIOD (TIME)	FREQUENCY (CYC/TIME)	FREQUENCY (RAD/TIME)	EIGENVALUE (RAD/TIME)**2
1	2.478593	0.403455	2.534981	6.426128
2	0.291195	3.434123	21.577230	465.576865
3	0.116831	8.559353	53.780003	2892.289
4	0.062681	15.953785	100.240587	10048.175

M O D A L P A R T I C I P A T I O N F A C T O R S

FOR UNIT ACCELERATION LOADS IN GLOBAL COORDINATES

MODE	PERIOD	UX	UY	UZ
1	2.478593	18.654914	.000000	1.57E-12
2	0.291195	-0.435858	.000000	-6.26E-12
3	0.116831	0.091597	.000000	2.87E-08
4	0.062681	0.031523	.000000	9.56E-07

M O D A L P A R T I C I P A T I N G M A S S R A T I O S

MODE	PERIOD	INDIVIDUAL MODE (PERCENT)			CUMULATIVE SUM (PERCENT)		
		UX	UY	UZ	UX	UY	UZ
1	2.478593	99.9425	0.0000	0.0000	99.9425	0.0000	0.0000
2	0.291195	0.0546	0.0000	0.0000	99.9971	0.0000	0.0000
3	0.116831	0.0024	0.0000	0.0000	99.9995	0.0000	0.0000
4	0.062681	0.0003	0.0000	0.0000	99.9997	0.0000	0.0000

PROGRAM SAP2000 - VERSION N6.11 FILE:ISOLATED1.OUT
NONLINEAR VERSION

M O D A L L O A D P A R T I C I P A T I O N R A T I O S

LOAD, ACC, OR NLLINK (TYPE)	DEF (NAME)	STATIC (PERCENT)	DYNAMIC (PERCENT)
LOAD	LOAD1	0.0000	0.0000
ACC	UX	100.0000	99.9997
ACC	UY	0.0000	0.0000
ACC	UZ	0.0000	0.0000

E F F E C T I V E M O D A L D A M P I N G R A T I O S

INCLUDING NLLINK EFFECTIVE DAMPING. MODAL CROSS-COUPLING TERMS ARE NEGLECTED

HIST HISTBU ----------

MODE	PERIOD	DAMP-RATIO
1	2.478593	0.050225
2	0.291195	0.050076
3	0.116831	0.050052
4	0.062681	0.050040

G L O B A L F O R C E B A L A N C E

TOTAL FORCE AND MOMENT AT THE ORIGIN, IN GLOBAL COORDINATES

LOAD LOAD1 ----------

	FX	FY	FZ	MX	MY	MZ
APPLIED	.000000	.000000	.000000	.000000	.000000	.000000
INERTIA	.000000	.000000	.000000	.000000	.000000	.000000
NLLINKS	.000000	.000000	.000000	.000000	.000000	.000000
REACTNS	.000000	.000000	.000000	.000000	.000000	.000000
CONSTRS	.000000	.000000	.000000	.000000	.000000	.000000
TOTAL	.000000	.000000	.000000	.000000	.000000	.000000

MODE 1 ----------

	FX	FY	FZ	MX	MY	MZ
APPLIED	.000000	.000000	.000000	.000000	.000000	.000000
INERTIA	119.878858	.000000	1.01E-11	.000000	884.111610	.000000
NLLINKS	-119.878858	.000000	.000000	.000000	.000000	.000000
REACTNS	.000000	.000000	-3.02E-06	.000000	-884.111604	.000000
CONSTRS	3.27E-09	.000000	.000000	.000000	7.76E-10	.000000
TOTAL	3.27E-09	.000000	-3.02E-06	.000000	5.86E-06	.000000

MODE 2 ----------

	FX	FY	FZ	MX	MY	MZ
APPLIED	.000000	.000000	.000000	.000000	.000000	.000000

INERTIA	-202.925224	.000000	-2.92E-09	.000000	28743.870	.000000
NLLINKS	202.925224	.000000	.000000	.000000	.000000	.000000
REACTNS	.000000	.000000	-5.03E-06	.000000	-28743.870	.000000
CONSTRS	9.51E-08	.000000	.000000	.000000	4.29E-07	.000000
TOTAL	9.33E-08	.000000	-5.04E-06	.000000	0.000146	.000000

MODE 3 ----------

	FX	FY	FZ	MX	MY	MZ
APPLIED	.000000	.000000	.000000	.000000	.000000	.000000
INERTIA	264.924583	.000000	8.29E-05	.000000	-5845.363	.000000
NLLINKS	-264.924583	.000000	.000000	.000000	.000000	.000000
REACTNS	.000000	.000000	-0.025429	.000000	5845.405	.000000
CONSTRS	2.32E-05	.000000	.000000	.000000	0.000148	.000000
TOTAL	2.31E-05	.000000	-0.025346	.000000	0.041987	.000000

G L O B A L F O R C E B A L A N C E

TOTAL FORCE AND MOMENT AT THE ORIGIN, IN GLOBAL COORDINATES

MODE 4 ----------

	FX	FY	FZ	MX	MY	MZ
APPLIED	.000000	.000000	.000000	.000000	.000000	.000000
INERTIA	316.753299	.000000	0.009602	.000000	-44015.397	.000000
NLLINKS	-316.753293	.000000	.000000	.000000	.000000	.000000
REACTNS	.000000	.000000	-0.739107	.000000	44016.093	.000000
CONSTRS	0.000337	.000000	.000000	.000000	0.002623	.000000
TOTAL	0.000343	.000000	-0.729505	.000000	0.698171	.000000

REFERENCES

Afet Bölgelerinde Yapılacak Yapılar Hakkında Yönetmelik, Afet İşleri Genel Müdürlüğü, Bayındırlık ve İskan Bakamlığı, 2 Eylül 1997 tarih ve 23 098 mükerrer sayılı Resmi Gazete.

Banerji, P., M. Murudi, A. H. Shah and N. Popplewell, 2000, "Tuned liquid dampers for controlling earthquake response of structures", *Earthquake Engineering and Structural Dynamics*, Vol.29, pp 587-602.

Ceccoli, C., C. Mazzotti and M. Savoia, "Non-linear Seismic Analysis of Base-Isolated RC Frame Structures", *Earthquake Engineering and Structural Dynamics*, Vol.28, pp.633-653, 1999.

Chunxiang, L., 2000, "Performance of multiple tuned mass dampers for attenuating undesirable oscillations of structures under the ground acceleration", *Earthquake Engineering and Structural Dynamics*, Vol.29, pp. 1405-1421.

Constantinou, M. C., T. T. Soong and T. Dargush, 1998, *Passive Energy Dissipation Systems for Structural Design and Retrofit, Multidisciplinary Center*, America.

Constantinou, M. C. and M. D. Symans, 1993, "Seismic Response of Structures with Supplemental Damping", *The Structural Design of Tall Buildings*, Vol.2, pp.77-92.

Constantinou, M. C. and M. D. Symans, 1993, "Experimental Study of Seismic Response of Buildings with Supplemental Fluid Dampers", *The Structural Design of Tall Buildings*, Vol.2, pp.93-132.

Dolce, M., D. Cardone and R. Marnetto, 2000, "Implementation and testing of passive control devices based on shape memory alloys", *Earthquake Engineering and Structural Dynamics*, Vol.29, pp. 945-968.

Edward, W., 1997, *Three Dimensional Dynamic Analysis of Structures with Emphasis on Earthquake Engineering, CSI. Computers and Structures Inc.*, Berkley, California,USA.

Fu, Y. and S. Cherry, 2000, "Design of friction damped structures using lateral force procedure" *Earthquake Engineering and Structural Dynamics*, Vol.29, pp. 989-1010.

Harry, W. S. and F. P. Hampton, September 1999, "Seismic Response of Isolated Elevated Water Tanks", *Journal Structural Engineering*, Vol.125, No.9.

Harry, W. S. and E. S. Holloway, 2000, "Effect of stiffness variability on the response of isolated structures", *Earthquake Engineering and Structural Dynamics*, Vol.29. pp. 19-36.

Kelly, J. M., 1999, "The Role of Damping in Seismic Isolation", *Earthquake Engineering and Structural Dynamics*, Vol.28, pp.3-20.

Kikuchi, M. and I. D. Aiken, 1997, "An Analytical Hysteresis Model For Elastomeric Seismic Isolation Bearings", *Earthquake Engineering and Structural Dynamics*, Vol.26, pp. 215-231.

Kikuchi, M. and I. D. Aiken, 1997, "An Analytical Hysteresis Model For Elastomeric Seismic Isolation Bearings", *Earthquake Engineering and Structural Dynamics*, Vol.26, pp. 215-231.

Levy, R., E. Marianchik, A. Rutenberg and F. Segal, 2000, "Seismic design Methodology for friction damped braced frames", *Earthquake Engineering and Structural Dynamics*, Vol.29, pp. 1569-1585.

Malhotra, P. K., 1997, "Dynamics of Seismic Impacts in Base-Isolated Buildings", *Earthquake Engineering and Structural Dynamics*, Vol.26, pp. 797-813.

Makris, N., M. C. Constantinou, Associate Member, ASCE, September 1991, "Fractional-Derivative Maxwell Model for Viscous Dampers", *Journal of Structural Engineering*, Vol.117, No.9.

Makris, N. and M. C. Constantinou, 1992, "Spring-Viscous Damper Systems for Combined Seismic and Vibration Isolation", *Earthquake Engineering and Structural Dynamics*, Vol.21, pp.649-664.

Makris, N. and M. C. Constantinou, July 1993, "Models of Viscoelasticity with Complex-Order Derivatives", *Journal of Engineering Mechanics*, Vol.119, No.7.

Makris, N., G.F. Dargush and M.C. Constantinou, August 1993, "Dynamic Analysis of Generalized Viscoelastic Fluids", *Journal of Engineering Mechanics*, Vol.119, No.8.

Makris, N., M. C. Constantinou, Associate Member, ASCE, G.F. Dargush, November 1993, "Analytical Model of Viscoelastic Fluid Dampers", *Journal of Structural Engineering*, Vol.119, No.11.

Makris, N., 1997, "Rigidity-Plasticity-Viscocity: Can Electrorheological Dampers Protect Base-Isolated Structures From Near-Source Ground Motions", *Earthquake Engineering and Structural Dynamics*, Vol.26, pp. 571-591.

Makris, N., G. F. Dargush and M. C. Constantinou, Members, ASCE, October 1995, "Dynamic Analysis of Viscoelastic-Fluid Dampers", *Journal of Engineering Mechanics*, Vol.121, No.10.

Makris, N. and S. Chang, 2000, "Effect of viscous, Viscoplastic and friction damping on the response of seismic isolated structures", *Earthquake Engineering and Structural Dynamics*, Vol.29, pp.85-107.

Nagarajaiah, S., A. M. Reinhorn, and M. C. Constantinou, 1991, *Nonlinear Dynamic Analysis of Three Dimensional Base Isolated Structures*, National Center for Earthquake Engineering Research, New York.

Nagarajaiah, S., Member, ASCE, Keith Ferrell, September 1999, "Stability of Elastomeric Seismic Isolation Bearings", *Journal of Structural Engineering*, Vol.125, No.9.

Naeim, F. and J. M. Kelly, 1999, *Design of Seismic Isolated Structures, John Wiley & sons. Inc.*, Canada.

Park, Y. J., Y. K. Wen and A. Ang, 1986, "Random Vibration of Hysteretic Systems under Bi-Directional Ground Motions" *Earthquake Engineering and Structural Dynamics*, Vol. 14

Pranesh, M. and R. Sinha, 2000, "VFPI: an isolation device for aseismic design", *Earthquake Engineering and Structural Dynamics*, Vol.29, pp. 603-627.

Ricciadelli, F. and B. J. Vickery, 1999, "Tuned Vibration Absorbers with Dry Friction Damping" *Earthquake Engineering and Structural Dynamics*, Vol.28, pp.707-723.

SAP2000 Version 6.11, *Integrated Finite Element Analysis and Design of Structures.*

SAP2000n *Analysis References* Volume1, CSI, California, USA, 1997.

SAP2000 Version 6.11, *Integrated Finite Element Analysis and Design of Structures.*

SAP2000n *Analysis References* Volume2, CSI, California, USA, 1997.

SAP2000n *Verification Manual*, CSI, California, USA, 1997.

Schmitendorf, W. E., 2000, "Designing tuned mass dampers via static output feedback: a numerical approach", *Earthquake Engineering and Structural Dynamics*, Vol.29, pp.127-137.

Shukla, A.K. and T.K. Datta, April 1999, "Optimal use of Viscoelastic Dampers in Building Frames for Seismic Force", *Journal of Structural Engineering*, Vol.125, No.4.

Skinner, R. I., W. H. Robinson and G. H. McVerry, 1996, *An Introduction To Seismic Isolation*, England.

Stewart, J. P., J. P. Conte and I. D. Aiken, Members, ASCE, September 1999, "Observed Behaviour of Seismically Isolated Buildings", *Journal of Structural Engineering*, Vol.125, No.9.

Takewaki, I., S. Yoshitomi, K. Uetani and M. Tsuji, 1999, "Non-Monotonic Optimal Damper Placement Via Steepest Direction Search", *Earthquake Engineering and Structural Dynamics*, Vol.28, pp. 655-670.

Tezcan, S. S., January 1982, "The Use of Isolation Techniques in Design", International Report No:82-41E, *Earthquake Engineering Research Institute*, Boğaziçi University.

Tezcan, S. S. and O. Uluca, 2000, *Reduction of Seismic Response by Viscoelastic dampers*, MS. Thesis, Boğaziçi University.

Todorovska, M. I., Member, ASCE, April 1999, "Base Isolation by A Soft First Story with Inclined Columns", *Journal of Engineering Mechanics*, Vol.125, No.4.

Uniform Building Code, International Conference of Building Officials, 5360 Workman Mill Rd, Whittier California, 90 601, USA, May 1985.

Uras, R. A., August 1996 "Use of a Viscoelastic Model for the Seismic Response of Base-Isolated Buildings", *Journal of Pressure Vessel Technology*, Vol.118.

Villaverde, R. and G. Mosqueda, 1999, "Aseismic Roof Isolation System: Analytical and Shake table Studies", *Earthquake Engineering and Structural Dynamics*, Vol.28, pp.217-234.

Vakakis, A. F. and A. N. Kounadis, I. G. Raftoyiannis,1999 "Use of non-Linear Localization for Isolating Structures from Earthquake-Induced Motions", *Earthquake Engineering and Structural Dynamics*, Vol.28, pp.21-36.

Wen Y. K., 1976, "Method for Random Vibration of Hysteretic Systems", *Journal of the Engineering Mechanics Division*, Vol.102

Whittaker, A., Michael C., Members, ASCE, Panos Tsopelas, Associate Member, ASCE, August 1998 "Displacement Estimates for Performance-Based Seismic Design", *Journal of Structural Engineering*, Vol.124, No.8.

Yamado, K., 2000 "Control strategy for variable damping element considering near-future excitation influence", *Earthquake Engineering and Structural Dynamics*, ol.29, pp. 1199-1217.

Yamazaki, F., M. A. Ansary, 1997, "Horizontal-to-Vertical Spectrum Ratio of Earthquake Ground Motion For Site Characterization", *Earthquake Engineering and Structural Dynamics*, Vol.26, pp. 671-689.

Zhao, B., Xilin L., Minzhe W., Zhanxin M., 2000, "Sliding mode control of buildings with base-isolated hybrid protective system", *Earthquake Engineering and Structural Dynamics*, Vol.29, pp.315-326.

Zhuge, Y., D. Thambiratnam, Member, ASCE, John Corderoy, Associate Member, ASCE, March 1998, "Non-linear Dynamic Analysis of Unreinforced Masonry", *Journal of Structural Engineering*, Vol.124, No.3.

Ziyaeifar, M., H. Noguchi, 1998, "Partial Mass Isolation in tall Buildings", *Earthquake Engineering and Structural Dynamics*, Vol.27, pp. 49-65.